University of São Paulo
"Luiz de Queiroz" College of Agriculture

Deciphering the role of early molecular interactions between *Eucalyptus* spp. x *Austropuccinia psidii* and its pathogenesis

Isaneli Batista dos Santos

Thesis presented to obtain the degree of Doctor in Science. Area: Agricultural Microbiology

Piracicaba
2019

Isaneli Batista dos Santos
Agronomist Engineer

Deciphering the role of early molecular interactions between *Eucalyptus* spp. x *Austropuccinia psidii* and its pathogenesis

versão revisada de acordo com a resolução CoPGr 6018 de 2011

Advisor:
Profa. Dra. **MARIA CAROLINA QUECINE VERDI**

Thesis presented to obtain the degree of Doctor in Science. Area: Agricultural Microbiology

Piracicaba
2019

Dados Internacionais de Catalogação na Publicação
DIVISÃO DE BIBLIOTECA – DIBD/ESALQ/USP

Santos, Isaneli Batista dos

Deciphering the role of early molecular interactions between *Eucalyptus* spp. x *Austropuccinia psidii* and its pathogenesis / Isaneli Batista dos Santos - - versão revisada de acordo com a resolução CoPGr 6018 de 2011. - - Piracicaba, 2019.

110 p.

Tese (Doutorado) - - USP / Escola Superior de Agricultura “Luiz de Queiroz”.

1. Lipdômica 2. Transcriptômica 3. Fungo biotrófico 4. Mecanismo pré-formado I. Título

AGRADECIMENTOS

"Entregue o seu caminho ao Senhor; confie nele, e ele o fará"
Salmos 37:5

À Deus pelo dom da vida, pela proteção e por sempre guiar meu caminho!

À minha família: Izabel, Izanielle, Jamille, Júnior e Samuel, pelo incentivo, apoio e compreensão!

Ao meu noivo, Fabrício, por sempre apoiar minhas decisões, por todo amor e companherismo!

À minha querida orientadora, Prof. Maria Carolina Quecine, obrigada por ser esse exemplo de pessoa e de profissionalismo! Obrigada por ter me dado a oportunidade de ser sua orientada, por não medir esforços na minha orientação, por ter me dado a chance de conviver com você e pela oportunidade de ter aprendido tanto! Você despertou em mim meu melhor lado: o cientista crítico! Sem dúvidas vc é uma inspiração pra mim!

Ao Prof. João Lúcio, pelo exemplo de dedicação, humildade e profissionalismo!

Aos colegas, amigos e ex-integrantes do "Laboratório de Genética de Microorganismos", obrigada pela convivência, pelas discussões científicas, pelos ensinamentos e pela companhia!

Ao grupo de pesquisa "Puccinia", unidos e com muita garra, superamos muitos obstáculos, aprendemos muito e discutimos muita ciência. Obrigada, sem a ajuda de vocês nada disso teria sido realizado!

Ao Prof. Carlos Labate, Mônica, Thaís e todos integrantes do "Laboratório Max Feffer de Genética de Plantas" pelo apoio nas análises e disponibilização de equipamentos!

À Prof. Luciana D. Silva e aos técnicos Natanael e Sabino do "Viveiro de mudas do Departamento de Ciências Florestais" pelo apoio inestimável na condução de mudas e na disponibilização de material vegetal. Sem dúvidas, conviver com vocês e aprender um pouco com suas experiências foi muito valioso pra mim!

À querida Lívia Franceschini, pelo apoio incondicional nas análises de RNASeq!

Ao time UAG na Esalq, Arthur, Pedro, Adijailton, Bruno, Everthon e demais, obrigada pelas conversas, companhia e apoio!

Aos amigos Mariana, Bruna W., Everthon, Camila, Jessica, Jaqueline, Bruno, Helena, Carolzinha e tantos outros, obrigada pela amizade e convívio, vcs foram essenciais nessa caminhada!

Aos amigos, Flaviana, Tiago e Raquel, apesar da distância vocês se fizeram sempre presentes! Obrigada pela amizade!

À minha querida ex orientadora, Prof. Júlia K. Sobral, pelas inúmeras conversas e pelo incentivo em cursar doutorado na Esalq. Sem seu incentivo nada disso teria acontecido!

À Escola Superior de Agricultura "Luiz de Queiroz", ao Programa de Pós-Graduação em Microbiologia Agrícola e a todos os professores dos departamentos de Solos, Genética, Fitopatologia, Ciências Florestais e Biologia, pelo auxílio em minha formação.

À Capes (Coordenação de Aperfeiçoamento de Pessoal de Nível Superior) pelo suporte financeiro.

Agradeço também a todos que direta ou indiretamente contribuíram para a realização desta tese.

Obrigada!

“A scientist in his laboratory is not a mere technician: he is also a child confronting natural phenomena that impress him as though they were fairy tales”

Marie Curie

CONTENTS

RESUMO **7**

ABSTRACT **8**

FIGURE LIST **9**

TABLE LIST **11**

ABBREVIATION LIST **12**

1. INTRODUCTION **13**

REFERENCES 18

2. THE *Eucalyptus* CUTICULAR WAXES CONTRIBUTE IN PREFORMED DEFENSE AGAINST *Austropuccinia psidii* **25**

ABSTRACT 25
INTRODUCTION 25
MATERIALS AND METHODS 26
- SUSCEPTIBILITY OG *EUCALYPTUS* SPP. TO *AUSTROPUCCINIA PSIDII*: FIELD INFERENCE .. 26
- *A. PSIDII* QUANTIFICATION BY QPCR IN CONTRASTING EUCALYPTUS SPECIES 27
- *EUCALYPTUS* SPP. CUTICULAR WAX EXTRACTION 27
- CHEMICAL CHARACTERIZATION OF *EUCALYPTUS* SPP. CUTICULAR WAXES USING CG-TOF-MS 28
- INFLUENCE OF CUTICULAR WAX ON *A. PSIDII* GERMINATION 29
- HEXADECANOIC ACID EFFECTS ON *A. PSIDII* GERMINATION 29
- SCANNING ELECTRON MICROSCOPY 29
- STATISTICAL ANALYSIS 30

RESULTS 30
- EVALUATION OF THE *EUCALYPTUS* SPP. RUST SUSCEPTIBILITY 30
- *EUCALYPTUS* SPP. CUTICLE WAX CHARACTERIZATION 33
- GERMINATION RATE OF *A. PSIDII* IN CUTICLE EXTRACTS AND HEXADECANOIC ACID ... 34
- EPICUTICULAR WAX MORPHOLOGY AND *A. PSIDII* GERMINATION *IN VIVO* 35

DISCUSSION 37
CONCLUSIONS 39
FUNDING 39
ACKNOWLEDGMENTS 40
SUPPLEMENTARY MATERIAL 40
REFERENCES 42

3. TRANSCRIPTOME ANALYSIS OF *Austropuccinia psidii* REVEALS THE ROLE OF CUTICULAR WAXES *Eucalyptus* spp. ON FUNGAL PATHOGEN GENE EXPRESSION **49**

ABSTRACT 49
INTRODUCTION 50
MATERIALS AND METHODS 52
- EXPERIMENTAL DESIGN 52
- RNA EXTRACTION, LIBRARY CONSTRUCTION AND RNA-SEQ 53
- DATA PROCESSING AND ASSEMBLY 54
- DIFFERENTIALLY EXPRESSED GENES ANALYSIS, ANNOTATION AND CATEGORIZATION 54
- REAL-TIME QUANTITATIVE PCR (RT-QPCR) ANALYSIS OF THE DEGS 55

RESULTS 57
- EXTRACTION OF TOTAL RNA FROM UREDOSPORES OF *A. PSIDII* 57
- SEQUENCE ANALYZING AND ALIGNING TO THE REFERENCE GENOME 58
- IDENTIFICATION AND DEGS ANALYSIS 58

- GO ENRICHMENT ANALYSIS 60
- DIFFERENTIAL EXPRESSION OF PATHOGENICITY RELATED GENES 62
- VALIDATION OF RNA-SEQ DATA BY QUANTITATIVE RT-QPCR 65

DISCUSSION 66
SUPPLEMENTARY MATERIAL 69
REFERENCES 71

4. ADDITIONAL INFORMATION 79

ADDITIONAL INFORMATION 1. TRIMMOMATIC 79
ADDITIONAL INFORMATION 2. KALLISTO 86
ADDITIONAL INFORMATION 3. SLEUTH 91

5. APPENDIX 99

RESUMO

Desvendando a patogênese e o papel das interações moleculares precoces entre *Eucalyptus* spp. x *Austropuccinia psidii*

Austropuccinia psidii é o agente causal da ferrugem das mirtáceas com crescimento biotrófico, ou seja, o patógeno depende dos tecidos do hospedeiro para crescer e se desenvolver. Os uredósporos de *A. psidii* infectam *Eucalyptus* por meio do contato inicial com a superfície do hospedeiro e também pela interação com a cutícula da folha que por sua vez fornece importantes sinais químicos e físicos capaz de desencadear o processo de infecção. Devido às características inerentes à cutícula de *Eucalyptus*, consideramos as hipóteses de que o mecanismo pré-formado, composto principalmente pelas ceras cuticulares, desempenha um papel crucial na resistência de *Eucalyptus* spp. contra *A. psidii*, e, também, é capaz de modular a expressão fúngica de genes associados a patogenicidade durante o estágio inicial de infecção de *A. psidii*. No capítulo 2, as ceras cuticulares de *Eucalyptus* spp. foram analisadas para determinar a composição/estrutura e sua correlação com suscetibilidade/resistência de *A. psidii*. Vinte e uma espécies de *Eucalyptus* foram classificadas em campo como resistentes ou suscetíveis. A análise de qPCR de seis *Eucalyptus* spp. revelou que o patógeno pode germinar na superfície de algumas espécies de eucaliptos sem se multiplicar no tecido hospedeiro. Foram identificados 26 compostos presentes na cutícula de *Eucalyptus* spp. e descobrimos o papel do ácido hexadecanóico na suscetibilidade de *E. grandis* e *E. phaeotricha* à ferrugem. Por meio da microscopia eletrônica de varredura encontramos uma correlação entre a morfologia epicuticular e a resistência contra *A. psidii*. No capítulo 3 para compreender a expressão gênica de *A. psidii* realizamos bioensaios (*in vitro*) contendo as ceras cuticulares de *E. grandis* (*E. g*), *E. urograndis* (*E. ug*) e *E. urophylla* (*E. u*). O tratamento com óleo mineral (MO) foi utilizado em todas as análises comparativas como controle negativo. A presença de ceras cuticulares de *E. g* induziu a expressão de genes que codificam proteínas relacionadas ao crescimento e colonização de *A. psidii*, como proteínas de ligação (*peptidylprolyl isomerase* e *ribosomal*) e proteínas de degradação da parede celular (*beta xilanase*). No entanto, outras proteínas patogênicas foram reprimidas na presença da cera cuticular de *E. g*, por exemplo, *triosephosphate isomerase, family 18 glycoside hydrolase, mitochondrial ATP carrier* e *glutamine-dependent NAD synthetase*. A análise de *E. ug* x MO resultou na ativação de proteínas associadas a transportadores e receptores de membrana, reparo de DNA e *glycine dehydrogenase*. Já a cera cuticular de *E. u* induziu a expressão de genes que codificam proteínas associadas a feromônios, cutinases e *prefoldin*. Pela primeira vez, está sendo apresentado a considerável variação interespecífica em espécies de *Eucalyptus* quanto à suscetibilidade a ferrugem, e, sua correlação com os compostos químicos de ceras cuticulares, os quais parecem ser um importante mecanismo de defesa pré-formado. Também foi revelado que as ceras cuticulares de *Eucalyptus* spp. são capazes de modular a expressão gênica de *A. psidii*, evidenciando o papel da interação molecular planta-patógeno precoce no desenvolvimento da ferrugem das mirtáceas.

Palavras-chave: Lipidômica, Transcriptoma, Fungo biotrófico, Mecanismo de defesa pré-formado

ABSTRACT

Deciphering the role of early molecular interactions between *Eucalyptus* spp. x *Austropuccinia psidii* and its pathogenesis

Austropuccinia psidii, the causal agent of myrtle rust, is a biotrophic pathogen, and therefore its growth and development depend on the host tissues. The uredospores of *A. psidii* infect *Eucalyptus* by engaging in close contact with the host surface and interacting with the leaf cuticle that provides important chemical and physical signals to trigger the infection process. Due to the inherent characteristics of the *Eucalyptus* cuticle, it was hypothesized that the preformed mechanism, comprised mostly by cuticular waxes, plays a crucial role in *Eucalyptus* resistance against *A. psidii* and its ability to modulate the expression of genes associated to the pathogenicity of *A. psidii* during the early stage of infection. In chapter 2, the cuticular waxes of *Eucalyptus* spp. were analyzed to determine their composition or structure and then correlated to susceptibility/resistance to *Austropuccinia psidii*. Twenty-one *Eucalyptus* spp. in the field were classified as resistant or susceptible. From these, the resistance/susceptibility level of six *Eucalyptus* spp. was evaluated in controlled conditions using qPCR, revealing that the pathogen can germinate on the eucalyptus surface of some species without multiplying in the host. CG-TOF-MS analysis detected 26 compounds in the *Eucalyptus* spp. cuticle and led to the discovery of the role of hexadecanoic acid in the susceptibility of *E. grandis* and *E. phaeotricha* to *A. psidii*. The scanning electron microscopy check revealed differences in *A. psidii* germination during host infection. It was found a correlation between epicuticular morphology and the resistance to *A. psidii*. In chapter 3, we investigated gene expression of *A. psidii* through bioassays *in vitro* containing cuticular waxes from *E. grandis* (*E. g*), *E. urograndis* (*E. ug*) and *E. urophylla* (*E. u*). Mineral oil (MO) treatment was used to all comparative analysis (negative control). The presence of cuticular waxes from *E. g* induced the expression of genes encoding proteins related to growth and colonization of *A. psidii* such as binding proteins (peptidylprolyl isomerase and ribosomal) and cell wall degrading proteins (beta-xylanase). However, other pathogenic proteins were repressed in presence of cuticular wax of *E. g*, for instance, triosephosphate isomerase, family 18 glycoside hydrolase, mitochondrial ATP carrier, and glutamine-dependent NAD synthetase. The *E. ug* x MO analysis resulted in DEGs associated with proteins related to membrane transporters and receptors, DNA repair and glycine dehydrogenase. As to the cuticular wax of *E. u*, it up-regulated the expression of genes encoding proteins associated with pheromone, cutinases, and prefoldin. Thus, for the first time, it was demostrated a considerable interspecific variation in *Eucalyptus* species on the susceptibility to *A. psidii* and its correlation with cuticular waxes chemical compounds that seem to play a synergistic role as a preformed defense mechanism. We also demonstrated that *Eucalyptus* spp. cuticular waxes may modulate the *A. psidii* gene expression, suggesting the importance of early plant-pathogen molecular interaction to the development of myrtle rust.

Keywords: Lipdomic, Transcriptome, Biotrophic fungal, Preformed defense mechanism

FIGURE LIST

THE *Eucalyptus* CUTICULAR WAXES CONTRIBUTE IN PREFORMED DEFENSE AGAINST *Austropuccinia psidii*

Figure 1. Infection process of *A. psidii* (MF1) in *Eucalyptus* spp. in controlled conditions. Legend: (a): 0 h.p.i. (hours post inoculation); (b): 72 h.p.i.; (c): 144 h.p.i.; (d): 336 h.p.i. Pustules in symptomatic leaves from *E. phaeotrica* and *E. grandis* and the hypersensitive response in *E. camaldulensis* and *E. robusta* leaves are indicated by black arrows where P: pustule and HR: hypersensitive response..... **32**

Figure 2. Metabolic profile from the cuticle waxes of susceptible (*E. grandis* and *E. phaeotricha*) and resistant (*E. camaldulensis, E. urophylla, E. robusta* and *E. urograndis*) *Eucalyptus* species against *A. psidii*. A) The Venn diagram shows the number of overlapping metabolites among the resistant (R) and susceptible (S) treatments. B) Principal component analysis (PCA) of the metabolic profile of cuticle *Eucalyptus* spp. in which susceptible species (*E. grandis* and *E. phaeotricha*) are represented by green and blue, respectively, and the resistant plants (*E. camaldulensis, E. urophylla, E. robusta* and *E. urograndis*) are shown in red, yellow, light blue and pink colors, respectively **33**

Figure 3. Abundance of metabolites present in the cuticle wax from susceptible (*E. grandis* and *E. phaeotricha*) and resistant (*E. urograndis, E. robusta, E. camaldulensis* and *E. urophylla*) *Eucalyptus* species. The data were submitted to an ANOVA followed by the Scott-Knott averages comparison test ($p < 0.05$) using the program Sisvar (v. 5. 6). Red color: indicates greater abundance of the metabolites between *Eucalyptus* spp.; orange color: less abundance of the metabolites between species, and the yellow color: indicates the absence of the metabolites in plants..... **34**

Figure 4. The germination rate of the *A. psidii* uredospores (MF1) at 24 h. p. i. A) Agar-water medium with or without cuticular extract from *Eucalyptus* species. B) Agar-water medium with palmitic acid (hexadecanoic acid). The data with equal letters did not differ statistically ($p < 0.05$) using the Scott-Knott (A) and Tukey (B) averages comparison test..... **35**

Figure 5. Leaf morphology (a-f) and scanning electron micrograph of the adaxial surface of the leaves of *Eucalyptus* species noninoculated (1-2) and inoculated (3) with *Austropuccinia psidii* at 144 h.a.i Epicuticular wax morphology: Group I - platelets; Group II – Wax sheet; Group III – Tubes or threads. (1) and (2) were observed using different magnifications (1100X and 3000X, respectively). CW: cuticular wax; ST: stomata; GT: germination tube; US: Uredospore. **36**

TRANSCRIPTOME ANALYSIS OF *Austropuccinia psidii* REVEALS THE ROLE OF CUTICULAR WAXES *Eucalyptus* spp. ON FUNGAL PATHOGEN GENE EXPRESSION

Figure 1. RNASeq bioassay to *A. psidii* uredospores germinated in cuticular waxes from *Eucalyptus* spp. with contrasting degree of resistance to pathogen (*E. grandis, E. urograndis* and *E. urophylla*) and mineral oil (negative control). **53**

Figure 2. Germination and differentiation of *A. psidii* uredospores (18 h.p.i) in agar-water medium containing dialysis membrane and cuticular waxes from of *Eucalyptus* spp. contrasting degree of resistance to pathogen (*E. grandis, E. urograndis* and *E. urophylla*) and mineral oil (control). Legend: gt- germ tube; us – uredospores; ap – appressorium. **57**

Figure 3. *A. psidii* DEGs in different cuticular waxes sources of *Eucalyptus* spp. Venn diagram (A and B): overlapping areas show the numbers of genes found to been congruently up/down regulated where A) total DEGs (known function, hypothetical function and uncharacterized/NA) and B) known

function DEGs. Heatmap (C): levels of expression are represented as Log2FC of TPM (transcripts per million) where dark blue indicates up-regulated and red signify down-regulated. **59**

Figure 4. GO enrichment analysis of DEGs from *A. psidii* uredospore according to the *E. grandis* x MO analysis. Only biological process terms were considered in the analysis. It was applied Fisher's Exact Test < 0.05. Legend: Nr reference: DEGs; Nr test: Genome. **60**

Figure 5. GO enrichment analysis of DEGs from *A. psidii* uredospore according to the *E. urograndis* x MO analysis. Only biological process terms were considered in the analysis. It was applied Fisher's Exact Test < 0.05. Legend: Nr reference: DEGs; Nr test: Genome. **61**

Figure 6. GO enrichment analysis of DEGs from *A. psidii* uredospore according to the *E. urophylla* x MO analysis. Only biological process terms were considered in the analysis. It was applied Fisher's Exact Test < 0.05. Legend: Nr reference: DEGs; Nr test: Genome. **61**

Figure 7. Relative gene expression of fourteen DEGs by RT-qPCR analysis. Relative gene expression was measured according to the Pfaffl method (PFAFFL, 2001). The statistical difference between the treatment (species) and the control (mineral oil) was calculated by the Pairwise Fixed Reallocation Randomization Test with bootstrap value = 1000. The significant comparison (specie x mineral oil) shows the symbol (*) at p <0.05. Error bars indicate standard error, n= 4. Four biological replicates including two technical replicates each were used for all samples in RT-qPCR analysis. Grey columns represent relative expression measured by RT-qPCR. Black columns represent corresponding RNASeq data. Legend: *E. g* x MO: 1- family 10 glycoside hydrolase; 2- Peptidylprolyl isomerase; 3- G2 mitotic-specific cyclin 1 2; 4- proline iminopeptidase; 5- aminotransferase; 6- pyruvate dehydrogenase kinase; 7- family 20 glycoside hydrolase. *E. ug* x MO: 8- proline iminopeptidase; 9- aminotransferase; 10- pyruvate dehydrogenase kinase. *E. u* x MO: 11- aminotransferase; 12- family 18 glycoside hydrolase; 13- carboxypeptidase C; and 14- pyruvate dehydrogenase kinase. **65**

Figure S1. Total RNA from *A. psidii* uredospores (18 h.p.i.) germinated in agar-water solid medium supplemented with different cuticular waxes. Gel source Agilent 2100 Bioanalyzer. Legend: R: biological replicates. The arrows indicate the typical ribosomal subunits of eukaryotes (28S and 18S rRNA) **69**

ADDITIONAL INFORMATION

Figure 1. Plots of the group comparison *E. g* x MO by Sleuth package (software R). Legend: a) Density x log mean tpm; b) Scatter x log counts; c) PCA (Principal Component Analysis); d) Mean variance **93**

Figure 2. Plots of the group comparison *E.u g* x MO by Sleuth package (software R). Legend: a) Density x log mean tpm; b) Scatter x log counts; c) PCA (Principal Component Analysis); d) Mean variance **96**

Figure 3. Plots of the group comparison *E. u* x MO by Sleuth package (software R). Legend: a) Density x log mean tpm; b) Scatter x log counts; c) PCA (Principal Component Analysis); d) Mean variance **98**

TABLE LIST

THE *EUCALYPTUS* CUTICULAR WAXES CONTRIBUTE IN PREFORMED DEFENSE AGAINST *AUSTROPUCCINIA PSIDII*

Table 1. Susceptibility level of *Eucalyptus* spp. to *A. psidii*.. **31**

Table 2. Quantification of *A. psidii* (MF1) during *Eucalyptus* spp. infection.. **32**

Table S1. The classification of twenty-six metabolites presents in cuticular wax *Eucalyptus* species according of The Human Metabolome Database. **41**

TRANSCRIPTOME ANALYSIS OF *Austropuccinia psidii* REVEALS THE ROLE OF CUTICULAR WAXES *Eucalyptus* spp. ON FUNGAL PATHOGEN GENE EXPRESSION

Table 1. List of primers used in the RT-qPCR. **56**

Table 2. *A. psidii* DEGs according to *Eucalyptus* spp. cuticular wax sources. **58**

Table 3. Top 20 DEGs from *A. psidii*, up/down regulated, with known function and annotated by Blast2GO. The comparative analyses were *E. g* x MO, *E. ug* x MO and *E. u* x MO. **63**

Table S1. Summary and alignment of paired-end reads with reference genome of *A. psidi*i by Kallisto software **70**

APPENDIX

Appendix A. GO terms of biological processes from *A. psidii* DEGs, up regulated and annotated by Blast2GO. The comparative analyses were: *E. g* x MO, *E. ug* x MO and *E. u* x MO. **99**

Appendix B. GO terms of biological processes from *A. psidii* DEGs, down regulated and annotades by Blast2GO. The comparative analyses were: *E. g* x MO, *E. ug* x MO and *E.u* x MO. **102**

Appendix C. Up-regulated DEGs from *A. psidii* annotated by Blast2GO. The comparative analyses were: *E. g* x MO, *E. ug* x MO and *E. u* x MO. **103**

Appendix D. Down-regulated DEGs from *A. psidii* annotated by Blast2GO. The comparative analyses were: *E. g* x MO, *E. ug* x MO and *E. u* x MO **106**

ABBREVIATION LIST

A. psidii	*Austropuccinia psidii* (G. Winter) Beenken
ID	Index disease
h. p. i.	Hours post inoculation
qPCR	Real-Time Quantitative PCR
GC-TOF-MS	Gas Chromatography coupled to Time-Of-Flight Mass Spectrometry
RNASeq	RNA sequencing
E. g	*Eucalyptus grandis*
E. ug	*Eucalyptus urograndis*
E. u	*Eucalyptus urophylla*
MO	Mineral oil
RT-qPCR	Reverse transcription - Quantitative PCR

1. INTRODUCTION

The planted forests are greatly important in ecosystems, they provide direct products, e.g. food, fuel and wood as well as environmental benefits such as including watershed protection, nutrient cycling, climate regulation, groundwater recharge, soil conservation, neutralization the negative effects of global warming and reduce the losses of natural forests. Moreover, planted forests have direct influence on economic, social and environmental development (Payn et al., 2015; Degroot et al., 2002; Laurance, 2007; Reddy et al., 2002).

It is estimated that between 1990 and 2010, the global area of planted forest increased by 7% up from 178 million hectares (ha) to 264 million ha (Jürgensen et al., 2014). A study conducted by FSC (Forest Stewardship Concil) showed that in 2012 roundwood production from planted forest was 520 millions m^3 and the forecast for 2050 will be 1082 million m^3, demonstrating great increase of the segment.

Concerning the planted forest areas, China has the largest cultivated area with forest (77.1 million ha – 29.3%), Brazil is in the eighth position (7.4 million ha – 2.6%). However, Brazil occupies the first position in the annual productivity, ranking to roundwood (131.878 million m^3). The largest producers (Brazil and United States) contributed with 43% of all produced timber, confirming the excellent management of planted forest in Brazil (Jürgensen et al., 2014; FAO, 2010).

Brazilian planted forests are composed by eucalyptus (76%), pinus (21%) and others (3%) (SNIF, 2016). Approximately 35% of the production is used as raw material to pulp and paper industries; 30% is composed by non-verticalized products; 13% to steel industry; 9% to TIMOs (Timber Investment Management Organizations); 6% to panel and flooring sectors; 4% of wood products and 3% others (IBGE, 2017). In 2014, the planted forestry sector was accountable for 1.1 % of total generated wealth in the country and 5.5 % of Gross Domestic Product. The international marketing of products from planted forests reached approximately US$ 8 billion, around 3% Brazilian exportation, as well as generation of 5 billion direct and indirect jobs (Virgens et al., 2016; IBÁ, 2015).

The *Eucalyptus* genus is originated from Australia and belongs to Family of Myrtaceae, which has more than 900 described species (Brooker, 2000; Boland et al., 2006). Several eucalyptus species have been used such as planted forests in Brazil, for instance: *E. grandis, E. saligna, E. camaldulensis, E. tereticornis, E. urophylla, E. cloeziana, E. citriodora, E. maculata, E. pellita, E. brassiana, E. dunni* and their several hybrids (Guimarães et al., 2010; Zauza et al., 2010). In Brazil, the expansion of planted forest is majorly due to the eucalyptus fast growth, high capacity of adaptation and production of wood of high quality. It is a consequence of continuous investments in research and development of genetic materials and improvement of sivicultural techniques (Ibá, 2015; Gonçalves et al., 2013).

The rise of planted forest sector is notable and shows the large growth potential for the next years. Nevertheless, the expansion of cultivated areas has favored the emergence of several diseases

that cause serious damage to the production of seedlings in clonal gardens and reforested areas, e.g. myrtle rust. Also, named eucalyptus rust, caused by *Austropuccinia psidii* (G. Winter) Beenken (Beenken, 2017).

A. psidii is a basidiomycete, previously known as *Puccinia psidii* Winter, the pathogen was newly redefined taxonomic position of Pucciniales family for Sphaerophragmiaceae family (Beenken, 2017). *A. psidii* is originated from South America. It was first described in Brazil by Winter in 1884 infecting guava (*Psidium guajava* L.) (Winter, 1884). Although the first recorded disease in *Eucalyptus* (*E. citriodora*) was in 1944, the first significant finding of economic damages in the crop occurred in 1973 in nurseries and plantations until eighteen months of age, in state of Espirito Santo (Joffily, 1944; Ferreira, 1983). Currently, *A. psidii* may be characterized as a cosmopolitan pathogen. It has been reported in different countries in America, including the Caribbean and Pacific Islands (Marlatt and Kimbrough, 1979; Coutinho et al., 1998; Uchida et al., 2006; Glen et al., 2007; Morin et al., 2012), Japan (Kawanishi et al., 2009), Australia (Carnegie et al., 2010), Africa (Roux et al., 2013) and China (Zhuang and Wei, 2011).

In 2000, a study was carried out and reported the areas with the highest risk of rust occurrence (*A. psidii*) in the Neotropical region. It was verified that Brazil has the largest region potentially affected by this phytopathogen (Booth et al., 2000). The researches conducted in seminal plantation of *E. grandis* in the state of Sao Paulo showed an incidence of rust in 35% of plants until 12 months of age, whose reduction was 35% in height and diameter of infected plants (Silveira and Higashi, 2003). These studies demonstrated the great epidemic potential of disease and the risk to productivity of eucalyptus planted forests as well to biodiversity. *A. psidii* can infect approximately 450 species, distributed in 73 genus of Myrtaceae, including *Eucalyptus*, *Corymbia, Eugenia* and *Melaleuca*, which demonstrates the serious global threat (Pegg et al., 2014; Carnegie and Cooper, 2011).

A. psidii attacks young, soft, actively-growing leaves, shoot tips and young stems. The presence of pathogen can be observed both in adult plants and in plantules in nursery stage (Ferreira, 1981). The first signs of rust infection are tiny spots or pustules loaded of yellow spores, characterizing the occurrence of disease (Ferreira, 1983). Symptoms can vary depending on the host species, susceptibility level within a host species, and age of the host leaf. In susceptible hosts, one-two weeks after infection, the attacked plant parts are atrophied and have areas with rust stains, in contrast in resistant hosts can occurs the hypersensitive response and the induction of cell death in plants (Ferreira, 1983; Glen et al., 2007).

The incidence and severity of disease depend on species, geographic region and time of year. *A. psidii* is very demanding as regards microclimate conditions and existence of juvenile organs (Abraf, 2013). Among *Eucalyptus* genus, the susceptible species are *E. grandis, E. cloeziana, E. phaeotricha, E. nitens* and *E. globulus*; and resistant: *E. pilularis, E. saligna, E. camaldulensis, E. urophylla, E. maculata, E. robusta, E. citriodora, E. tereticornis* and *E. torreliana* (Dianese et al., 1984; Ferreira, 1989, Santos et al. 2019).

The biotrophic pathogens such as *A. psidii* establishes intimate interactions with their hosts, whose success depends on the manipulation of host physiology (Eckardt, 2011). Concerning to *A. psidii*, little is known about genetic variability in pathogen populations and its correlation with the degree of host susceptibility (Quecine et al., 2014, Santos et al., 2019). Furthermore, there are no reports about the successful multiplication of uredospores in culture medium, hampering the molecular studies of this pathogen. This certainly contributes to the scarce number of studies related to genomic and transcriptomic of *A. psidii*, resulting in little knowledge about the genetics and pathogenicity mechanisms this fungus. Therefore, the understanding of *A. psidii* genetic approaches is critical for comprehension of host associations, especially in *Eucalyptus* plants, potential pathways of spread and climatic requirements, all of which facilitate the development of management strategies (Stewart et al., 2018).

The inter-intra specific genetic variability for resistance to rust in eucalyptus species allows the control of disease through clones, progenies and resistant species (Silva et al., 2014). However, the selection of resistant progenies from eucalyptus clones has been a challenge for forest industry and particular importance to eucalyptus breeding programs (Quecine et al., 2014). Little is known about the life cycle of *A. psidii*, which is essential to predict evolutionary potential and developing control strategies, as creation of durable host resistance or the removal of alternative hosts (Billiard et al., 2012; Mcdonald and Linde, 2002).

A. psidii has three known stages of life cycle: i) uredinial, mitotic and dicariotic stage used to differentiate other rust in mirtaceae; ii) telial stage – teliospores are diploid; and iii) basidial stage – basidiospores with one or two nuclei, its necessary for sexual reproduction (Maier et al., 2015; Morin et al., 2014). The optimum environmental conditions for development of spores in Brazil are 15-20ºC (uredospores), 21-25ºC (teliospores) and 21ºC (basidiospores) (Aparecido, 2001). There are many controversies related to *A. psidii* life cycle, however the life cycle proposed by Glen et al. (2007) is more accepted by the scientific community. These authors consider this fungal as autoecious and macrocyclic rust, i.e. this pathogen complete life cycle in just one host and there is no evidence of spermacia/spermagonia and aecia/aeciospore stages. *A. psidii* is pleomorphic because can development/alter several forms, according to the life cycle stage, reproduction and environmental conditions. There is no information concerning the basidia stage on another host except in fruits of *Syzygium jambos* (McTaggart et al., 2018). Until now, only uredospores have been described as infective agents and sporulation structure in *Eucalyptus* species (Morin et al., 2014).

In the patossystem *Eucalyptus* spp. x *A. psidii* the host tissues penetration occurs differently of most other rust caused by fungi of order Pucciniales, with direct penetration through the cuticle and epidermis, following after appressorium formation (Xavier et al., 2001). Thus, the leaf surface features can strongly influence the development of infection structures and directly contributing to increase resistance or susceptible some species (Bushnell, 1972).

Constitutive or inducible plant defense mechanisms may be either structural or biochemical. Chemical composition and thickness of cuticular wax as well as the presence of trichomes can affect the pre-penetration, penetration and colonization process configuring important plant preformed mechanisms of resistance to phytopathogens (Wynn and Staples, 1981). There are also mechanisms involved in plant resistance after the interaction of pathogen with the host, such as cell wall appositions, tylosis, phenolic compounds accumulation, abscission layer, induction of reactive oxygen species, activation of defense genes, hypersensitivity reactions and others (Boava et al., 2010).

Among the possible plant preformed defense mechanisms, the composition of cuticular wax vary considerably within species, ontogeny and environmental growth conditions (Jenks and Ashworth, 1999). Commonly, the outermost plant barrier is the epidermis that is covered by a lipophilic layer composed mainly of cutin, hydroxylated acids, esterified aliphatic acids, ferulic acid, flavonoids and phenylpropanoids (Albersheim et al., 2011; Yeats and Rose, 2013). The level of plant resistance should be related with leaf cuticular thicknesses, conformations and chemical composition. Moreover, cuticular waxes are one of the first barriers to fungal infection (Stockwell and Hanchey, 1983; Smith et al., 2006).

The cuticle is a limiting region for PAMPs and DAMPs signaling and the host resistance. The increase of thickness as well as alterations in cuticular topography are plant responses associated with the presence of pathogens (Serrano et al., 2014; Marques et al., 2016). Many studies have demonstrated the cuticular waxes effects on pathogen germination such as Santos et al. 2019, Zabka et al., 2014, Hansjakob et al., 2011, Zabka et al., 2007, Reisige et al., 2006, Inuyang et al., 1999 and Kolattukudy et al., 1995.

The development of molecular biology allowed the emergence of omics approaches as powerful analyses tools. The mass spectrometry and the next-generation sequencing, for instance, RNASeq, allowed a better understanding about the first contact between plant x fungal pathogen mediating the morphogenesis of fungal structures and preformed defense mechanisms in the target plant tissue surface (Padliya et al., 2007; Naidoo et al., 2018). Since no single approach can fully clear up the complexity of living organisms, each tool does contributes synergistically to a better knowledge of pathosystems (González-Fernández et al., 2010).

The mass spectrometry is a powerful analytical technique to identify and quantify a diversity of compounds, as instance lipids, due to the combination of sensibility, specificity and selectivity in a short time of analysis as well as being an effective tool for studies with fungal pathogens (Baldwin, 1995; Hopfgartner and Varesio, 2012). Thus, the lipidomic researches play a vital role in identification the biochemical mechanism condition of lipid-related disease progressions through categorizing the changes found in lipid composition (Koriem, 2017). In spite of all those advantages, it is incipient the lipidomic studies of plant x microbe interaction.

The emergence of RNASeq enabled of novel gene discovery and has provided insight into the exploration and understanding of gene expression, allowing in turn to accelerate the description of

complex biological machineries used by fungi, specially by phytophatogens (Janasz et al., 2018). The first study that used this technique was Velculescu et al. (1977), which analyzed the set of genes expressed from the model yeast during the fungal growth. The transcriptome analysis of 60.633 transcripts revealed 4665 genes, with expression levels varied, providing insight into global patterns of gene expression in yeast. Since then several studies with pathogen x plant interaction are been investigated such as Flor-Parra et al., (2006), López-Berges et al. (2010), Haddadi et al. (2015), Silva et al. (2017) among others.

Therefore, based on the scarcity of knowledge about the molecular mechanisms involved in the early interaction between *A. psidii* and *Eucalyptus* spp., this study aimed to analyze the lipid profile of the host and the transcriptomic of *A. psidii* modulated by cuticular wax from *Eucalyptus* spp. with different degree of susceptibility. Due to the inherent characteristics of the *Eucalyptus* cuticle, it was hypotheses that the preformed mechanism, comprised mostly by cuticular waxes, plays a crucial role in *Eucalyptus* resistance against *A. psidii* and it's able of modular the expression of genes associated to pathogenicity of *A. psidii* during the early stage of infection.

Thus, the specific objectives were to analyze the cuticular waxes composition and their structure of *Eucalyptus* spp. in relation with susceptibility/resistance to *A. psidii*. It was also evaluated the influence of cuticular wax from three *Eucalyptus* species (*E. grandis, E. urograndis* and *E. urophylla*) in *A. psidii* gene expression. In the chapter 2, it was demonstrated that *A. psidii* can germinate on *Eucalyptus* spp. surface of some species without multiplying in the host and revealed the role of hexadecanoic acid in the susceptibility of *E. grandis* and *E. phaeotricha* to *A. psidii*. It was provided the first report of considerable interspecific variation in *Eucalyptus* spp. on the susceptibility to *A. psidii* and its correlation with cuticular waxes chemical compounds, that seem to play a synergistic role as a preformed defense mechanism. Already, in the chapter 3, it was showed that the presence of cuticular wax from *E. g* induced the expression of genes encoding proteins related to growth and colonization of *A. psidii* such as binding proteins (peptidylprolyl isomerase and ribosomal) and cell wall degrading proteins (beta-xylanase). The *E. ug* x MO analysis resulted in DEGs associated to proteins related to membrane transporters and receptors, DNA repair and glycine dehydrogenase. The cuticular from *E.u* up-regulated the expression of genes econding proteins associated to pheromone, cutinases and prefoldin. To our knowledge, this is the first report proving that *Eucalyptus* spp. cuticular waxes may act as preformed defense mechanisms stimulating the fungal germination as well as modulating the *A. psidii* gene expression, suggesting the importance of early plant-pathogen molecular interaction to development of myrtle rust.

References

ABRAF, Anuário estatístico ABRAF (Associação Brasileira de Produtores de Florestas Plantadas). 2013. http://www.ipef.br/estatisticas/relatorios/anuario-abraf13-br.pdf (accessed: 02 august 2018).

Albersheim, P., Darvill, A., Roberts, K., Sederoff, R., Staehelin, A. 2011. Plant Cell Walls. New York, NY: Garland Science, Taylor and Francis Publishing Group.

Aparecido CC (2001). Ecological studies of *Puccinia psidii* Winter – Myrtaceae rust. Dissertation, School of São Paulo State University Julio de Mesquita Filho, Botucatu, Brazil.

Baldwin, M. A. 1995. Modern mass spectrometry in bioorganic analysis. Natural Product Reports, 12: 1: 33. doi:10.1039/np9951200033.

Beenken, L. 2017. *Austropuccinia*: A new genus name for the myrtle rust *Puccinia psidii* placed within the redefined family Sphaerophragmiaceae (Pucciniales). Phytotaxa, 297: 53–61. doi: 10.11646/phytotaxa.297.1.5.

Billiard, S., López-Villavivencio, M., Hood, M. E., Giraud, T. 2012. Sex, out crossing and mating types: unsolved questions in fungi and beyond. Journal of Evolutionary Biology, 25: 6: 1020-1038. doi: 10.1111/j.1420-9101.2012.02495.x.

Boland, D. J., Brooker, M. I. H., Chippendale, G. M., 2006. Forest Trees of Australia. CSIRO Publishing, Collingwood.

Booth, T. H., Old, K. M., Jovanovic, T. 2000. A preliminary assessment of high risk areas for *Puccinia psidii* (*Eucalyptus* rust) in the Neotropics and Australia. Agriculture, Ecosystems and Environment, 82: 295–301. doi: 10.1016/S0167-8809(00)00233-4.

Boava, L. P., Kuhn, O. J., Pascholati, S. F., Di Piero, R. M., Furtado, E. L. 2010. Atividade de quitinases e peroxidases em folhas de eucalipto em diferentes estágios de desenvolvimento após tratamento com acibenzolar-S-metil (ASM) e inoculação com Puccinia psidii. Tropical Plant Pathology, 35: 124–128. doi: 10.1590/S1982-56762010000200009.

Brooker, M. I. H. 2000. A new classification of the genus *Eucalyptus* L'Hér. (Myrtaceae). Australian Systematic Botany, 13: 79–148. doi: 10.1071/SB98008.

Bushnell, W. R. 1972. Physiology of fungal haustoria. Annual Review of Phytopathology, 10: 151–176. doi: 10.1146/annurev.py.10.090172.001055.

Carnegie, A. J., Lidbetter, J. R., Walker, J., Horwood, M. A., Tesoriero, L., Glen, M., Priest, M. 2010. *Uredo rangelii*, a taxon in the guava rust complex, newly recorded on Myrtaceae in Australia. Australasian Plant Pathology, 39: 463–466. doi: 10.1071/AP10102.

Carnegie, A. J., Cooper, K. 2011. Emergency response to the incursion of an exotic myrtaceous rust in Australia. Australasian Plant Pathology, 40: 4: 346-359. doi: 10.1007/s13313-011-0066-6.

Coutinho, T. A., Wingfield, M. J., Alfenas, A. C., Crous, P. W. 1998. *Eucalyptus* rust – a disease with the potential for serious international implications. Plant Disease, 82: 819–825. doi: 10.1094/PDIS.1998.82.7.819.

Degroot, R. S., Wilson, M. A., Boumans, R. M. J. 2002. A typology for the classification, description and valuation of ecosystem functions, goods and services. Ecological Economics, 41: 3: 393–408. doi: 10.1016/S0921-8009(02)00089-7.

Dianese, J. C. 1984. Response of Eucalyptus species to field infection by *Puccinia-psidii*. Plant Disease, 68: 314-316. doi: 10.1094/PD-69-314.

Eckardt, N. A. 2011. Interconnected metabolism of host plants and obligate biotrophic pathogens. The Plant Cell, 23: 2475. doi: 10.1105/tpc.111.230714.

FAO, Global Forest Resource Assessment. 2010. FAO Forestry Paper. http://www.fao.org/docrep/013/i1757e/i1757e.pdf (accessed 12 may 2018).

Ferreira, F. A. 1981. *Eucalyptus* rust – occurrence, temperature for the germination of urediniospores, the production of teliospores, alternative hosts and resistance. Fitopatologia Brasileira, 5: 603-604.

Ferreira, F. A. 1983. Ferrugem do eucalipto. Revista árvore, 7: 91-109.

Ferreira, F. A. 1989. Ferrugem do eucalipto. In: Patologia florestal - principais doenças florestais no Brasil. Sociedade de Investigações Florestais/Universidade Federal de Viçosa, 129-146.

Flor-Parra, I., Vranes, M., Kämper, J., Pèrez-Martin, J. 2006. Biz1, a Zinc Finger Protein Required for Plant Invasion by Ustilago maydis, Regulates the Levels of a Mitotic Cyclin. The Plant Cell, 18: 2369–2387. doi: 10.1105/tpc.106.042754.

FSC, Forest Stewardship Council (FSC). 2012. Strategic Review on the Future of Forest Plantations. http://www.fao.org/forestry/42701-090e8a9fd4969cb334b2ae7957d7b1505.pdf (accessed 12 may 2018).

Glen, M., Alfenas, A. C., Zauza, E. A. V., Wingfield, M. J., Mohammed, C. 2007. *Puccinia psidii*, a threat to the Australian environment and economy – a review. Australasian Plant Pathology, 36: 1–16. doi: 10.1071/AP06088.

Gonçalves, J. L. M., Alvares, C. A., Higa, A. R., Silva, L. D., Alfenas, A. C., Stahl, J., Ferraz, S. F. B., Lima, W. P., Brancalion, P. H. S., Hubner, A., Winter, G. 1884. Repertorium. Rabenhorst fungi europaei et extra-euraopaei. Centuria XXXI et XXXII. Hedwigia, 23: 164-175. doi: https://www.biodiversitylibrary.org/page/474236#page/188/mode/1up.

González-Fernández, R., Prats, E., Jorrín-Novo, J. 2010. Proteomics of plant pathogenic fungi. Jornal of Biomedicine and Biotechnology, 2010: 1-37. doi: 10.1155/2010/932527.

Guimarães, L. M. S., Titon, M., Lau, D., Rosse, L., Oliveira, L. S. S. , Rosado, C. C. G., Christo, G. G. O., Alfenas, A. C. 2010. *Eucalyptus pellita* as a source of resistance to rust, ceratocystis wilt and leaf blight. Crop Breeding and Applied Biotechnology, 10: 124-131. doi: 10.12702/1984-7033.v10n02a04

Haddadi, P., Ma, L., Wang, H., Borhan, M. H. 2015. Genome-wide transcriptomic analyses provide insights into the lifestyle transition and effector repertoire of Leptosphaeria maculans during the colonization of Brassica napus seedlings. Molecular Plant Pathology, 17: 8: 1196-1210. doi: 10.1111/mpp.12356.

Hansjakob, A., Riederer, M., Hildebrandt, U. 2011. Wax matters: absence of very-long-chain aldehydes from the leaf cuticular wax of the glossy11 mutant of maize compromises the pre penetration processes of Blumeria graminis. Plant Pathology, 60: 1151-1161. doi: 10.1111/j.1365-3059.2011.02467.x.

Hopfgartner, G., Varesio, E. 2012. The life sciences mass spectrometry research unit. Chimia, 66: 5: 335-8. doi: 10.2533/chimia.2012.335.

Horbach, R., Navarro-Quesada, A. R., Knogge, W., Deising, H. B. 2011. When and how to kill a plant cell: infection strategies of plant pathogenic fungi. Journal Plant Physiology, 168: 51–62. doi: 10.1016/j.jplph.2010.06.014.

IBÁ, Indústria Brasileira de Árvores. Relatório IBÁ 2015. 100 p. 2016. http://iba.org/images/shared/Biblioteca/IBA_RelatorioAnual2016_.pdf (accessed 13 may 2018).

Inuyang, E. N., Butt, T. M., Beckett, A., Archer, S. 1999. The effect of crucifer epicuticular waxes and leaf extracts on the germination and virulence of Metarhizium anisopliae conidia. Mycological Research, 103: 419-426. doi: 10.1017/S0953756298007333.

Janasz, G., Mazur, A., Wielbo, J., Koper, P., Zebracki, K., Pawlik, A., Ciolek, B., Paszczynski, A., Kubik-Komar, A. 2018. Comparative transcriptomic analysis of Cerrena unicolor revealed differencial expression of genes engaged in degradation of various kinds of wood. Microbiological Research, 207: 256-268. doi: 10.1016/j.micres.2017.12.007.

Jenks, M. A., Ashworth, E. N. 1999. Plant epicuticular waxes: function, production and genetics. Horticultural Reviews, 23: 1–68. doi: 10.1002/9780470650752.ch1.

Joffily, J. 1944. *Eucalyptus* Rust. Bragantia, 4: 475-487. doi: 10.1590/S0006-87051944000300001.

Jürgensen, C., Kollert, W., Lebedys, A. 2014. Assessment of industrial round wood production from planted forests. http://www.fao.org/3/a-i3384e.pdf (accessed 13 may 2018).

Kawanishi, T., Uemastu, S., Kakishima, M., Kagiwada, S., Hamamoto, H., Horie, H., Namba, S. 2009. First report of rust disease on ohia and the causal fungus, *Puccinia psidii*, in Japan. Journal of General Plant Pathology, 75: 428–431. doi: 10.1007/s10327-009-0202-0.

Kolattukudy PE, Rogers LM, Li DX, Hwang CS, Flaishman MA. 1995. Surface signaling in pathogenesis. Proceedings of the National Academy of Sciences 92: 4080–4087.

Koriem, K. M. M. 2017. A lipidomic concept in infectious diseases. Asian Pacific Journal of Tropical Biomedicine, 7: 3: 265-274. doi: 10.1016/j.apjtb.2016.12.010.

Kubicek, C. P., Trevor, L. S., Glass, N. L. 2014. Plant cell wall-degrading enzymes and their secretion in plant-pathogenic fungi. Annual Review of Phytopathology, 52: 427-451. doi: 10.1146/annurev-phyto-102313-045831.

Laurance, W. F. 2007. Environmental science: forests and floods. Nature, 449: 7161: 409–410. doi: 10.1038/449409a.

Leite, T. F., Moon, D. H., Lima, A. C. M., Labate, C. A., Tanaka, F. A. O. 2013. A simple protocol for whole leaf preparation to investigate the interaction between *Puccinia psidii* and *Eucalyptus grandis*. Australasian Plant Pathology, 42: 79-84. doi: 10.1007/s13313-012-0179-6.

López-Berges, M. S., Rispail, N., Prados-Rosales, R. C., Di Pietro, A. 2010. A Nitrogen Response Pathway Regulates Virulence Functions in Fusarium oxysporum via the Protein Kinase TOR and the bZIP Protein MeaB. Plant Cell, 22: 7: 2459-75. doi: 10.1105/tpc.110.075937.

Maier, W., McTaggart, A. R., Roux, J., Wingfield, M. J. 2015. *Phakopsora myrtacearum* sp. nov., a newly described rust (Pucciniales) on eucalypts in eastern and southern Africa. Plant Pathology, 65: 189–195. doi: 10.1111/ppa.12406.

Marlatt, R. B., Kimbrough, J. W. 1980. *Puccinia psidii* on Pimenta dioica in south Florida. Plant Disease Reporter, 63: 6: 510-512.

Marques JPR, Amorim L, Spósito MB, Appezzato-da-Glória B. 2016. Ultrastructural changes in the epidermis of petals of the sweet orange infected by Colletotrichum acutatum. Protoplasma 253: 5: 1233-42.

McDonald, B. A., Linde, C. 2002. Pathogen population genetics, evolutionary potential and durable resistance. Annual Review Phytopathology, 40: 349-379. doi: 10.1146/annurev.phyto.40.120501.101443.

McTaggart, A. R., Shuey, L. S., Granados, G., M., Du Plessis, E., Fraser, S., Naidoo, S., Wingfield, M., J., Roux, J. 2018. Evidence that *Austropuccinia pdisii* may complete its sexual life cycle on Myrtaceae. Plant Pathology, 67: 3: 729-734. doi: 10.1111/ppa.12763.

Morin, L., Aveyard, R., Lidbetter, J. R., Wilson, P. G. 2012. Investigating the host-range of the rust fungus *Puccinia psidii* sensu lato across tribes of the family Myrtaceae present in Australia. Plos One, 7: 4: 1-7. doi: 10.1371/journal.pone.0035434.

Morin, L., Talbot, M. J., Glen, M. 2014. Quest to elucidate the life cycle of *Puccinia psidii* sensu lato. Fungal Biology, 118: 253–263. doi: 10.1016/j.funbio.2013.12.004.

Naidoo, S., Visser, E. A., Zwart, L., Toit, Y. du, Bhadauria, V., Shuey, L. S. 2018. Dual RNA-seq to elucidate the plant-pathogen duel. Current Issues in Molecular Biology, 27: 127-141. doi: 0.21775/cimb.027.127.

Padliya, N. D., Garrett, W. M., Campbell, K. B., Tabb, D. L., Cooper, B. 2007. Tandem mass spectrometry for the detection of plant pathogenic fungi and the effects of database composition on protein inferences. Proteomics, 7: 21: 3932-42. doi: 10.1002/pmic.200700419.

Payn, T., Carnus, J. M., Freer-Smith, P., Kimberley, M., Kollert, W., Liu, S., Orazio, C., Rodriguez, L., Silva, L. N., Wingfield, M. J. 2015. Changes in planted forests and future global implications. Forest Ecology and Management, 352: 57-67. doi: 10.1016/j.foreco.2015.06.021.

Pegg, G. S., Giblin, F. R., McTaggart, A. R., Guymer, G. P., Taylor, H., Irelenad, K. B., Shivas, R. G., Perry, S. 2014. *Puccinia psidii* in Queensland, Australia: disease symptoms, distribution and impact. Plant Pathology, 63: 1005-1021. doi: 10.1111/ppa.12173.

Potts, B. M., Karanjeet, S. S., Wardlaw, T., Freeman, J., Li, H., Tilyard, P., Park, R. F. 2016. Evolutionary history shapes the susceptibility of an island tree flora to an exotic pathogen. Forest Ecology and Management, 368: 183-193. doi: 10.1016/j.foreco.2016.02.027.

Quecine, M. C., Bini, A. P., Romagnoli, E. R., Andreote, F. D., Moon, D. H., Labate, C. A. 2014. Genetic variability in *Puccinia psidii* populations as revealed by PCR-DGGE and T-RFLP markers. Plant disease, 98: 1: 16- 23. doi: 10.1094/PDIS-03-13-0332-RE.

Quecine, M. C., Leite, T. F., Bini, A. P., Regiani, T., Franceschini, L. M., Budzinski, I. G. F., Marques, F. G., Labate, M. T. V., Guidetti-GonzaleZ, S., Moon, D. H., Labate, C. A. 2016. Label-free quantitative proteomic analysis of *Puccinia psidii* uredospores reveals differences of fungal populations infecting eucalyptus and guava. Plos One, 11: 1: 1-19. doi: 10.1371/journal.pone.0145343.

Reddy, K. N., Jadhav, S. N., Reddy, C. S., Raju, V. S. 2002. Life forms and biological spectrum of Marriguda Reserve forest Khammam district, Andhra Pradesh. Indian Forester, 128: 7: 751-756.

Reisige, K., Gorzelanny, C., Daniels, U., Moerschbacher, B. M. 2006. The C28 aldehyde octacosanal is a morphogenetically active component involved in host plant recognition and infection structure differentiation in the wheat stem rust fungus. Physiological and Molecular Plant Pathology, 68: 33–40. doi: 10.1016/j.pmpp.2006.05.006.

Roux, J., Greyling, I., Coutinho, T. A., Verleur, M., Wingfield, M. J. 2013. The Myrtle rust pathogen, *Puccinia psidii*, discovered in Africa. International Mycological Association Fungus, 4: 1: 155-159. doi: 10.5598/imafungus.2013.04.01.14.

Santos, I. B., Lopes, M. S., Bini, A. P., Tschoeke, B. A. P., Verssani, B. A. W., Figueredo, E. F., Cataldi, T. R., Marques, J. P. R., Silva, L. D., Labate, C. A., Quecine, M. C. 2019. The Eucalyptus cuticular waxes contribute in preformed defense against Austropuccinia psidii. Frontiers in Plant Science, 9: 1-13. doi: 10.3389/fpls.2018.01978.

Serrano, M., Coluccia, F., Torres, M., L'Haridon, F., Metraux, J. P. 2014. The cuticle and plant defense to pathogens. Frontiers in Plant Science, 5: 274. doi: 10.3389/fpls.2014.00274.

Silva, R. R., Silva, A. C., Rodella, R. A., Serrão, J. E., Zanuncio, J. C., Furtado, E. L. 2017. Pre-infection stages of Austropuccinia psidii in the epidermis of Eucalyptus hybrid leaves with diferente resistance levels. Forests, 8: 362. doi:10.3390/f8100362.

Silva, D. E. M., Azevedo, L. A. S., Poltronieri, T. P. S. 2014. Avaliação da resistência de espécies de eucalipto à ferrugem (*Puccinia psidii* Winter). Summa Phytopathology, 40: 1: 54-62. doi: 10.1590/S0100-54052014000100008.

Silveira, R. L. V. A., Higashi, E. N. 2003. Aspectos nutricionais envolvidos na ocorrência de doenças com ênfase para o eucalipto. Circular Técnica, Instituto de Pesquisa e Estudos Florestais, 200: 1-13.

Smith, A. H., Pinkard, E. A., Hunter, G. C., Wingfield, M. J., Mohammed, C. L. 2006. Anotamical variation and defence responses of juvenile Eucalyptus nitens leaves to Mycophaerella leaf disease. Australasian Plant Pathology, 35: 725-731. doi: 10.1071/AP06070.

SNIF, Sistema Nacional de Informações Florestais. BOLETIM SNIF 2016. 7 p. 2016. http://www.florestal.gov.br/documentos/publicacoes/2231-boletim-snif-recursos-florestais-2016/file (accessed 30 march 2019).

Stewart, J. E., Ross-Davis, A. L., Graça, R. N., Alfenas, A. C., Peever, T. L., Hanna, J. W., Uchida, J. Y, Hauff, R. S., Kadooka, C. Y., Kim, M. S., Cannon, P. G., Namba, S., Simeto, S., Pérez, C. A., Rayamajhi, M. B., Lodge, D. J., Arquedas, M., Medel-Ortiz, R., Lópes-Ramirez, M. A., Tennant, P., Glen, M., Machado, P. S., McTaggart, A. R., Carnegie, A. J., Klopfenstein, N. B. 2018. Genetic diversity of the myrtle rust pathogen (Austropuccinia psidii) in the Americas and Hawaii: Global implications for invasive threat assessments. Forest Pathology, 48: 1: 1-13. doi: 10.1111/efp.12378.

Stockwell, V., Hanchey, P. 1983. The role of the cuticle in resistance of beans to Rhizoctonia solani. Phytopathology, 74: 1640-1642.

Uchida, J., Zhong, S., Killgore, E. 2006. First report of a rust disease on Ohia caused by *Puccinia psidii* in Hawaii. Plant Disease, 90: 4: 524. doi: 10.1094/PD-90-0524C.

Van der Does, H. C., Rep, M. 2007. Virulence genes and the evolution of host specificity in plant-pathogenic fungi. Molecular Plant-Microbe Interactions, 20: 1175–82. doi: 10.1094/MPMI-20-10-1175.

Velculescu, V. E., Zhang, L., Zhou, W., Vogeistein, J., Basrai, M. A., Bassett, D. E., Hieter, P., Vogeistein, B., Kinzier, K. W. 1997. Charaterization of the Yeast transcriptome.Cell, 88: 2: 243-251. doi: 10.1016/S0092-8674(00)81845-0.

Virgens, A., FreitaS, L., Leite, A. 2016. Economic and sensitivity analysis in a settlement established in Southwestern Bahia. Floresta e Ambiente, 23: 2: 211-219. doi: 10.1590/2179-8087.104914.

Wynn, W.R, Staples, R.C. 1981. Tropism of fungi in host recognition. In: Staples, R. C, Toenniessen GH (eds) Plant disease control: resistance and susceptibility. Wiley Interscience, 45–69.

Winter, G. 1884. Repertorium. Rabenhorstii fungi europaei et extraeuraopaei. Cent. XXXI et XXXII. Hedwigia 23:164–172.

Xavier, A. A., Alfenas, A. C., Matsuoka, K., & Hodges, C. S. 2001. Infection of resistant and susceptible *Eucalyptus grandis* genotypes by urediniospores of *Puccinia psidii*. Australasian Plant Pathology, 30: 277-281. doi: 10.1071/AP01038.

Yeats, T. H., Rose, J. K. C. 2013. The formation and function of plant cuticles. Plant Physiology, 163: 5-20. doi: 10.1104/pp.113.222737.

Zabka, M., Pavela, R., Prokinova, E. 2014. Antifungal activity and chemical composition of twenty essential oils against significant indoor and outdoor toxigenic and aeroallergenic fungi. Chemosphere, 112: 443-448. doi: 10.1016/j.chemosphere.2014.05.014.

Zabka, V., Stangl, M., Bringmann, G., Vogg, G., Riederer, M., Fildebrandt, U. 2007. Host surface properties affect pre penetration processes in the barley powdery mildew fungus. New Phytologist, 177: 251-263. doi: 10.1111/j.1469-8137.2007.02233.x.

Zauza, E. A. V., Alfenas, A. C., Old, K., Couto, M. M. F., Graça, R. N., Maffia, L. A. 2010. Myrtaceae species resistance to rust caused by Puccinia psidii. Australasian Plant Pathology, 39: 406-411. doi: 10.1071/AP10077.

Zhuang, J. Y., Wei, S. X. 2011. Additional materials for the rust flora of Hainan Province, China. Mycosystema, 30: 853–860.

2. THE *Eucalyptus* CUTICULAR WAXES CONTRIBUTE IN PREFORMED DEFENSE AGAINST *Austropuccinia psidii*

Abstract

Austropuccinia psidii, the causal agent of myrtle rust, is a biotrophic pathogen whose growth and development depends on the host tissues. The uredospores of *A. psidii* infect *Eucalyptus* by engaging in close contact with the host surface and interacting with the leaf cuticle that provides important chemical and physical signals to trigger the infection process. In this study, the cuticular waxes of *Eucalyptus* spp. were analyzed to determine their composition or structure and correlation with susceptibility/resistance to *Austropuccinia psidii*. Twenty-one *Eucalyptus* spp. in the field were classified as resistant or susceptible. The resistance/susceptibility level of six *Eucalyptus* spp. were validated in controlled conditions using qPCR, revealing that the pathogen can germinate on the eucalyptus surface of some species without multiplying in the host. CG-TOF-MS analysis detected 26 compounds in the *Eucalyptus* spp. cuticle and led to the discovery of the role of hexadecanoic acid in the susceptibility of *E. grandis* and *E. phaeotricha* to *A. psidii*. We characterized the epicuticular wax morphology of the six previously selected *Eucalyptus* spp. using scanning electron microscopy and observed different behavior in *A. psidii* germination during host infection. It was found a correlation of epicuticular morphology on the resistance to *A. psidii*. However, in this study, we provide the first report of considerable interspecific variation in *Eucalyptus* spp. on the susceptibility to *A. psidii* and its correlation with cuticular waxes chemical compounds that seem to play a synergistic role as a preformed defense mechanism.

Keywords: GC-TOF-MS; Preformed defense; Rust; Susceptibility

Introduction

Austropuccinia psidii (G. Winter) Beenken (syn. *Puccinia psidii*) is a basidiomycete that belongs to the Pucciniales order and is the causal agent of myrtle rust (Beenken, 2017; Miranda et al., 2013). The pathogen infects approximately 460 species in 73 genera of the Myrtaceae (Beenken, 2017; Giblin and Carnegie, 2014; Roux et al., 2016). Its hosts include *Eucalyptus* spp. that are important to the forestry industry (Coutinho et al., 1998). Different degrees of severity are observed in *Eucalyptus*, and the disease occurs primarily in young trees and infects actively growing leaves, shoots, inflorescences and apical buds (Glen et al., 2007). The disease is characterized by the production of yellow and pulverulent pustules containing the uredospores that cause the deformation of the leaves, intense defoliation of the branches, stunted growth and even the death of the plants (Ferreira, 1981). Despite the importance of myrtle rust, the mechanisms of resistance of *Eucalyptus* spp. to *A. psidii* remain unclear. The host penetration by rust pathogens occurs preferentially through stomata; however, *A. psidii* penetrates inner *Eucalyptus* tissues through the cuticle and epidermis following the formation of appressoria (Xavier et al., 2001).

Leaf cuticular waxes cover all the aerial plant surfaces and have a multifunctional role, serving as an interface between the plant and biotic or abiotic stresses; its composition includes a polymeric

skeleton of cutin covalently attached to a type of lipid known as waxes (Kock et al., 2010; Yeats and Rose, 2013). Plant cuticles are known to be primary barriers against herbivores and pathogens that perform a key factor in the adaptation and evolution of terrestrial plants and that the cutin monomers released are signaling molecules for both the pathogens and plants (Serrano et al., 2014; Tucker et al., 2010). Leaf surface cuticles have been described to be a source of signals that influence the germination and specificity of the host to biotrophic pathogens (Lazniewska et al., 2012). Thus, the effect of cuticular waxes on pathogen germination has been examined by several authors (Hansjakob et al., 2011; Inuyang et al., 1999; Kolattukudy et al., 1995; Reisige et al., 2006; Zabka et al., 2007; Zabka et al., 2014). These extracts obtained from the leaf surface can induce up to 50% germination and appressorium production by pathogenic fungi (Reisige et al., 2006). A long-chain hydrocarbon with a 436 MW ($C_{31}H_{64}$) known as hentriacontane was characterized from an active fraction of *Syzygium jambos* leaf wax extract. The active fraction induced up to 88% of uredospore germination and was determined to be involved with the stimulation of rust uredospore germination (Tessmann and Dianese, 2002).

Due to the unique characteristics of the *Eucalyptus* cuticle, our hypothesis supports the concept that the preformed mechanism plays an important role in *Eucalyptus* resistance. Thus, we selected *Eucalyptus* spp. with varying responses to rust myrtle infection in the field and validated the results in controlled conditions. The leaf cuticular wax composition of the six eucalyptus species was characterized using gas chromatography coupled to mass spectrometry (GC-TOF-MS). We also assessed the uredospores germination rate of *A. psidii* exposed to cuticular waxes and specific metabolites identified in susceptible and resistant *Eucalyptus* spp. The morphology of the *Eucalyptus* spp. cuticle was observed using electron microscopy. The polyphasic analysis of the leaf cuticle greatly contributed to a better understanding of the dynamics of the early infection process of *A. psidii* on *Eucalyptus* spp.

Materials and Methods

Susceptibility of *Eucalyptus* spp. to *Austropuccinia psidii*: field inference

Natural *Eucalyptus* infection by *A. psidii* was evaluated in young trees up to two years old. The trees were located at the Anhembi Experimental Station of Forestry Sciences (EECFA), Anhembi, São Paulo, Brazil (22°40'S and 48°10'W). The disease scores representing the percentage of leaves with rust symptoms were based on the Takahashi scale (2002) modified by Zamprogno et al. (2008): S0 (no pustules or healthy plants); S1 (isolated punctate pustules on the limbs and young leaves); S2 (rust pustules generally sparse or occasionally abundant on the limbs and young leaves), and S3 (pustules abundant on the limbs, petioles and leaves, at the tips of branches and the primary stem and apical necrosis). The index disease (ID) was calculated as described by McKinney (1923). The

experiment was a randomized design with 21 genotypes (nineteen species and two hybrids) and 72 biological replicates per genotype. Each replicate consisted of one tree.

After the field assessment, species with enough plantlets to further assays: susceptible (*E. grandis* and *E. phaeotricha*) and resistant (*E. urophylla, E. camaldulensis, E. urograndis* and *E. robusta*) were selected to validate the data in controlled conditions as described by Leite et al. (2013) with modifications (Quecine et al., 2016). Plantlets of each species were grown under greenhouse conditions for 120 days and transferred to a controlled growth chamber under a 12 h photoperiod (200 µmol m-1 s-1) at 20°C for acclimatization for seven days. A suspension of *A. psidii* MF-1 containing 10^5 uredospores mL^{-1} and 0.05% Tween 20 was sprayed onto the plants. The plants were enclosed in transparent plastic bags for the first 48 h with the first 24h in complete darkness at 20°C to enable the fungus to germinate. The plants were returned to the growth conditions previously described. The symptoms were assessed in the third to 14th day after inoculation based on the scale adapted from Zamprogno et al. (2008). The experiment was conducted in a completely randomized design.

A. psidii quantification by qPCR in contrasting *Eucalyptus* species

The leaves from *E. grandis, E. phaeotricha, E. urophylla, E. camaldulensis, E. urograndis* and *E. robusta* were harvested at: 0 hour post inoculation (h.p.i) (control treatment); 72 h.p.i (start of the colonization phase – susceptible species, and no detection of the pathogen – resistant species); 144 h.p.i: colonization of mesophyll cells (susceptible species) and no detection of the pathogen (resistant species); and 336 h.p.i: pustules developed (susceptible species) and no detection of the pathogen (resistant species) based on an assay previously described (Bini et al., 2018). At each time, leaves from the first two pairs of five plantlets per species were collected, immediately frozen in liquid nitrogen and stored at -80ºC. Leaves of the control plants were collected at 0 h.p.i. The DNA was extracted from 100 mg of leaves using a DNeasy Plant Mini Kit (Qiagen) according to the manufacturer's instructions.

The qPCR (Real-Time Quantitative PCR) reaction was performed using an iCycleiQ Real-Time PCR Detection System (BioRad) in a final volume of 25 µL. The *A. psidii* genomic DNA quantification in the *Eucalyptus* spp. leaves was based on an IGS region described by Bini et al. (2018). The *A. psidii* MF-1 DNA serial dilution was performed in triplicate, and the time-course assay samples were generated in duplicates of all five biological replicates per sampled time.

Eucalyptus spp. cuticular wax extraction

Cuticular wax from the young branches (first pair of leaves) of *E. grandis, E. phaeotricha, E. urophylla, E. camaldulensis, E. urograndis* and *E. robusta* was extracted as described by Viana et al. (2010) modified by Bini (2016). One milligram of wax was obtained by immersing and gentle agitating the leaves in 5 mL of chloroform (JT Baker) for 30 s and vacuum concentration (SpeedVac-

Eppendorf) for 20 min. Each replicate consisted of 6-8 young leaves from one plantlet. Four plantlets were used for each species.

Chemical characterization of *Eucalyptus* spp. cuticular waxes using CG-TOF-MS

The GC-TOF-MS (Gas Chromatography coupled to Time-Of-Flight Mass Spectrometry) analysis was performed immediately after the wax extraction. The samples were derivatized as described by Hoffman et al. (2010) with 30 µL of methoxyamine hydrochloride (15 mg mL^{-1}) in pyridine for 16 h at room temperature in the dark. The samples were trimethylsilylated by adding 30 µL of N-methyl-N-(trimethylsilyl) trifluoroacetamide (MSTFA) containing 1% trimethylchlorosilane (TMCS) and incubating the mixture at room temperature for 1 h. Thirty microliters of heptane was added after silylation. Stable isotope reference compounds [1 mg mL^{-1}each of ($^{13}C_3$) - myristic acid, ($^{13}C_4$) - palmitic acid and ($^{2}H_4$) - succinic acid] were added to the samples prior to derivatization and used as external standards for quality control. The derivatized samples were analyzed as described by Gullberg et al. (2004). Blank control samples and a series of n-alkanes (C12–C40) were also used to obtain the retention indices (Schauer et al., 2005).

One microliter of each derivatized sample was injected splitless into a gas chromatograph 7890A (Agilent Technologies, Santa Clara, USA) coupled with a Comb-xt Autosampler (Leap Technologies, Carrboro, USA). The injector temperature was 280 °C; the septum purge flow rate was 20 mL min^{-1}, and the purge was turned on after 60 s. The gas flow rate through the column was 1 mL min^{-1}. The column used for the GCxGC separation was a DB-5 (20 m × 0.18 mm × 0.18 µm; Agilent Technologies, Santa Clara, USA) as the first-dimension column and a RTX-17 (0.9 m × 0.10 mm × 0.10 µm; Restek Corporation, U.S., Bellefonte) for the second-dimension column. The column temperature was held at 80°C for 2 min, increased by 10°C min^{-1} to 305°C and held for 10 min. The column effluent was introduced into the ion source of a GC×GC/TOFMS (Pegasus 4D, Leco Corp., St. Joseph, USA). The transfer line and the ion source temperatures were 280 and 250°C, respectively. The ions were generated using a 70 eV electron beam at an ionization current of 2.0 mA, and 10 spectra/s were recorded in the mass range m/z 45 to 800.

ChromaTOF software v. 4.51 (Leco Corp., St. Joseph, USA) was used to correct the baseline and export all the MS files into a NetCDF format. Peak detection, retention time alignment and library matching were performed using the Target Search package (Cuadros-Inostroza et al., 2009). Metabolites were identified by comparing their retention indexes (±2 s) and spectra (similarity > 600) against the compounds stored in the Golm-Metabolome-Database (http://csbdb.mpimp-golm.mpg.de/csbdb/gmd/gmd.html) (Kopka et al., 2005). Metabolite intensities were normalized using dry weight and total ion chromatogram (TIC).

Influence of cuticular wax on *A. psidii* germination

The cuticular waxes from *E. grandis, E. phaeotricha, E. urophylla, E. camaldulensis, E. urograndis* and *E. robusta* were obtained as described above. One milligram of extracted waxes was diluted in 1 mL of dichloromethane (JT Baker) to remove chloroform residues and vacuum concentrated (SpeedVac-Eppendorf). The waxes were solubilized in 1 mL of dichloromethane (JT Baker) and sonicated for 10 min. This final solution was used in the germination assay. The uredospore solution of *A. psidii* MF-1 was prepared separately in mineral oil (Sigma Aldrich) (10^5 uredospores per Petri dish), which was mixed with 20 ppm of the cuticle extracts (Tessmann and Dianese, 2002). The uredospore solution was inoculated in Petri dishes containing solid water agar medium (8 g L^{-1}) amended with mineral oil and cuticle extracts and incubated for 24 h at 20ºC in the dark. Five hundred uredospores were observed for each treatment per replicate, and the germination rate was calculated based on the number of uredospores with a germ tube. The experiment was conducted in three randomized blocks. Water, mineral oil and dichloromethane were considered to be the controls. Uredospore germination was observed using a light microscope (Aziophot) with a digital coupled camera (Zeiss).

Hexadecanoic acid effects on *A. psidii* germination

To validate the results obtained using GC-TOF-MS, a bioassay was performed using commercial palmitic acid (hexadecanoic acid) (Sigma Aldrich) and a uredospore solution of *A. psidii* MF-1 (10^5 per Petri dish) diluted in mineral oil (Sigma Aldrich). The palmitic acid was diluted in dichloromethane (JT Baker) at concentrations of 0 (control), 0.5, 2.5, 5.0, 10 and 20 ppm and combined with the solution of uredospores before inoculation in Petri dishes with solid water agar medium (8 g L^{-1}) and incubation for 24 h at 20ºC in the dark. Germination rates were obtained as described above. The experiment was conducted in a randomized block design with six hexadecanoic acid concentrations using three replicates (Petri dishes) per treatment.

Scanning electron microscopy

We examined the morphology of the epicuticle wax morphology by evaluating the middle third adaxial leaf surface of non-inoculated and inoculated (144 h.p.i.) plantlets of *E. grandis, E. phaeotricha, E. urophylla, E. camaldulensis, E. urograndis* and *E. robusta*. The leaves were sampled and fixed in Karnovsky solutions (Karnovsky, 1965), washed in 0.1 M phosphate buffer and post fixed in 1% osmium tetroxide in 0.1 M phosphate buffer (pH 7.2). The samples were washed three times in distilled water and then dehydrated in graded acetones (10% 1x, 30% 1x, 50% 1x, 70% 1x, 90% 1x, 100% 2x, for 15 min each). All these steps were performed at room temperature. The samples were dried to their critical point (Horridge and Tamm, 1969), glued on aluminum stubs and sputter coated with gold. The samples were examined at 20 kV using an LEO VP435 (Zeiss, Oberkochen, Germany) scanning electron microscope.

Statistical analysis

Fungal quantification qPCR data were analysed for significance ($p < 0.05$) according to Tukey's test. The profile of the metabolites from the cuticular waxes was submitted to multivariate analysis to visualize the separation among the Eucalyptus spp. using the program Metaboanalyst (http://www.metaboanalyst.ca/). Principal component analysis (PCA) was also utilized to identify the tendency of group separation, and an ANOVA (Analysis of variance) was used to identify differentially abundant metabolites among the groups ($p <0.05$), followed by a comparison test of Scott-Knott averages ($p <0.05$) (Chong et al., 2018). The results of the germination rate of *A. psidii* in different cuticular waxes and hexadecanoic acid concentrations were submitted to an analysis of variance (ANOVA), followed by Scott-Knott's and Tukey tests ($p < 0.05$) using software R (version 3.4.1), respectively.

Results

Evaluation of the *Eucalyptus* spp. rust susceptibility

Among the 19 species and two hybrids evaluated in the field, just two species were classified as S0 - high level of resistance to the pathogen (*E. resinifera* and *E. toreliana x E. citriodora* – *E. toreliodora*); four species were classified as susceptible to *A. psidii*, i.e., more than 50% of the individuals were categorized in the S1, S2 and S3 scale (*E. botryoides, E. deglupta, E. grandis* and *E. phaeotricha*) with IDs ranging from 40.51% to 56.30%. Other species demonstrated a low level of resistance, and more than 50% of the individuals were asymptomatic to rust (ID: 0.64% – 18.65%) (Table 1).

Table 1. Susceptibility level of *Eucalyptus* spp. to *A. psidii* in field conditions.

Species	Susceptibility Scale (%) [a]				Classification [b]	ID (%) [c]
	S0	S1	S2	S3		
E. botryoides	44.44	20.83	26.39	8.33	Susceptible	45.65
E. brassiana	91.67	1.39	2.78	4.17	Low resistance	9.00
E. camaldulensis	70.83	19.44	8.33	1.39	Low resistance	18.65
E. cloeziana	75.00	11.11	12.50	1.39	Low resistance	18.65
E. deglupta	34.72	19.44	34.72	11.11	Susceptible	56.58
E. dunni	72.22	20.83	5.56	1.39	Low resistance	16.72
E. exserta	98.61	1.39	0.00	0.00	Low resistance	0.64
E. grandis	47.22	25.00	20.83	6.94	Susceptible	40.51
E. microcorys	83.33	12.50	2.78	1.39	Low resistance	10.29
E. paniculata	91.67	5.56	1.39	1.39	Low resistance	5.79
E. pellita	93.06	2.78	2.78	1.39	Low resistance	5.79
E. phaeotricha	45.83	26.39	4.17	23.61	Susceptible	48.87
E. pilularis	75.00	19.44	1.39	4.17	Low resistance	16.08
E. propínqua	94.44	2.78	1.39	1.39	Low resistance	4.50
E. resinifera	100.00	0.00	0.00	0.00	High resistance	0.00
E. robusta	97.22	0.00	0.00	2.78	Low resistance	3.86
E. saligna	65.28	31.94	2.78	0.00	Low resistance	17.36
E. tereticornis	87.50	6.94	4.17	1.39	Low resistance	9.00
E. toreliana x E. citriodora (E. toreliodora)	100.00	0.00	0.00	0.00	High resistance	0.00
E. urophylla x E. grandis (E. urograndis)	83.33	11.11	5.56	0.00	Low resistance	10.29
E. urophylla	93.06	4.17	1.39	1.39	Low resistance	5.14

[a] Susceptibility scale adapted from Zamprogno et al. (2008): S0: hypersensitive and /or immune response; S1 to S3: detection of pustules with different sporulation intensities. The experiment was a randomized design with 21 genotypes (19 species and two hybrids) and 72 replicates.
[b] Susceptible: the total susceptibility scale of S1, S2 and S3 is greater than 50%; low resistance: the total susceptibility scale of S0 is greater than 50%, and high resistance: the total susceptibility scale of S0 is the same as 100%.
[c] ID: Disease index was calculated as described by McKinney (1923).

The susceptible/resistance level of the *Eucalyptus* spp. against *A. psidii* was validated in controlled condition: *E. urophylla, E. camaldulensis, E. robusta* and *E. urograndis* were classified as S0, i.e., resistant to *A. psidii* in these conditions with a hypersensitive response in *E. camaldulensis* and *E. robusta* at 336 h.p.i. The susceptibility of *E. grandis* and *E. phaeotricha* was confirmed by visualization of the typical symptoms of rust: chlorotic stains which turned into pustules, resulting in a mass of uredospores. The symptoms on the *E. phaeotricha* leaves occurred earlier compared to those on *E. grandis* (Figure 1).

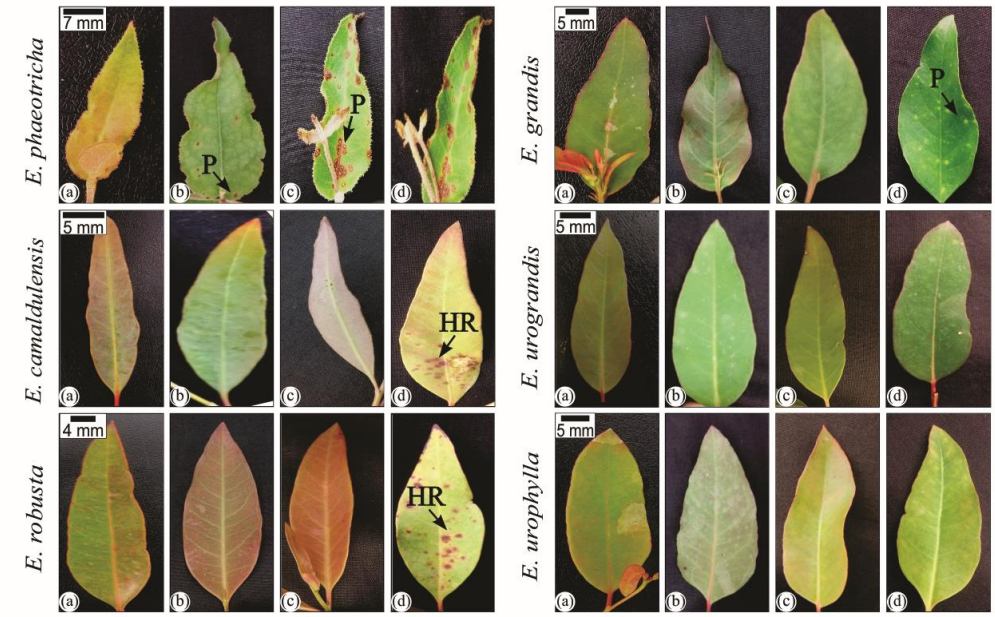

Figure 1. Infection process of *A. psidii* (MF1) in *Eucalyptus* spp. in controlled conditions. Legend: (a): 0 h.p.i. (hours post inoculation); (b): 72 h.p.i.; (c): 144 h.p.i.; (d): 336 h.p.i. Pustules in symptomatic leaves from *E. phaeotrica* and *E. grandis* and the hypersensitive response in *E. camaldulensis* and *E. robusta* leaves are indicated by black arrows where P: pustule and HR: hypersensitive response.

The infection was also monitored over time by the temporal quantification of *A. psidii* in the leaf tissues of *E. grandis, E. phaeotricha, E. urophylla, E. camaldulensis, E. urograndis* and *E. robusta* using qPCR. *A. psidii* was not detected in non-inoculated control samples. The pathogen was detected up to 72 h.p.i in all the species inoculated with *A. psidii* uredospores ranging between 0.04 (*E. camaldulensis*) to 0.95 pg (*E. phaeotricha*). Non-pathogenicity was detected at 144 and 336 h.p.i. in the resistant species (*E. urophylla, E. camaldulensis, E. urograndis* and *E. robusta*) (Table 2).

Table 2. Absolute quantification of *A. psidii* (MF1) during *Eucalyptus* spp. infection.

Species	***A. psidii* quantification (DNA pg)***			
	0 h.p.i	**72 h.p.i**	**144 h.p.i**	**336 h.p.i**
E. grandis	0.21 (± 0.09)^{b}	0.28 (± 0.16)^{b}	0.58 (± 0.42)^{b}	2.71 (± 1.31)^{a}
E. phaeotricha	0.42 (± 0.09)^{c}	0.95 (± 0.41)^{c}	6.75 (± 3.43)^{b}	11.8 (± 6.53)^{a}
E. urograndis	0.51 (± 0.12)^{a}	0.14 (± 0.08)^{b}	0,00 (± 0.00)^{c}	0,00 (± 0.00)^{c}
E. urophylla	0.05 (± 0.04)^{b}	0.29 (± 0.13)^{a}	0,00 (± 0.00)^{c}	0,00 (± 0.00)^{c}
E. robusta	0.20 (± 0.13)^{a}	0.04 (± 0.04)^{a}	0,00 (± 0.00)^{b}	0,00 (± 0.00)^{b}
E. camaldulensis	0.04 (± 0.04)^{b}	0.21 (± 0.12)^{a}	0,00 (± 0.00)^{c}	0,00 (± 0.00)^{c}

* *A. psidii* (MF1) quantification in *Eucalyptus* spp. was measured in pg of the pathogen DNA present in 5 µg of total DNA from infected leaves. The average of five biological replicates was determined at each sampling time; values between the parentheses represent the standard error. Values with the same letter within a line are not significantly ($p < 0.05$) different according to Tukey's test.

***Eucalyptus* spp. cuticle wax characterization**

GC-TOF-MS analysis enabled the identification of 26 metabolites present in the cuticular waxes from the *Eucalyptus* spp. Two metabolites of the 26 compounds were only identified in the susceptible species of *Eucalyptus*, and 6 were exclusive to resistant Eucalyptus species (Figure 2A). The total metabolites obtained from the cuticular waxes were submitted to multivariate analysis to visualize the separation among the treatments in relation to the metabolic content. The PCA revealed a clear tendency of the clustering among susceptible (*E. grandis* and *E. phaeotricha*) and resistant (*E. camaldulensis, E. urograndis, E. robusta* and *E. urophylla*) species. The sum of the first two principal components explained 54.8% of the total variance (Figure 2B).

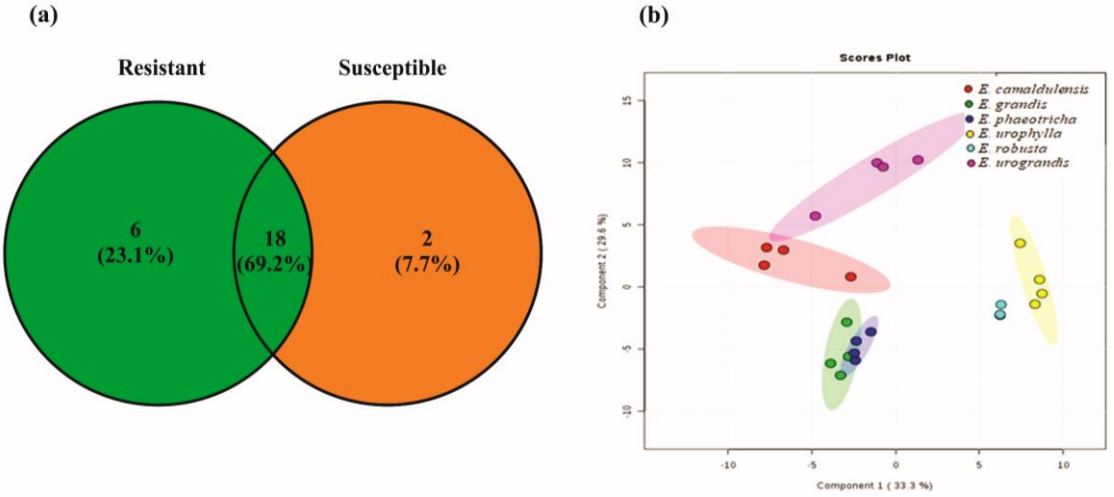

Figure 2. Metabolic profile from the cuticle waxes of susceptible (*E. grandis* and *E. phaeotricha*) and resistant (*E. camaldulensis, E. urophylla, E. robusta* and *E. urograndis*) *Eucalyptus* species against *A. psidii*. A) The Venn diagram shows the number of overlapping metabolites among the resistant (R) and susceptible (S) treatments. B) Principal component analysis (PCA) of the metabolic profile of cuticle *Eucalyptus* spp. in which susceptible species (*E. grandis* and *E. phaeotricha*) are represented by green and blue, respectively, and the resistant plants (*E. camaldulensis, E. urophylla, E. robusta* and *E. urograndis*) are shown in red, yellow, light blue and pink colors, respectively.

The cuticular wax compounds were classified as fatty acyls (38%), alkanes (23%), steroids (12%), organooxygen compounds (11%), hydrocarbons (4%), keto acids (4%), carboxylic acids (4%) and cinnamic acids (4%). Twenty-three compounds identified in this study have been previously described to be components of plant cuticular waxes (Table S1). The heat map obtained shows that among the identified metabolites previously described as cuticular wax compounds, hexadecanoic acid is present only in *E. grandis* and *E. phaeotricha* and absent in the resistant species (Figure 3).

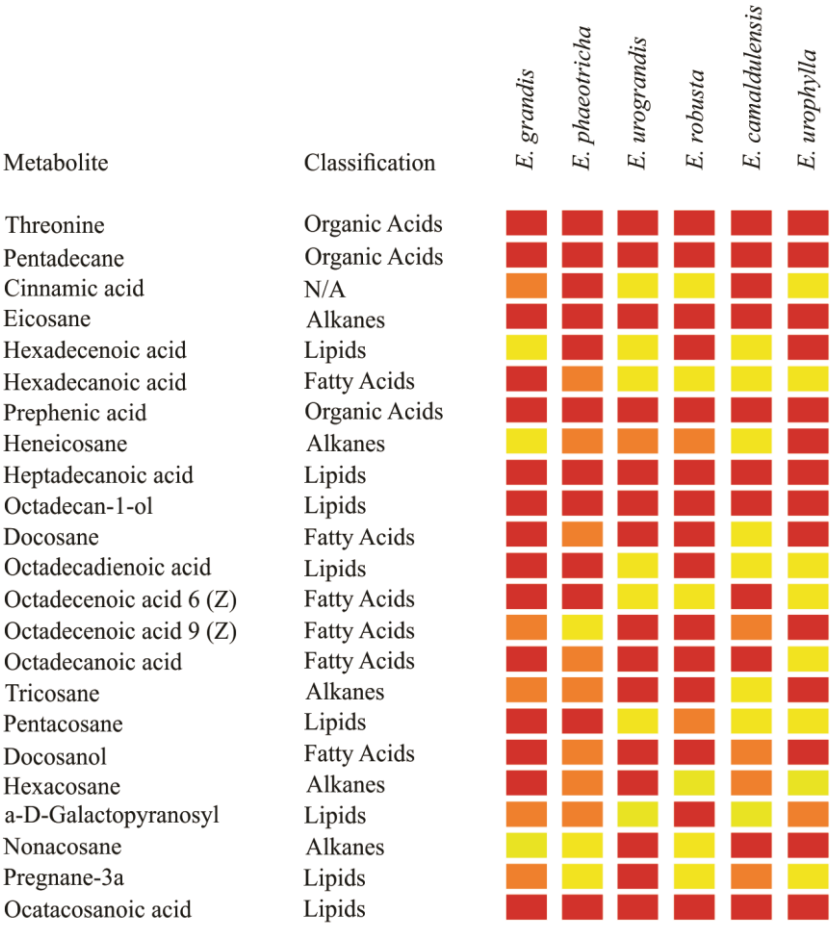

Figure 3. Abundance of metabolites present in the cuticle wax from susceptible (*E. grandis* and *E. phaeotricha*) and resistant (*E. urograndis, E. robusta, E. camaldulensis* and *E. urophylla*) *Eucalyptus* species. The data were submitted to an ANOVA followed by the Scott-Knott averages comparison test ($p < 0.05$) using the program Sisvar (v. 5. 6). Red color: indicates greater abundance of the metabolites between *Eucalyptus* spp.; orange color: less abundance of the metabolites between species, and the yellow color: indicates the absence of the metabolites in plants.

Germination rate of *A. psidii* in cuticle extracts and hexadecanoic acid

The germination rate of *A. psidii* was significantly higher in the media supplemented with 20 ppm cuticle extract of *E. grandis* (44.06%) followed by E. urograndis (16.26%). With the exception of *E. grandis*, the addition of cuticular wax from *Eucalyptus* spp. did not seem to influence the germination rates of the uredospores compared to mineral oil. Non-significant germination was observed using only the solvent dichloromethane and water (Figure 4A). To confirm the ability of hexadecanoic acid to induce germination, the germination rate of *A. psidii* was determined at 24 h. p. i. we observed the highest germination rate of 8% using 5.0 ppm hexadecanoic acid. The data showed a polynomial curve from 0 - 20 ppm. The lowest rate of 1.46% was observed in the absence of hexadecanoic acid (Figure 4B).

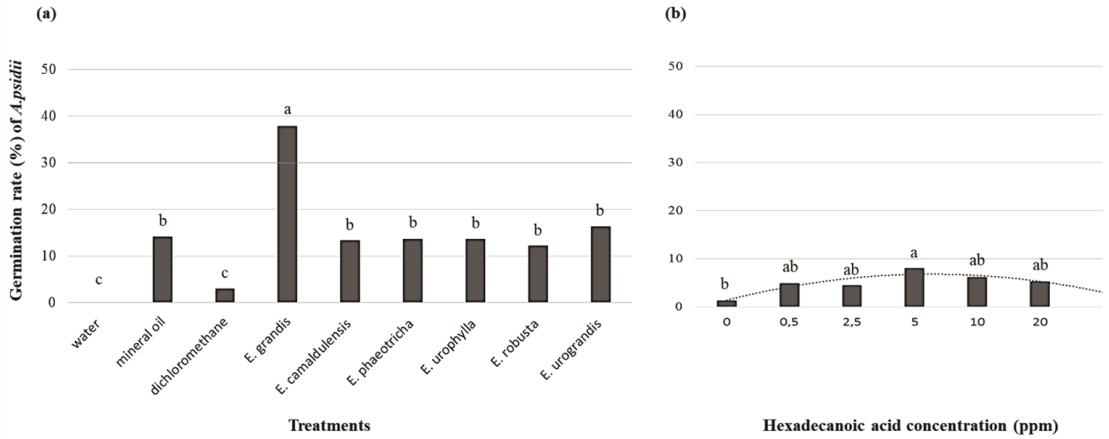

Figure 4. The germination rate of the *A. psidii* uredospores (MF1) at 24 h. p. i. A) Agar-water medium with or without cuticular extract from *Eucalyptus* species. B) Agar-water medium with palmitic acid (hexadecanoic acid). The data with equal letters did not differ statistically ($p < 0.05$) using the Scott-Knott (A) and Tukey (B) averages comparison test.

Epicuticular wax morphology and *A. psidii* germination *in vivo*

It was possible to group the six *Eucalyptus* spp. into three different groups based on the epicuticular wax morphology: Group I is comprised of species that contain parallel platelets wax crystals and include *E. grandis, E. urograndis*, and *E. robusta* and *E. urophylla* (Figure 5A – 5D). Group II includes *E. phaeotricha* in which the wax crystals are absent, and the cuticle presents a smooth surface comprised of a thin wax film that can be folded in some regions (Figure 5E). Group III includes *E. camaldulensis* and exhibits epicuticular wax distributed as tubes or threads (Figure 5F). Another difference among them is that only *E. phaeotricha* possess a pubescent leaf covered by non-glandular trichomes (data not shown).

There are some differences in the members of Group 1 in the orientation and size of the platelets. *E. grandis* and *E. urograndis* possess epicuticular wax crystals of different sizes (Figure 5A1-2, B1-2). The large wax crystals are primarily located on the epidermis anticlinal walls, while the smaller ones are on the periclinal walls. In *E. robusta*, the majority of the wax plates was parallel and arranged perpendicularly to the proximodistal leaf axis (Figure 5D1-2). *E. urophylla* possesses parallel wax plates, but they seem to be distributed in a different direction (Figure 5C1-2).

We found germinated uredospores in all species at 24 h.p.i (data not shown). In the susceptible species *E. grandis* and *E. phaeotricha*, germ tubes were observed at144 h.p.i. along with the possible presence of a degraded cuticle represented by grooves (Figure 5A3). Pustules and a substantial amount of trichomes were only observed in *E. phaeotricha* (Figure 5E3). In *E. urograndis*, described as a low resistance species, we also observed germinated uredospores (Figure 5B3). However, the germination was visually higher than the germinated uredospores found in *E. urophylla* and *E. camaldulensis* (Figure 5C3-F3). Non-germinated uredospores were found in *E. robusta* (Figure 5D3).

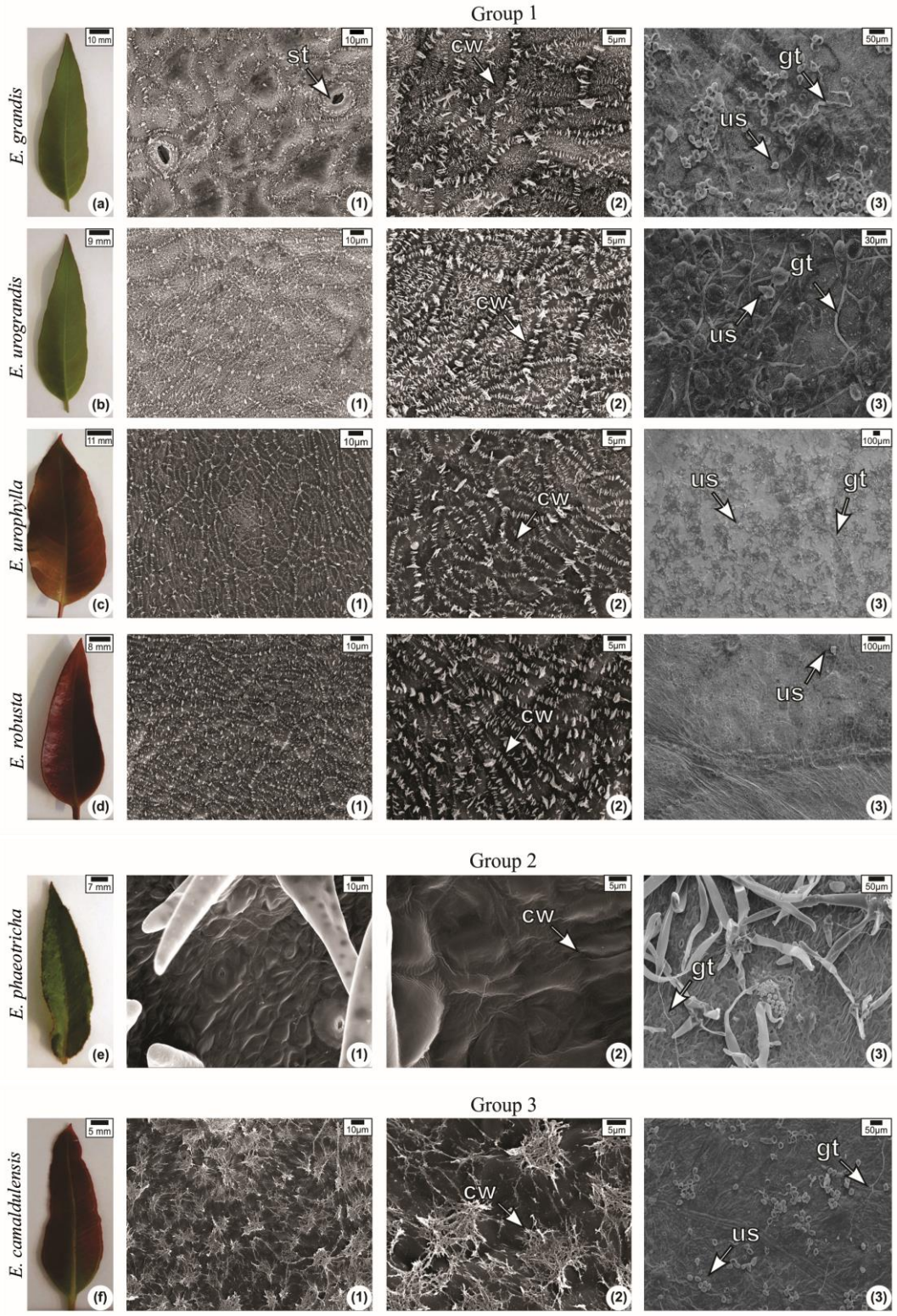

Figure 5. Leaf morphology (a-f) and scanning electron micrograph of the adaxial surface of the leaves of *Eucalyptus* species noninoculated (1-2) and inoculated (3) with *Austropuccinia psidii* at 144 h.a.i Epicuticular wax morphology: Group I - platelets; Group II – Wax sheet; Group III – Tubes or threads. (1) and (2) were observed using different magnifications (1100X and 3000X, respectively). CW: cuticular wax; ST: stomata; GT: germination tube; US: Uredospore.

Discussion

The susceptibility level to *A. psidii* and the ID of *Eucalyptus* spp. revealed high variability among the species, as well as individuals within the same species. The susceptibility and resistance levels found in *E. grandis, E .cloeziana, E. microcorys, E. robusta, E. tereticornis, E. urograndis, E. saligna* and *E. urophylla* have been reported previously (Carnegie and Lidbetter, 2012; Carvalho et al., 1998; Silva et al., 2014; Zauza et al., 2010). However, we observed low resistance in *E. cloeziana, E. dunii* and *E. microcorys* that had been previously described as species susceptible to *A. psidii* (Carnegie and Lidbetter, 2012; Dianese et al., 1984; Kawanishi et al., 2009; Silva et al., 2014; Zauza et al., 2010). Our research is the first report that describes the susceptibility of *E. botryoides* and *E. deglupta* to rust, as well as the resistance of *E. brassiana, E. exserta* and *E. toreliodora* to the disease.

The variability within the *Eucalyptus* species has resulted in a controversial susceptibility classification of *A. psidii*, which could be explained by the high level of allogamy found in *Eucalyptus*. The pathogen *A. psidii* has also been described to possess a wide genetic variability (Quecine et al., 2014). In addition, it is known that the incidence and severity of the disease varies among genotypes within the same species, geographic region and time of the year (Alfenas et al., 2004), demonstrating the importance of the genotype–environment interaction on myrtle rust studies.

In controlled conditions, we validated the data obtained in the field. The assay demonstrated the ability of the uredospores from *E. grandis* to infect the susceptible species *E. phaeotrica*. In addition, the symptoms of the disease were visualized early in *E. phaeotrica* when compared to *E. grandis*. At 336 h.p.i., *E. camaldulensis* and *E. robusta* showed a hypersensitive response, which was not observed in *E. urophylla* and *E. urograndis*. The different defense responses exhibited in the species evaluated against *A. psidii* reflect the enormous complexity in the plant responses. The SYBR Green-based qPCR assay was used for the first time to detect *A. psidii* on six different *Eucalyptus* species in initial infection times, validating the sensitivity of the set IGS7/IGS9 primers used to quantify the rust pathogen in *E. grandis* (Bini et al., 2018).

The qPCR corroborated the field results. Temporal monitoring of *A. psidii* showed its presence in a very low abundance until 72 h.p.i in all the species, independently of their susceptibly level. After 72 h.p.i., *A. psidii* was found only in *E. grandis* and *E. phaeotricha* (susceptible species). Our data is consistent with that of Xavier et al. (2001) and Leite (2012). The authors compared the *A. psidii* infection process in two contrasting genotypes of *E. grandis* and verified that fungal germination, appressoria formation and penetration occur within 12 h.p.i., independent of the genotype. The defense response starts in the resistant species at 24 h.p.i. After 72 h.p.i, is not possible to detect the pathogen in the resistant hosts, while in the susceptible plants, a succession of events occurs, including mesophyll colonization, development and sporulation pustules. The success of the *A. psidii* x *Eucalyptus* interaction is primarily defined in the first stage of infection, and the preformed mechanisms probably play an important role in resistance. Further, the qPCR assay to quantify *A. psidii* should be proceeding with other *Eucalyptus* species.

GC-TOF-MS identified 26 compounds from the cuticular waxes of *Eucalyptus* leaves. Twenty-three compounds were plant specific, belonging to different classes, such as fatty acyls, alkanes, steroids and hydrocarbon carboxylic acids. Commonly, the compounds of cuticular waxes are derived from very long chain fatty acids (VLCFA), including alkanes, alcohols, and sterols as found in this study (Racovita et al., 2015). The fatty acids in the cuticles of plants and insects have significant effects on spore germination and fungal differentiation, and may be toxic, fungistatic and stimulatory for some pathogenic species. For example, Golebiowski et al. (2008) obtained the profiles of cuticular fatty acids of three species (*Calliphora vicina, Dendrolimus pini* and *Galleria mellonella*) in relation to the susceptibility to infection caused by *Conidiobolus coronatus*. The species resistant to *C. vicina* had a different lipid profile compared to the susceptible species *D. pini* and *G. mellonella*. The exclusive presence of three fatty acids in the cuticle of the resistant genotype could inhibit fungal growth and reduce the production of conidia. Our data revealed differences in the lipid profile among *Eucalyptus* spp. resistant and susceptible to *A. psidii* in a manner consistent with these results.

We found a specific fatty acid, hexadecanoid acid, in susceptible E. grandis and *E. phaeotricha* that improved the uredospore germination rates of *A. psidii*. The role of this compound in the biosynthesis of cuticular wax is highly diverse. Hexadecanoic acid participates in the biosynthetic pathways of fatty acids, cutin, suberin, wax, unsaturated fatty acids and secondary metabolites from plants and contributes to the elongation and degradation of fatty acids (Kanehisa and Goto, 2000).

Unexpectedly, only the cuticle waxes from *E. grandis* stimulated the germination of *A. psidii* uredospores, and the germination rate in *E. phaeotricha* did not differ from the control. Our data is supported by other research, such as that of Song-Jiang et al. (2014) who used cuticular waxes from pingguoli pear to stimulate the germination and mycelial growth of *Alternaria alternata*. Another study showed that an epicuticular wax extract of wheat leaf (*Triticum compactum* L.) had an active component capable of inducing up to 50% the formation of the germ tube, appressorium, substomatal vesicle and penetrating hyphae of *Puccinia graminis* f.sp. tritici (Reisige et al., 2006). These data enhance the importance of cuticular wax as physical and chemical signaling patterns in the recognition of the host by the pathogen.

Tessmann and Dianese (2002) observed that a long-chain hydrocarbon with 436 MW (C31H64), hentriacontane, obtained from *Syzygium jambos* leaf wax extract could induce uredospore germination up to 88% in *A. psidii*. We observed that the effect of hexadecanoic acid on the *A. psidii* germination rate was lower than in the media supplemented with *Eucalyptus* cuticular waxes. However, our data confirm the influence of hexadecanoic acid on the susceptibility of *Eucalyptus* spp. to the pathogen *A. psidii* and suggest a complex *A. psidii* x *Eucalyptus* spp. interaction related to probable physical and chemical signaling.

Our data also revealed global differences in the lipid profile between *Eucalyptus* spp. resistant and susceptible to *A. psidii*, and not only the chemical profile of possible preformed mechanism related to resistance in *Eucalyptus* spp. was evaluated. It was possible to assemble *Eucalyptus* spp. in

three groups based on their epicuticular wax morphologies. In the 1970s, Hallam and Chamber undertook a large study to characterize the wax morphology from a survey of 315 *Eucalyptus* species and classified them in groups. These authors found that *E. camaldulensis* has the most plastic epicuticular wax. In this study, we observed that *E. camaldulensis* has tubes or threads-shaped epicuticular wax that resemble the *E. globulus* wax pattern (Steinbauer et al., 2009), but this was differed from the observations of Guzmán et al. (2014) who described the epicuticular wax arrangements as plates with different orientations. Previous studies demonstrated that topography is important for the formation of appressoria (Read et al., 1992; Marques et al., 2013). We believed in a correlation of epicuticular morphology as a determining factor to *Eucalyptus* susceptibility or resistance. However, this characteristic is better related with the cuticular wax chemical composition. It is clear that *A. psidii* infects species with different cuticular morphologies suggesting that the morphology it is not the key factor for susceptibility.

Conclusions

Eucalyptus spp. has more than one mechanism (preformed and induced resistance) responsible for their resistance against *A. psidii*. The cuticular chemical composition is strongly related to the susceptibility of *E. grandis* and *E. phaeotricha*. However, our data suggest that there are many cuticular signals that act at different stages of fungal infection, uredospore germination, appressorium formation, invasion and survival on the eucalyptus leaves, corroborating the hypothesis that the Eucalyptus spp. resistance to *A. psidii* is related to synergistic preformed and induced resistance mechanisms that should be studied in more detail.

Funding

This study was supported by the Fundação de Amparo à Pesquisa do Estado de São Paulo - FAPESP (Grant 2014/16804-4). We also thank the FAPESP for its fellowship awards to A.P.B. (2013/07596-6), E.F.F. (2017/11026-1) and J.P.R.M. (2012/25315-1). We thank Coordenação de Aperfeiçoamento de Pessoal de Nível Superior (CAPES) for their fellowship awards to I.B.S., M.S.L., B.A.P.T. and B.A.W.V.

Acknowledgments

We thank Dr. Beatriz Appezato da Glória (ESALQ/USP, Brazil) for providing the structure for the epicuticular morphology analysis. The authors also thank Dr. Elliot Watanabe Kitajima from NAP/MEPA (ESALQ/USP, Brazil) for support with the SEM analysis.

Supplementary Material

frontiers in Plant Science

ORIGINAL RESEARCH
published: 09 January 2019
doi: 10.3389/fpls.2018.01978

The *Eucalyptus* Cuticular Waxes Contribute in Preformed Defense Against *Austropuccinia psidii*

*Isaneli Batista dos Santos[1], Mariana da Silva Lopes[1], Andressa Peres Bini[1], Bruno Augusto Profmann Tischoeke[1], Bruna Aparecida Wruck Verssani[2], Everthon Fernandes Figueredo[1], Thais Regiani Cataldi[3], João Paulo Rodrigues Marques[3], Luciana Duque Silva[4], Carlos Alberto Labate[1] and Maria Carolina Quecine[1]**

[1] Departament of Genetics, "Luiz de Queiroz" College of Agriculture, University of São Paulo, Piracicaba, Brazil, [2] Departament of Exact Sciences, "Luiz de Queiroz" College of Agriculture, University of São Paulo, Piracicaba, Brazil, [3] Departament of Phytopathology, "Luiz de Queiroz" College of Agriculture, University of São Paulo, Piracicaba, Brazil, [4] Departament of Forest Science, "Luiz de Queiroz" College of Agriculture, University of São Paulo, Piracicaba, Brazil*

OPEN ACCESS

Edited by:
Jens Staal,
Ghent University, Belgium

Reviewed by:
Walter Gassmann,
University of Missouri, United States
Fei Gao,
University of Missouri, United States

***Correspondence:**
Maria Carolina Quecine
mquecine@usp.br

Specialty section:
This article was submitted to Plant Microbe Interactions, a section of the journal Frontiers in Plant Science

Received: 26 September 2018
Accepted: 19 December 2018
Published: 09 January 2019

Citation:
Santos IB, Lopes MdS, Bini AP, Tischoeke BAP, Verssani BAW, Figueredo EF, Cataldi TR, Marques JPR, Silva LD, Labate CA and Quecine MC (2019) The *Eucalyptus* Cuticular Waxes Contribute in Preformed Defense Against Austropuccinia psidii. *Front. Plant Sci.* 9:1978. doi: 10.3389/fpls.2018.01978

Austropuccinia psidii, the causal agent of myrtle rust, is a biotrophic pathogen whose growth and development depends on the host tissues. The uredospores of *A. psidii* infect *Eucalyptus* by engaging in close contact with the host surface and interacting with the leaf cuticle that provides important chemical and physical signals to trigger the infection process. In this study, the cuticular waxes of *Eucalyptus* spp. were analyzed to determine their composition or structure and correlation with susceptibility/resistance to *A. psidii*. Twenty-one *Eucalyptus* spp. in the field were classified as resistant or susceptible. The resistance/susceptibility level of six *Eucalyptus* spp. were validated in controlled conditions using qPCR, revealing that the pathogen can germinate on the eucalyptus surface of some species without multiplying in the host. CG-TOF-MS analysis detected 26 compounds in the *Eucalyptus* spp. cuticle and led to the discovery of the role of hexadecanoic acid in the susceptibility of *Eucalyptus grandis* and *Eucalyptus phaeotricha* to *A. psidii*. We characterized the epicuticular wax morphology of the six previously selected *Eucalyptus* spp. using scanning electron microscopy and observed different behavior in *A. psidii* germination during host infection. It was found a correlation of epicuticular morphology on the resistance to *A. psidii*. However, in this study, we provide the first report of considerable interspecific variation in *Eucalyptus* spp. on the susceptibility to *A. psidii* and its correlation with cuticular waxes chemical compounds that seem to play a synergistic role as a preformed defense mechanism.

Keywords: cuticular waxes, GC-TOF-MS, preformed defense, rust, susceptibility

INTRODUCTION

Austropuccinia psidii (G. Winter) Beenken (syn. *Puccinia psidii*) is a basidiomycete that belongs to the Pucciniales order and is the causal agent of myrtle rust (Miranda et al., 2013; Beenken, 2017). The pathogen infects approximately 460 species in 73 genera of the Myrtaceae (Roux et al., 2013; Giblin and Carnegie, 2014; Beenken, 2017). Its hosts include *Eucalyptus* spp. that

Table S1. The classification of twenty-six metabolites presents in cuticular wax *Eucalyptus* species according of The Human Metabolome Database.

Metabolite	Class [a]	Organism	Reference
Alpha-D-Galactopyranosyl-(1,4)	Organooxygen compounds	Plant	Horbowicz et al., (1998).
Androst-4-en-3,17- dione	Steroids and Steroid derivatives	Fungal	Faramarzi et al., (2008).
Cinnamic acid, 4-hydroxy	Cinnamic acids and derivatives	Plant	Freitas et al., (2016).
Corticosterone	Steroids and Steroid derivatives	Animal	Samtani & Jusko (2007).
Docosan-1-ol	Fatty Acyls	Plant	Stashenki & Martínez (2012).
Docosane	Alkanes	Plant	Lytovchenko et al., (2009).
Eicosane	Alkanes	Plant	Asha et al., (2017).
Erythronic acid	Organooxygen compounds	Human	Nikolova et al., (2016).
Heneicosane	Alkanes	Plant	Bini (2016); Moussa & Almaghrabi (2016).
Heptadecanoic acid	Fatty Acyls	Plant	Moussa & Almaghrabi (2016).
Hexacosane	Alkanes	Plant	Kumar et al., (2017).
Hexadecanoic acid	Fatty Acyls	Plant	Moussa & Almaghrabi (2016).
Hexadecenoic acid	Fatty Acyls	Plant	Cahoon et al., (1994); Moussa & Almaghrabi (2016).
Nonacosane	Alkanes	Plant	Lytovchenko et al., (2009).
Octacosanoic acid	Fatty Acyls	Plant	Lytovchenko et al., (2009).
Octadecadienoic acid	Fatty Acyls	Plant	Bini (2016); Moussa & Almaghrabi (2016).
Octadecan-1-ol	Fatty Acyls	Plant	Lytovchenko et al., (2009).
Octadecanoic acid	Fatty Acyls	Plant	Moussa & Almaghrabi (2016). Lytovchenko et al., (2009).
Octadecenoic acid, 6-(Z)	Fatty Acyls	Plant	Rajeswari & Rani (2015); Vijisaral & Arumugam (2014).
Octadecenoic acid, 9-(Z)	Fatty Acyls	Plant	Moussa & Almaghrabi (2016).
Pentacosane	Organooxygen compounds	Plant	Kumar et al., (2017).
Pentadecane	Saturated	Plant	Lytovchenko et al., (2009).

	hydrocarbons		
Pregnane-3alpha	Steroids and Steroid derivatives	Plant	Cioffi et al., (2006)
Prephenic acid	Keto acids and derivatives	Plant	Bini (2016).
Threonine	Carboxylic acids and derivatives	Plant	Bini (2016).
Tricosane	Alkanes	Plant	Casuga et al., (2016).

[a] The class of metabolites was determinate in The Human Metabolome Database. Acess in May 2, 2018. Available in: http://www.hmdb.ca/

References

Alfenas, A. C., Zauza, E. A. V., Mafia, R. G., Assis, T. F. (2004). Clonagem e doenças do eucalipto. Viçosa, MG, Brazil: Editora UFV.

Asha, K. R., Priyanga, S., Hemmalakshmi, S., Devaki, K. (2017). GC-MS Analysis of the Ethanolic Extract of whole plant Drosera indica L. J. Pharmacogn. Phytochem. Res. 9, 5, 685-688. doi: 10.25258/phyto.v9i2.8149

Beenken, L. (2017). Austropuccinia: A new genus name for the myrtle rust Puccinia psidii placed within the redefined family Sphaerophragmiaceae (Pucciniales). Phytotaxa. 297, 53–61. doi: 10.11646/phytotaxa.297.1.5.

Bini, A. P., Quecine, M. C., Silva, T. M., Silva, L. D., Labate, C. A. (2018). Development of a quantitative real-time PCR assay using SYBR Green for early detection and quantification of Austropuccinia psidii in Eucalyptus grandis. Eur. J. Plant Pathol. 150, 735–746. doi: 10.1007/s10658-017-1321-7.

Bini, A. P. (2016). Estudo molecular do desenvolvimento de Puccinia psidii Winter in vitro e no processo de infecção em Eucalyptus grandis. [PhD's thesis]. [Piracicaba (SP)]: College of Agriculture "Luiz de Queiroz", University of São Paulo.

Cahoon, E. B., Cranmer, A. M., Shanklin, J., Ohlrogge, J. B. (1994). Delta-6 Hexadecenoic acid is synthesized by the activity of a soluble Delta-6 palmitoyl-acyl carrier protein desaturase in Thunbergia alata endosperm. J. Biol. Chem. 44, 519-26.

Carnegie, A. J., Lidbetter, J. R. (2012). Rapidly expanding host range for Puccinia psidii sensu lato in Australia. Australas. Plant Pathol. 41, 13-29. doi: 10.1007/s13313-011-0082-6

Carvalho, A. D. O., Alfenas, A. C., Maffia, L. A., Carmo, M. G. F. (1998). Resistance of Eucalyptus species, progenies and provenances to Puccinia psidii. Pesq. Agropec. Bras. 33, 139-147.

Casuga, F. P., Castillo, A. L., Corpuz, M. J. T. (2016). GC-MS analysis of bioactive compounds present in different extracts of an endemic plant Broussonetia luzonica (Blanco) (Moraceae) leaves. Asian Pac. J. Trop. Biomed. 6, 957-961. doi: 10.1016/j.apjtb.2016.08.015.

Chong, J., Soufan, O., Li, C., Caraus, I., Li, S., Bourque, G., et al. (2018). MetaboAnalyst 4.0: towards more transparent and integrative metabolomics analysis. Nucleic Acids Res. 46, 486-489. doi:10.1093/nar/gky310.

Cioffi, G., Sanogo, R., Vassallo, A., Dal Piaz, F., Autore, G., Marzocco, S., et al. (2006). Pregnane glycosides from Leptadenia pyrotechnica. J. Nat. Prod. 69, 625-635. doi: 10.1021/np050493r.

Coutinho, T. A., Wingfield, M. J., Alfenas, A. C., Crous, P. W. (1998). Eucalyptus rust: A disease with the potential for serious international implications. Plant Dis. 82(7), 819-825 doi: 10.1094/PDIS.1998.82.7.819.

Cuadros-Inostroza, A., Caldana, C., Redestig, H., Kusano, M., Lisec, J., Peña-Cortés, H., et al. (2009). TargetSearch - a Bioconductor package for the efficient preprocessing of GC-MS metabolite profiling data. BMC Bioinformatics 10, 428. doi: 10.1186/1471-2105-10-428.

Dianese, J. C., Moraes, T. S. A., Silva, A. R. (1984). Response of Eucalyptus to field infection by Puccinia psidii. Plant Dis. 68, 314-316. doi: 10.1094/PD-69-314.

Faramarzi, M. A., Aghelnejad, M., Yazdi, M. T., Amini, M., Hajarolasvadi, N. (2008). Metabolism of androst-4-em-3, 17-dione by the filamentous fungus Neurospora crassa. Steroids. 73,13-18. doi: 10.1016/j.steroids.2007.06.008.

Ferreira, F. A. (1981). Ferrugem de eucalipto - ocorrência, temperatura para germinação de uredósporos, produção de teliósporos, hospedeiro alternativo e resistência. Fitopatol. Bras. 6, 603-604.

Freitas, C. A. S., Vieira, I. G. P., Sousa, P. H. M., Muniz, C. R., Gonzaga, M. L. C., Guedes, M. I. F. (2016). Carnauba wax p-methoxycinnamic diesters: Characterization, antioxidant activity and simulated gastrointestinal digestion followed by in vitro bioaccessibility. Food Chem. 196, 1293-1300. doi: 10.1016/j.foodchem.2015.10.101.

Glen, M., Alfenas, A. C., Zauza, E. A. V., Wingfield, M. J., Mohammed, C. (2007). Puccinia psidii: a threat to the Australian environment and economy – a review. Australas. Plant Pathol. 36, 1–16. doi: 10.1071/AP06088.

Giblin, F. R., and Carnegie, A. J. (2014). Puccinia psidii (Myrtle rust) - Australian host list. Version current at 23 Oct. 2014. Available at: http://www.anpc.asn.au/myrtle-rust

Golebiowski, M., Malinski, E., Bogus, M. I., Kumirska, J., Stepnowski, P. (2008). The cuticular fatty acids of Calliphora vicina, Dendrolimus pini and Galleria mellonella larvae and their role in resistance to fungal infection. Insect Biochem. Mol. Biol. 38:619-627. doi: 10.1016/j.ibmb.2008.03.005.

Gullberg, J., Jonsson, P., Nordstrom, A., Sjostrom, M., Moritz, T. (2004). Design of experiments: an efficient strategy to identify factors influencing extraction and derivatization of Arabidopsis thaliana samples in metabolomics studies with gas chromatography/mass spectrometry. Anal. Biochem. 331, 283-295. doi: 10.1016/j.ab.2004.04.037.

Guzmán, P., Fernández, V., Graça, J., Cabral, V., Kayali, N., Khayet, M., et al. (2014). Chemical and structural analysis of Eucalyptus globulus and E. camaldulensis leaf cuticles: a lipidized cell wall region. Front. Plant. Sci. 5, 1-12. doi: 10.3389/fpls.2014.00481.

Hallam, N. D., Chambers, T. C. (1970). The leaf waxes of the genus Eucalyptus L'heritier. Aust. J. Bot. 18, 335-86. doi: 10.1071/BT9700335.

Hansjakob, A., Riederer, M., Hildebrandt, U. (2011). Wax matters: absence of very-long-chain aldehydes from the leaf cuticular wax of the glossy11 mutant of maize compromises the pre penetration processes of Blumeria graminis. Plant Pathol. DOI: 10.1111/j.1365-3059.2011.02467.x.

Hoffman, D. E, Jonsson, P., Bylesjö, M., Trygg, J., Antti, H., Eriksson, M. E., et al. (2010). Changes in diurnal patterns within the Populus transcriptome and metabolome in response to photoperiod variation. Plant Cell Environ. 60, 1151-1161. doi: 10.1111/j.1365-3040.2010.02148.x.

Horbowicz, M., Brenac, P., Obendorf, R. L. (1998). Fagopyritol B1, O-α-D-galactopyranosyl-(1→2)-D-chiro-inositol, a galactosyl cyclitol in maturing buckwheat seeds associated with desiccation tolerance. Planta 205, 1-11. doi: 10.1007/s004250050290.

Horridge, G. A, Tamm, S. L. (1969). Critical point drying for scanning electron microscopic sthdy of ciliary motion. Science 163, 817-818. doi: 10.1126/science.163.3869.817.

Inuyang, E. N., Butt, T. M., Beckett, A., Archer, S. (1999). The effect of crucifer epicuticular waxes and leaf extracts on the germination and virulence of Metarhizium anisopliae conidia. Mycol. Res. 103, 419-426. doi: DOI.org/10.1017/S0953756298007333.

Kanehisa, M., Goto, S. (2000). KEGG: Kyoto encyclopedia of genes and genomes. Nucleic Acids Res. 28, 27-30.

Karnovsky, M. J. (1965). A formaldehyde-glutaraldehyde fixative of high osmolality for use in electron microscopy. J. Cell. Biol. 27, 137-138.

Kawanishi, T., Uemastu, S., Kakishima, M., Kagiwada, S., Hamamoto, H., Horie, H., Namba, S. 2009. First report of rust disease on ohia and the causal fungus, Puccinia psidii, in Japan. Journal of General Plant Pathology, 75, 428–431. doi: 10.1007/s10327-009-0202-0

Koch, K., Bhushan, B., Barthlott, W. (2010). “Multifunctional plant surfaces and smart materials” in Handbook of Nanotechnology, ed. B. Bhushan (New York, NY: Springer Press), 1399-1436.

Kolattukudy, P. E., Rogers, L. M., Li, D. X., Hwang, C. S., Flaishman, M. A. (1995). Surface signaling in pathogenesis. Proc. Natl. Acad. Sci. USA. 92, 4080–4087.

Kopka, J., Schauer, N., Krueger, S., Birkemeyer, C., Usadel, B., Bergmüller, E., et al. (2005). GMD@CSB.DB: the Golm Metabolome Database. Bioinformatics 21, 1635-1638. doi: 10.1093/bioinformatics/bti236.

Kumar, J., Paul, B., Nebapure, S. M., Singh, S. (2017). Comparative GC-MS analysis of two Brassica rapa L. varieties for identification of volatile compounds. Ch. Sc. Rev. Lett. 6, 22, 884-889.

Lazniewska, J., Macioszek, V. K., Kononowicz, A. K. (2012). Plant-fungus interface: the role of surface structures in plant resistance and susceptibility to pathogenic fungi. Physiol. Mol. Plant Path. 78, 24–30. doi: 10.1016/j.pmpp.2012.01.004.

Leite, T. F., Moon, D. H., Lima, A. C. M., Labate, C. A., Tanaka, F. A. O. (2013). A simple protocol for whole leaf preparation to investigate the interaction between Puccinia psidii and Eucalyptus grandis. Australas. Plant Pathol. 42, 79-84. doi: 10.1007/s13313-012-0179-6.

Leite, T. F. (2012). Estabelecimento de um patossistema modelo e análise da interação molecular planta-patógeno entre Eucalyptus grandis e Puccinia psidii Winter por meio da técnica de Rna-seq. [PhD's Thesis]. [Piracicaba (SP)] College of Agriculture "Luiz de Queiroz", University of São Paulo.

Lytovchenko, A., Beleggia, R., Schauer, N., Isaacson, T., Luendorf , J. E., Hellmann, H., et al. (2009). Application of GC-MS for the detection of lipophilic compounds in diverse plant tissues. Plant Methods. 5, 1-11. doi: 10.1186/1746-4811-5-4.

Marques, J. P. R., Amorim, L., Spósito, M. B, Appezzato-da-Glória, B. (2013). Histopathology of postbloom fruit drop caused by Colletotrichum acutatum in citrus flowers. Eur. J. Plant Pathol. 135, 783–790. doi: 10.1007/s10658-012-0120-4.

McKinney, H. H. (1923). Influence of soil, temperature and moisture on infection of wheat seedlings by Helminthosporium sativum. J. Agric. Res. 26, 195-217.

Miranda, A. C., Moraes, M. L. T., Tambarussi, E. V., Furtado, E. L., Mori, E. S., Silva, P. H. M., et al. (2013). Heritability for resistance to Puccinia psidii Winter rust in Eucalyptus grandis Hill ex Maiden in Southwestern Brazil. Tree Genet. Genomes. 9, 321–329. doi: 10.1007/s11295-012-0572-x.

Moussa, T. A. A., Almaghrabi, O. A. (2016). Fatty acid constituents of Peganum harmala plant using Gas Chromatography-Mass Spectroscopy. Saudi J. Biol. Sci. 23, 397-403. doi: 10.1016/j.sjbs.2015.04.013.

Nikolova, M., Aneva, I., Berkov, S. (2016). GC-MS metabolic profiling and free radical scavenging activity of Micromeria dalmatica. Biologica Nyssana 7, 159-165. doi: 10.5281/zenodo.200415.

Quecine, M. C., Bini, A. P., Romagnoli, E. R., Andreote, F. D., Moon, D. H., Labate, C. A. (2014). Genetic variability in Puccinia psidii populations as revealed by PCR-DGGE and T-RFLP markers. Plant Dis. 98,16-23. doi: 10.1094/PDIS-03-13-0332-RE.

Quecine, M. C., Leite, T. F., Bini, A. P., Regiani, T., Franceschini, L. M., Budzinski, I. G. F., et al. (2016). Label-free quantitative proteomic analysis of Puccinia psidii uredospores reveals differences of fungal populations infecting eucalyptus and guava. Plos One. 11, e0145343. doi: 10.1371/journal.pone.0145343.

Racovita, R. C., Peng, C., Awakawa, T., Abe, I., Jetter, R. (2015). Very-long-chain-3-hydroxy fatty acids, 3-hidroxy fatty acid methyl esters and 2-alkanols from cuticular waxes of Aloe arborescens leaves. Phytochemistry 113, 183-194. doi: 10.1016/j.phytochem.2014.08.005.

Rajeswari, J., Rani, S. (2015). GC-MS analysis of phytochemical compounds in the ethanolic extract of root Lawsonia inermis Linn. Int. J. ChemTech Res. 7, 389-399.

Read, N. D., Kellock, L. J., Knight, H., Trewavas, A. J. (1992). "Contact sensing during infection by fungal pathogens" in Perspective in plant cell recognition, ed. J. A. Gallow, J. R. Green (Cambridge, UK: Cambridge University Press), 137-172.

Reisige, K., Gorzelanny, C., Daniels, U., Moerschbacher, B. M. (2006). The C28 aldehyde octacosanal is a morphogenetically active component involved in host plant recognition and infection structure differentiation in the wheat stem rust fungus. Physiol. Mol. Plant Path. 68, 33–40. doi: 10.1016/j.pmpp.2006.05.006.

Roux, J., Greyling, I., Coutinho, T. A., Verleur, M., Wingfield, M. J. 2013. The Myrtle rust pathogen, Puccinia psidii, discovered in Africa. IMA Fungus 4, 155-159. doi: 10.5598/imafungus.2013.04.01.14.

Samtani, M. N., Jusko, W. (2007). Quantification of dexamethasone and corticosterone in rat biofluids and fetal tissue using highly sensitive analytical methods: assay validation and application to a pharmacokinetic study. Biomed. Chromatogr. 21, 585-597. doi: 10.1002/bmc.788.

Schauer, N., Steinhauser, D., Strelkov, S., Schomburg, D., Allison, G., Moritz, T., et al. (2005). GC-MS libraries for the rapid identification of metabolites in complex biological samples. FEBS Let. 579, 1332-1337. doi: 10.1016/j.febslet.2005.01.029.

Serrano, M., Coluccia, F., Torres, M., L'Haridon, F., Metraux, J. P. (2014). The cuticle and plant defense to pathogens. Front. Plant Sci. 5,274. doi: 10.3389/fpls.2014.00274.

Silva, D. E. M., Azevedo, L. A. S., Poltronieri, T. P. S. (2014). Avaliação da resistência de espécies de eucalipto à ferrugem (Puccinia psidii Winter). Summa Phytopathol. 40, 54-62.

Song-Jiang, C., Yong-Cai, L., Yan, Y., Yong-Hong, G., Yi, W. (2014). Solvent effects on the ultrastructure and chemical composition of cuticular wax and its potential bioactive role against Alternaria alternate in Pingguoli pear. J. Integr. Agric. 13, 1137-1145. doi: 10.1016/S2095-3119(13)60374-3.

Stashenki, E. E., Martínez, J. R. (2012). "GC-MS analysis of volatile plant secondary metabolites" in Gas chromatography in plant science, wine technology, toxicology and some specific applications, eds. B. Salih, Ö. Çelikbiçak (InTech), 247-270.

Steinbauer, M. J., Davies, N. W., Gaertner, C., Derridj, S. (2009). Epicuticular waxes and plant primary metabolites on the surfaces of juvenile Eucalyptus globulus and E. nitens (Myrtaceae) leaves. Aust. J. Bot. 57, 474-485. doi: 10.1071/BT09108.

Takahashi, S. S. 2002. Ferrugem do eucalipto: Índice de infecção, análise temporal e estimativas de danos relacionados à intensidade da doença no campo. [Dissertation]. [Botucatu (SP)], Universidade Estadual Paulista.

Tessmann, D. J., Dianese, J. C. (2002). Hentriacontane: a leaf hydrocarbon from Syzygium jambos with stimulatory effects on the germination of uredósporos of Puccinia psidii. Fitopatol. Bras. 27, 538-542. doi: 10.1590/S0100-41582002000500017.

Tucker, D., Wallis, I., Bolton, J., Marsh, K., Rosser, A., Brereton, I., et al. (2010). A metabolomic approach to identifying chemical mediators of mammal–plant interactions. J. Chem. Ecol. 36, 727–735. doi: 10.1007/s10886-010-9803-5.

Viana, R. G., Tuffi-Santos, L. D., Demuner. A. J., Ferreira, F. A., Ferreira, L. R., Ferreira, E. A., et al. (2010). Quantification and chemical composition of epicuticular wax of Eucalyptus leaves. Planta Daninha. 28, 753-758. doi: 10.1590/S0100-83582010000400007.

Vijisaral, E. D., Arumugam, S. (2014). GC-MS analysis of bioactive constituents of Indigofera suffruticosa leaves. J. Chem. Pharm. Res. 6, 294-300.

Xavier, A. A., Alfenas, A. C., Matsuoka, K., Hodges, C. S. (2001). Infection of resistant and susceptible Eucalyptus grandis genotypes by urediniospores of Puccinia psidii. Australas. Plant Pathol. 30, 277-281, doi: 10.1071/AP01038.

Yeats, T. H., Rose, J. K.C. (2013). The formation and function of plant cuticles. Plant Physiol. 163,5-20. doi: 10.1104/pp.113.222737.

Zabka, M., Pavela, R., Prokinova, E. (2014). Antifungal activity and chemical composition of twenty essential oils against significant indoor and outdoor toxigenic and aeroallergenic fungi. Chemosphere 112, 443-448. doi: 10.1016/j.chemosphere.2014.05.014.

Zabka, V., Stangl, M., Bringmann, G., Vogg, G., Riederer, M., Fildebrandt, U. (2007). Host surface properties affect pre penetration processes in the barley powdery mildew fungus. New Phytol. 177, 251-263. doi: 10.1111/j.1469-8137.2007.02233.x.

Zamprogno, K. C., Furtado, E. L., Marino, C. L., Bonine, C. A. V., Dias, D. C. (2008). Utilização de análise de segregantes agrupados na identificação de marcadores ligados a genes que controlam resistência à ferrugem (Puccinia psidii) em Eucalyptus spp. Summa Phytopathol. 34, 253-255. doi: 10.1590/S0100-54052008000300009.

Zauza, E. A. V., Alfenas, A. C., Old, K., Couto, M. F., Graça, R. N., Maffia, L. A. (2010). Myrtaceae species resistance to rust caused by Puccinia psidii. Australas. Plant Pathol. 39,106-411. doi: 10.1071/AP10077.

3. TRANSCRIPTOME ANALYSIS OF *Austropuccinia psidii* REVEALS THE ROLE OF CUTICULAR WAXES *Eucalyptus* spp. ON FUNGAL PATHOGEN GENE EXPRESSION

Abstract

Eucalyptus productivity has been affected by myrtle rust, which is caused by the basidiomycete fungus *Austropuccinia psidii*. This species is a biotrophic fungus and, thus, molecular studies concerning its interaction with the host are scarce. It is known that preformed physical and chemical defenses may affect the plant-pathogen interaction. Among those, the cuticular wax composition has been related to the resistance or susceptibility of the host. Thus, our hypothesis is that the cuticular waxes from *Eucalyptus* spp. with different levels of resistance may modulate the gene expression of the pathogen *A. psidii* during the early plant-pathogen interaction. In order to understand gene expression of *A. psidii*, we realized bioassays in vitro containing cuticular waxes from *E. grandis* (*E. g*: susceptible), *E. urograndis* (*E. ug*: intermediate) and *E. urophylla* (*E. u*: resistant). Mineral oil (MO) treatment was used to all comparative analysis as a negative control. The chemical stimulus provided by cuticular waxes from *E. g* and *E. ug* enabled the *A. psidii* uredospore germination and the differentiation of germ tubes in infection structures known as appressoria. Fungal RNA was extracted at 18 hours after inoculation. The paired-end sequencing was performed using HiSeq SBS Kit v4 through Illumina HiSeq 2500 platform. In total, it was processed 320.570.660 PE reads. Using Kallisto software, the alignment average rate was of 80.36%, having *A. psidii* draft genome as a reference. Differentially expressed genes (DEGs) were obtained by Sleuth package of RStudio software. Three comparisons analysis were performed, *E. g* x MO (487 DEGs), *E. ug* x MO (209 DEGs) and *E. u* x MO (851 DEGs). The GO enrichment analysis was performed and to *E. g* x MO it was observed an abundance of DEGs related to the pathogen establishment, localization, cellular response to stimulus and organelle organization. Regarding *E. ug* x MO, the most predominant GO terms were related to anatomical structure development, regulation of gene expression, reproduction, among others. As to *E. u* x MO, highlighted processes was reciprocal meiotic recombination, cell budding, and protein maturation. The presence of cuticular waxes from *E. g* induced the expression of genes encoding proteins related to growth and colonization of *A. psidii* such as binding proteins (peptidylprolyl isomerase and ribosomal) and cell wall degrading proteins (beta-xylanase). However, other pathogenic proteins were repressed in presence of cuticular wax of *E. g*, for instance, triosephosphate isomerase, family 18 glycoside hydrolase, mitochondrial ATP carrier, and glutamine-dependent NAD synthetase. The *E. ug* x MO analysis resulted in DEGs associated with proteins related to membrane transporters and receptors, DNA repair and glycine dehydrogenase. The cuticular wax of *E. u* up-regulated the expression of genes encoding proteins associated to pheromone, cutinases, and prefoldin. Some DEGs down-regulated in presence of cuticular wax of *E. u* were hydrolases families (family 18 and 23 glycoside hydrolase) and enzyme cofactors (thiamine pyrophosphokinase). The qRT-PCR with the same samples used to perform RNA-Seq was realized and validated the transcriptomic assay. Thus, for the first time, we demonstrated that *Eucalyptus* spp. cuticular waxes may act as pre-formed defense mechanisms, besides modulating the *A. psidii* gene expression, suggesting the importance of early plant-pathogen molecular interaction to the development of myrtle rust.

Keywords: RNA-Seq; Plant x pathogen; Interaction; Biotrophic fungal

Introduction

Myrtle rust, also known as eucalyptus rust, is caused by *Austropuccinia psidii* (G. Winter) Beenken (Basidiomycota, Pucciniales). It is a biotrophic fungus, autoecious, that was first reported in Brazil (1984) infecting guava (*Psidium guajava*). Later this pathogen was found infecting *Eucalyptus citriodora* (Beenken, 2017; Winter, 1884; Joffily, 1944). *A. psidii* is native to Central and South America and has rapid global dissemination with reports its occurrence in several countries and continents such as South, Central and North America (Granados et al., 2017; Kern and Toro, 1935; Mohali and Aime, 2016; Pérez et al., 2011; Tommerup et al., 2003; MacLachlan, 1938; Uchida et al., 2006), Asian (Kawanishi et al., 2009; Zhuang and Wei, 2011; Du Plessis et al., 2017), Australia (Carnegie et al., 2010), South Africa (Roux et al., 2013) and Indonesia (McTaggart et al., 2016). In many countries as Australia, the center of diversity to Myrteceae, the *A. psidii* pandemic represents a threat for local biodiversity due to its quick dissemination, severe damage and wide host range (Carnegie et al., 2016; Pegg et al., 2017).

This pathogen attacks young, growing leaves and shoots, flowers and fruits. In early stages of infection, chlorotic flecks can be observed, followed by the production of masses yellow uredospores, can be resulting in shoot dieback and reduced recruitment. In eucalypt trees, *A. psidii* attack result in a significative reduction in height and diameter of approximately 25-35% and wood-volume losses of 41% (Pegg et al., 2014; Silveira and Higashi, 2003; Takahashi, 2002).

Studies conducted by Xavier et al. (2001) and Leite et al. (2013) allowed to describe the structures of *A. psidii* during infection in different *E. grandis* genotypes (resistant and susceptible) . Three hours post inoculation (h.p.i.) starts the germination of uredospores; and 6 h.p.i. it is observed appressorium formation, responsible for anchoring and application of mechanical pressure in plants tissues. The penetration into plant cell occurs in 12 h.p.i. with visualization of hyphae resulting from appressorium. In 18-24 h.p.i. haustoria is emerged, a fungal structure specialized in the absorption of nutrients in hosts cells. In spite of the importance of *A. psidii*, little is known about its biology and mechanisms involved in the host attacking.

Currently, the high-throughput sequencing has contributed with a better understing of plant pathogens with significant economic importance and with incipient molecular information, as the biotrophic fungus. The sequencing of transcriptomes by RNASeq has provided important genetic and functional information to many organisms at unprecedented scale and speed (Haas et al., 2013). Some studies have demonstrated the efficiency and applicability of RNASeq to better understanding key pathogenicity mechanisms from biotrophic pathogenic fungi *in vitro* and *in vivo* assays. For instance, Garnica et al. (2013) studied the transcriptome of infection structures (haustories) and germinated uredospores of *Puccinia striiformis* f. sp. *tritici* (Pst), causal agent of wheat rust (*Triticum sativum* L.). The 454 sequencing provided 12282 transcripts of these 400 genes encoding secreted proteins (effector candidates) were identified from the haustorial transcriptome and 65% genes were up-regulated in comparison to germinated spores transcriptome. The authors confirmed the expression

pattern of 94 effector candidates effectors by RT-qPCR and that uredospores depend mainly on the host's energy reserves for their growth and development, while the haustories assimilates from of the plants the nutrients for spore production. These data corroborate the importance of transcriptome analysis in uncovering key mechanisms of phytopathogens attack during the infection.

De Carvalho et al. (2017) studied the transcriptome of *Phakopsora pachyrhizi*, causal agent of soybean rust (*Glycine max*). The RNAseq resulted in a total of 36350 *P. pachyrhizi* contigs expressed *in plant* and a predicted secretome of 851 proteins. As expected, some of these proteins had specific characteristics of candidate effectors: small size, rich cysteine without PFAM domains and strongly by expressed *in plant*. The effectors candidates selected were able to suppress immunity in transient assays, and were localized in the cytoplasm and nucleus of plant.

Bini (2016) obtained by RNASeq some genes differentially expressed by *A. psidii* during during the pathogen morphogenesis *in vitro*. The sequencing resulted in 170,000,000 reads, which assembled in 61,343 transcripts grouped in 31,393 putative genes. A total of 18,593 transcripts were annotated, among those, 74.12% were related to fungal pathogenicity, such as effectors, proteases, proteasomes, chitinases and lipases, evidencing the direct relationship with activation of mechanisms of recognition, germination and initial process of interaction of the pathogen with its host. These studies clearly show the existence of a large and wide universe in the transcriptomes of phytopathogenic fungi that needs to be explored to better understanding of their interaction with host plants.

In vivo assays, plant tissue and the stage of infection have been crucial to determine which genes are induced during interaction plant-pathogen, especially in pathosystems with forest species, where the stature, long generation times and large genomes are specially complexes (Rampant et al., 2011). Hayden et al. (2014) undertook the transcriptome of tonoak (forest host) infected by *Phytophthora ramorum* (Oomycetes). The authors detected more than 850 *P. ramorum* transcripts at 5 days post-inoculation (d.p.i) and a concurrent upregulation of host genes usually associated with pathogenicity. However, in one d.p.i was not detected pathogen expression or significant enrichment of functional categories of host transcripts relative to controls, demonstrating how challenging and complex are the researches with pathosystems *in vivo*.

Thus, another strategy is monitoring the development of disease over time combined with *in vitro* conditions that partially simulate the host, for instance the surface of plant. It is important to note that these approaches do not establish causal relationships, i.e. genes induced after host colonization is not necessarily required for growth of pathogen. Taniguti et al. (2015) analyzed the *Sporisorium scitamineum* transcriptome profiling from *in vitro* and during the interaction with sugarcane. It was discovered that 13.5% of the genes were differentially expressed in planta and particular to each development stage with expression of plant cell wall degrading enzymes, proteases, lipases, chitin modification and lignin degradation enzymes, sugar transporters and transcriptional factors. The *S. scitamineum* also was able to modulate the plant gene expression. These researches support

hypotheses about the metabolic processes, pathogenicity mechanisms and other artifacts necessary for successful infection. Also, it is possible to identify candidate genes to effectors, enzymes secreted during colonization, among others (Van Der Does and Rep, 2017).

In general the first interaction of biotrophic pathogenic fungi is the contact with the host tissue. The pathogen recognizes the host surface (cuticle) through its hydrophobicity and chemical composition during the early stages of infection. It is known that the cuticles have complex composition formed by cutin, polymers of fatty acids and cuticular waxes (Buschhaus and Jetter, 2011). The signals emitted by host may modulate the gene expression related to fungal growth as well as its morphgenesis and formation of apressorium. Briefly, during the early pathogen x plant interaction, the host produces specific reactions of living cells in response to presence of microorganisms, resulting in detection and settle of pathogen in plant surface (Lanver et al., 2014).

Santos et al. (2019) initially classified twenty-one *Eucalyptus* spp. in the field as resistant or susceptible to *A. psidii*. The resistance/susceptibility level of six *Eucalyptus* spp. were validated in controlled conditions using qPCR, revealing that the pathogen can germinate on the eucalyptus surface of some species without multiplying in the host. By CG-TOF-MS analysis the authors detected 26 compounds derivated from in the *Eucalyptus* spp. cuticle and led to the discovery of the role of hexadecanoic acid in the susceptibility of *E. grandis* and *E. phaeotricha* to *A. psidii*. The authors also characterized the epicuticular wax morphology of the six previously selected *Eucalyptus* spp. using scanning electron microscopy and observed different behavior in *A. psidii* germination during host infection. In this study, it was provided the first report of considerable interspecific variation in *Eucalyptus* spp. on the susceptibility to *A. psidii* and its correlation with cuticular waxes chemical compounds that seem to play a synergistic role as a preformed defense mechanism.

Thus, we aimed to analyze the influence cuticular waxes from three *Eucalyptus* species (*E. grandis*: susceptible, *E. urograndis*: intermediate and *E. urophylla*: resistant) with different degree of susceptibility in the transcriptome of *A. psidii* looing for genes associated with the pathogen to circumvent the preformed defense in eucalyptus.

Materials and Methods

Experimental design

To evaluate the influence of cuticular waxes in the differentially expressed genes (DEGs) profile of *A. psidii* MF1 the bioassay was conducted in controlled conditions using Petri dishes containing 20 ml of agar-water (8 g l^{-1}), 50 µl of mineral oil (Sigma) or 50 µl of cuticular wax (20 ppm) obtained as described in Santos et al. (2019) and 7 mg of *A. psidii* uredospores (Figure 1). The Petri dishes were incubated at 20 °C in the absence of light for 18 hours, time in which occurs the penetration into plant cell upon appressorium formation (Leite et al., 2013). After incubation were observed the *A. psidii* uredospores germination and the development of infection structures by

photomicroscope (Aziophot) with digital coupled camera (Zeiss). The experimental design was completely randomized blocks containing three treatments (wax cuticular: *E. grandis, E. urograndis* and *E.urophylla*) and the control (mineral oil). The assay was perfomed with four biological replicates, each one composed by two Petri dishes (Figure 1). The RNA extraction, the dialysis membranes with *A. psidii* uredospores were macered with liquid nitrogen and stored at -80ºC (Xavier et al., 2001, Leite, 2012, Bini, 2016).

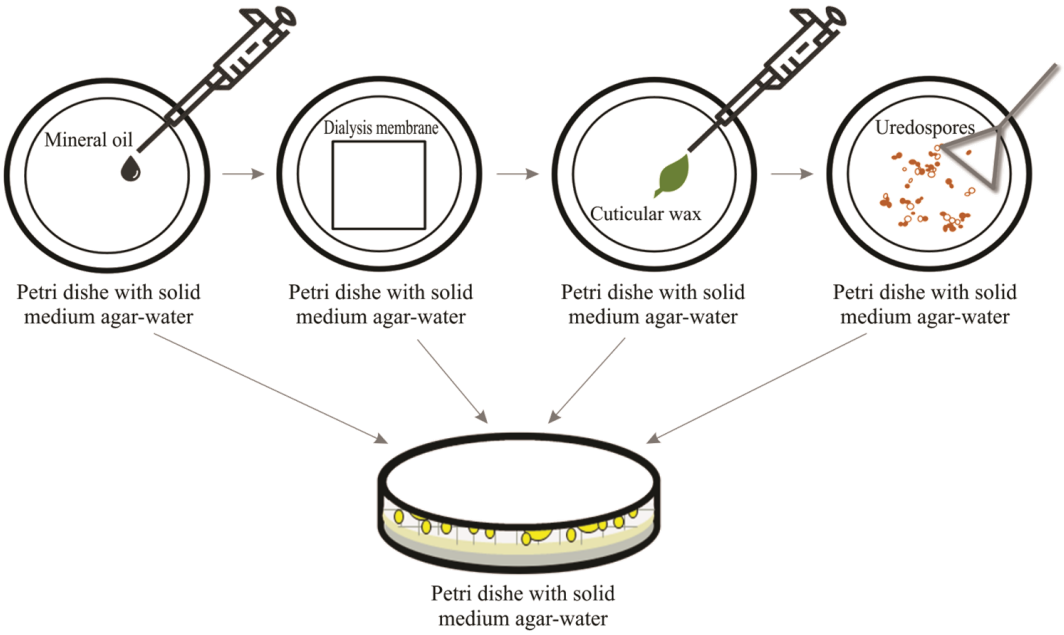

Figure 1. RNASeq bioassay to *A. psidii* uredospores germinated in cuticular waxes from *Eucalyptus* spp. with contrasting degree of resistance to pathogen (*E. grandis*, *E. urograndis* and *E. urophylla*) and mineral oil (negative control).

RNA Extraction, Library Construction and RNA-Seq

Total RNA was extracted using the Rneasy Mini Plant Kit (Qiagen) according to the manufacturer's recommendations. Sample quantification was obtain by agarose gel (1.4% w/v), NanoDrop (Thermo Fisher Scientific) and Agilent 2100 Bioanalyzer (Agilent Technologies). Subsequently, one µg of total RNA of each replicate was sent to construct the cDNA libraries and sequencing. The preparation of cDNA libraries and sequencing (RNASeq) were performed at the Centralized Multiuser Laboratory of Functional Genomics Applied to Agriculture and Agroenergy (ESALQ/USP). The libraries were prepared with Illumina TruSeq Stranded mRNA LT Sample Prep Protocol (Illumina, San Diego, CA, USA). Paired-end sequencing was performed using HiSeq SBS Kit v4 through Illumina HiSeq 2500 platform (Illumina, San Diego, CA, USA) generating the reads size of 100 bp.

Data processing and assembly

The demultiplex process of samples and conversion of files generated by the Illumina sequencing system were performed using FASTQ Generation (version 1. 0. 0) (Illumina, San Diego, CA, USA). For each sample, four files (. * Fastq) were generated: two to paired-end 1 (R1: lane 1 and 2) and two to paired-end 2 (R2: lane 1 and 2).

The trimmomatic software (version 0. 32) (http://www.usadellab.org/cms/index.php?page=trimmomatic) was used to remove of adapters utilizing the following parameters: Illumina Clip TruSeq 3-PE.fa: 2: 30: 10: 5 true; Maxinfo: 60: 0: 80 and Millen: 60 (Bolger et al., 2014). The Trimmomatic scripts used to trimming were detailed in the Additional Information 1. The FASTQC (version 0.11.7) (https://www.bioinformatics.babraham.ac.uk/projects/fastqc/) was applied to analyze the quality of the sequences. Remaining segments of contaminant sequences (rRNAs, adapters and bases with low quality) were removed with BBDuk2 (version 37.25) (BBMap: http://sourceforge.net/projects/ bbmap /) using the parameters: k: 27; mink: 6. Sequencing depth was verified by RSEQC package (version 2.3.7) (http://rseqc.sourceforge.net/) with junction_saturation parameter (Wang et al., 2012).

Kallisto software (version 0.44.0) (https://pachterlab.github.io/kallisto/) was used to perform the pseudoalignment of the pathogen genes with reference genome of *A. psidii* (Bray et al., 2016). Briefly, sequencing of *A. psidii* was performed in several sequencing technologies: MiSeq, Hiseq2500 (Pair end and Mate Pair), PacBio and Roche 454. The data were processed, assembled and annotated using several programs: SPAdes (v.3.9.1), RepeatMasker (v. 4.0.7), TopHat, Augustus (v. 1.1), PASA (v. 2.1.0), EvidenceModeler (v 1.1.1), Blast (v. 2.6.0), InterproScan, Blast2go (v. 4.1.9 PRO), among others (Trapnell et al., 2009; Altschul et al., 1990; Conesa et al., 2005). Alignment of RNASeq data was performed with masked reference genome of *A. psidii* (without the presence of transposable elements and retrotransposons) which contains 47121 ORFs (unpublished data).

The parameters used to measurement of estimates of ets_counts (Estimated Counts) and TPM (Transcripts Per Million) were k-mer: 31, bias, bootstrap-samples: 100, seed: 42, rf-stranded and threads (Bray et al., 2016). The software provided three output files: *i)* abundances.h5: binary file containing performance information, abundance estimates, bootstrap and transcript length; *ii)* abundaces.tsv: simple text file with abundance estimates, bootstrap, ets_counts, TPM and effective count; and *iii)* run_info.json: file with information about running the software. The Kallisto scripts used for pseudoalignment are detailed in the Additional Information 2.

Differentially expressed genes analysis, annotation and categorization

The DEG analysis was performed using the input abundance estimation file (abundaces.tsv) through Sleuth package (v. 0. 30. 0) (http://pachterlab.github.io/sleuth/) from RStudio software (v. 1. 1. 463) (Pimentel et al., 2017). According to the lipidomic analysis previously obtained by Santos et al. (2019) three comparative analysis were performed in this study: *A. psidii* uredospore germination in

cuticular waxes from *E. grandis* (*E. g* - susceptible) x mineral oil (MO), cuticular waxes from *E. urograndis* (*E. ug* - intermediate) x mineral oil (MO) and cuticular waxes from *E. urophylla* (*E. u* - resistant) x mineral oil (MO).

The experimental information, details of model used in the tests and the results were stored in "Sleuth object". Sleuth package performed two "full" and "reduced" measurement models for Likelihood Ratio Test (LRT). The genes with qval < 0.05 (treatment/control) were considered as DEG. The R scripts utilized in this analysis are detailed in the Additional Information 3.

Functional annotation and Gene Ontology categorization to each DEG were obtained using Blast2GO (v. 5) (https://www.blast2go.com/support/blog/21-news/174-blast2go-release-version-5) with default parameters settings. In addition, manual annotation of the DEGs was performed using the NCBI database (Blastx - v. 2.8.0) (https://blast.ncbi.nlm.nih.gov/Blast.cgi?PROGRAM=blastx&PAGE_TYPE=BlastSearch&LINK_LOC=blasthome) and InterPro (v.70 - UniProt) (https://www.uniprot.org/). Enrichment analysis of GO annotations was carried out in Blast2GO (v. 5) using the hypergeometric test and Benjamini and Hochberg's false discovery rate (FDR) multiple testing correction ($p \leq 0.05$) (Conesa et al., 2005).

Real-Time Quantitative PCR (RT-qPCR) analysis of the DEGs

The primer design to randomly selected DEGs was performed using the Primer3 software (v. 0.4.0). The dimers presence was verified using Oligo Analysis Tool (http://goo.gl/37JHNg) (Table 1). Firstly, the primers set were validated by conventional PCR (PCR) to verify the best annealing temperature and specificity. The reactions were prepared with a final volume of 25 µl containing: 2.5 µl Taq Buffer with KCl (10X), 3.5 µl $MgCl_2$ (25 mM), 0.5 µl dNTP (0.2 mM), 0.5 µl primer Forward-Reverse (5 pmol), 0.5 µl BSA (10 mg mL^{-1}), 0.25 µl Taq DNA Polymerase (5 U μL^{-1}) (ThermoFisher), 20 ng DNA template (*A. psidii* MF-1, *E. grandis* without spores and *E. grandis* 144 h.p.i) and ultrapure water. The samples were submitted to PCR in thermocycler Profex PCR System (Applied Biosystems) programmed for following cycles: initial denaturation of 95 ºC for 3 min; 35 cycles of amplification contining: 95 °C for 30 sec, 52-62 °C for 30 sec, 72 °C for 30 sec; and, final extension of 72 °C for 10 min. The PCR products were observed in gel electrophoresis (1.5% agarose gel) with TAE 1x buffer (40 mM Tris-acetate and 1 mM EDTA) at 4 volts cm^{-1} for 2 hours. After, gels were stained with ethidium bromide (1 µg mL^{-1} in 0.1 M NH_4 acetate) for ten minutes and then visualized under ultraviolet light and documented.

Table 1. List of primers used in the RT-qPCR.

Putative Function	Primers	Sequence 5' – 3'
Family 18 glycoside hydrolase	Fam18hydrolase F	TGATGCCCTTATTCCTCTGG
	Fam18hydrolase R	TGGGTTTTGGTCTTTTGAGG
Family 10 glycoside hydrolase	Betaxylanase F	CTATCGCATCCACACCATTG
	Betaxylanase R	AGGTTCTGTCGGATTTGTGC
G2 mitotic-specific cyclin 1 2	G2cyclin F	CGCACAAGTGAACCAGAAGA
	G2cyclin R	CAGCGCGCATAGTTTCATAA
Peptidylprolyl isomerase	Peptidyiso F	TTTGATTCATCTCGCTCACG
	Peptidyiso R	TTTGGTGGGATAGCGTTAGG
Beta-hexosaminidase	Betaaminidase F	CCTCTTGGTGTGATCCGTTT
	Betaaminidase R	GATTTTGCTCATCGGCTTGT
Carboxypeptidase	Carbopeptidase F	CGCTGGGGAAGATGATTTTA
	Carbopeptidase R	TCCAGCGGATCTAACCATTC
Proline iminopeptidase	Proimunopep F	ACTTTGTCAACCGAGGATGG
	Proimunopep F	GAGTGTCCCGCATCTGAAAT
Pyruvate dehydrogenase kinase	Pyrukinase F	AAGGCTCAGCGATTAGACCA
	Pyrukinase R	AAGGTTCGCTGCTTGTTGAT
Aminotransferase	Aminotransferase F	GGCTTGGATTGTTGGAGTGT
	Aminotransferase R	GCTTCATAAATTCGGGTGGA

Following RNA isolation and DNase treatment performed previously to RNASeq, complementary DNA synthesis was performed with Kit RevertAid H Minus First Strand cDNA Synthesis (Fermentas) according to the manufacturer's recommendations. The cDNA was diluted in ultrapure water (1/20 v/v). The Bt2a/Bt2b and Ef5/Ef2, which encodes the beta-tubulin (BTub) and the elongation factor (EF) genes of *A. psidii*, respectively, were selected as the reference (Bini et al., 2018).

The reactions were prepared in final volume of 12.5 µl containing: 6.25 µl of Platinum® SYBR® Green qPCR SuperMix-UDG, 1 µl of each primer pair (10 pmol), 0.25 µl BSA (10 mg mL $^{-1}$), 0.25 µl ROX Reference Dye (50 nM), 2.5 µl cDNA and 1.25 µl ultrapure water. The samples were amplified in 7500 Fast Real-Time PCR System (Applied Biosystems) programmed for following conditions: 95 °C for 5 min; 35 cycles: 95 °C for 30 sec, 58 °C 45 sec; e, 95 °C for 15 sec, 60 °C for 1 min; 95 °C for 15 sec, and 60 °C for 15 sec (melting). The assay was conducted in duplicate techniques containing four biological replicates per sample.

The fluorescence-per-cycle data for each reaction were imported into the LinRegPCR program (Ramakers et al., 2003; Ruijter et al., 2009). LinReg-PCR was used to determine the cycle threshold

(Ct) value for each reaction and to determine the average amplification efficiency of each primer set. Only primers with amplification efficiencies of 1.6 or greater were used. The Pfaffl method was used to determine a relative quantification of the target genes in comparison to the reference gene (Pfaffl, 2001). Results were evaluated statistically using the relative expression software tool (Pfaffl et al. 2002).

Results

Extraction of total RNA from uredospores of *A. psidii*

The physical and chemical stimulus provided by dialysis membrane and cuticular waxes from *E. grandis, E. urophyla* and *E. urograndis* enabled *A. psidii* uredospore germination. However, the presence of infection structures as appressorium and germ tube was only observed when used cuticular waxes from *E. grandis* and *E. urograndis* (Figure 2).

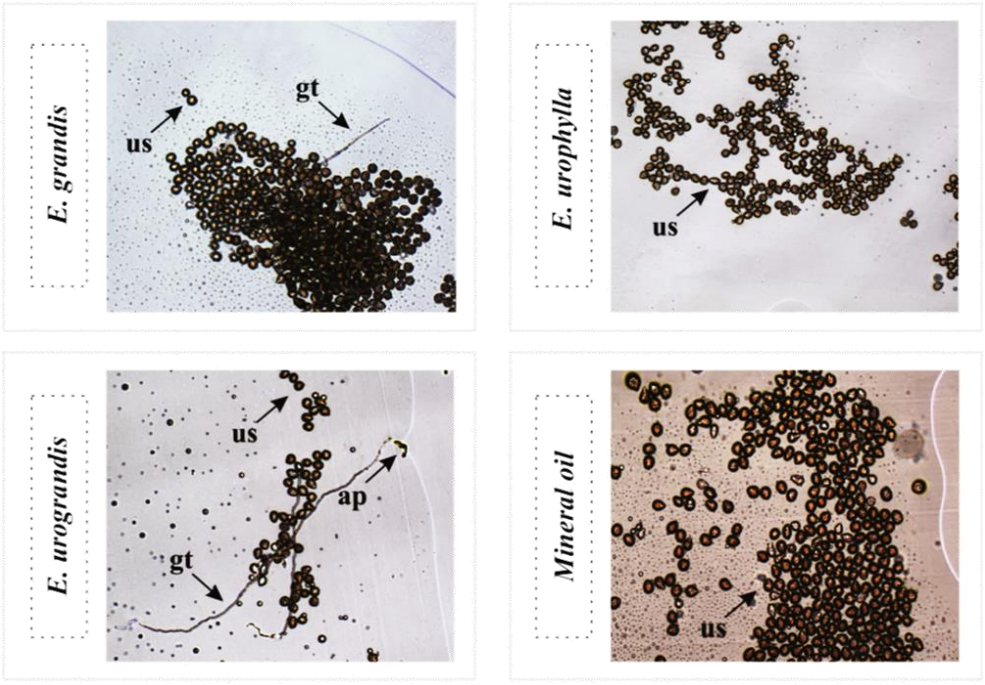

Figure 2. Germination and differentiation of *A. psidii* uredospores (18 h.p.i) in agar-water medium containing dialysis membrane and cuticular waxes from of *Eucalyptus* spp. contrasting degree of resistance to pathogen (*E. grandis, E. urograndis* and *E. urophylla*) and mineral oil (control). Legend: gt- germ tube; us – uredospores; ap – appressorium.

The sample RNA were extracted and the mean 260/280 nm and 260/230 ratios were 2.24 and 2.00, respectively. The extracted RNA integrity was analyzed by Agilent 2100 BioAnalyzer and the RIN (RNA integrity number) values were higher than the 8.6. None samples showed RNA degradation (Supplementary Figure 1).

Sequence Analyzing and Aligning to the Reference Genome

Sequencing provided 326,054,313 million paired-end (PE) reads per lane from Illumina HiSeq 2500 with average of 20,378,395 million PE reads per sample. After data preprocessing, i. e. removal of remaining adapter sequences and reads trimming, average number PE reads for each sample was 20,083,848 million and 101 (pb) length read, in a total 321,341,568 million PE reads (Supplementary Table S1). The assembly of preprocessed PE reads was using the unpublished *A. psidi* reference genome by Kallisto software. In total was processed 320,570,660 PE reads and 257,715,111 million pseudoalignments with average rate of 80.36% alignment (Supplementary Table 1).

Identification and DEGs analysis

Three comparative analyses were performed to identify the DEGs: *E. grandis* (*E. g* - susceptible) x mineral oil (MO), *E. urograndis* (*E. ug* - intermediate) x mineral oil (MO) and *E. urophylla* (*E. u* - resistant) x mineral oil (MO). In *E. u* x MO analysis were obtained the highest amount of DEG (851) followed by *E. g* x MO (487) and *E. ug* x MO (209). In average to all comparative analyses were obtained half of up/down regulated DEGs (Table 2).

Table 2. *A. psidii* DEGs according to *Eucalyptus* spp. cuticular wax sources.

Comparative analyses	DEG amount	DEG characterization		
		Known function	Hypothetical function	Uncharacterized function/NA
E. grandis x Mineral oil	Up: 224	54	123	47
	Down: 263	86	156	21
	Total: 487	140	279	68
E. urograndis x Mineral oil	Up: 109	24	55	30
	Down: 100	37	56	7
	Total: 209	61	111	37
E. urophylla x Mineral oil	Up: 402	108	220	74
	Down: 449	132	277	40
	Total: 851	240	497	114

* DEG *q-value* < 0.05

Venn's diagrams were constructed for a better view of distribution of DEGs with total (known, hypothetical and uncharacterized/NA) and known function. The total DEGs, 36 (up) and 40 (down) were exclusive in *E. g* x MO, followed by 16 (up) and 12 (down) in *E. ug* x MO; and 200 (up) and 204 (down) in *E. u* x MO (Figure 3 – A). Already, the total DEGs common in at least two comparison groups were 6 (up) and 1 (down) in susceptible (*E. g* x MO) and intermediate (*E. ug* x MO); 115 (up) and 158 (down) in susceptible (*E. g* x MO) and resistant (*E. u* x MO); 19 (up) and 24 in

intermediate (*E. ug* x MO) and resistant (*E. u* x MO) (Figure 3 – A). Finally, the total DEGs shared in the three comparison groups were 68 (up) and 63 (down) (Figure 3 – A).

The DEGs only with known function were can be viewed in Figure 3 (B). In relation to DEGs restricted to each comparison group 8 (up) and 9 (down) were exclusive in *E. g* x MO, followed by 6 (up) and 7 (down) in *E. ug* x MO, and 60 (up) and 49 (down) in *E. u* x MO. The DEGs common in at least two comparison groups were grouped this way: 1 (up) in susceptible (*E. g* x MO) and intermediate (*E. ug* x MO); 30 (up) and 53 (down) in susceptible (*E. g* x MO) and resistant (*E. u* x MO); and 3 (up) and 6 in intermediate (*E. ug* x MO) and resistant (*E. u* x MO) (Figure 3 – B). Ultimately, the known function DEGs shared in the three comparison groups were 15 (up) and 24 (down) (Figure 3 –B).

An overview of DEGs can be visualized in the figure 3 (C). The hierarchical clustering of DEGs to the three comparative analyses revealed a different profile according to *Eucalyptus* species cuticular waxes sources. In the comparison group *E. g* x MO showed a profile with a highest amount of DEG down-regulated. In contrasting, *E. u* x MO reveled a profile with a high amount of DEG up-regulated.

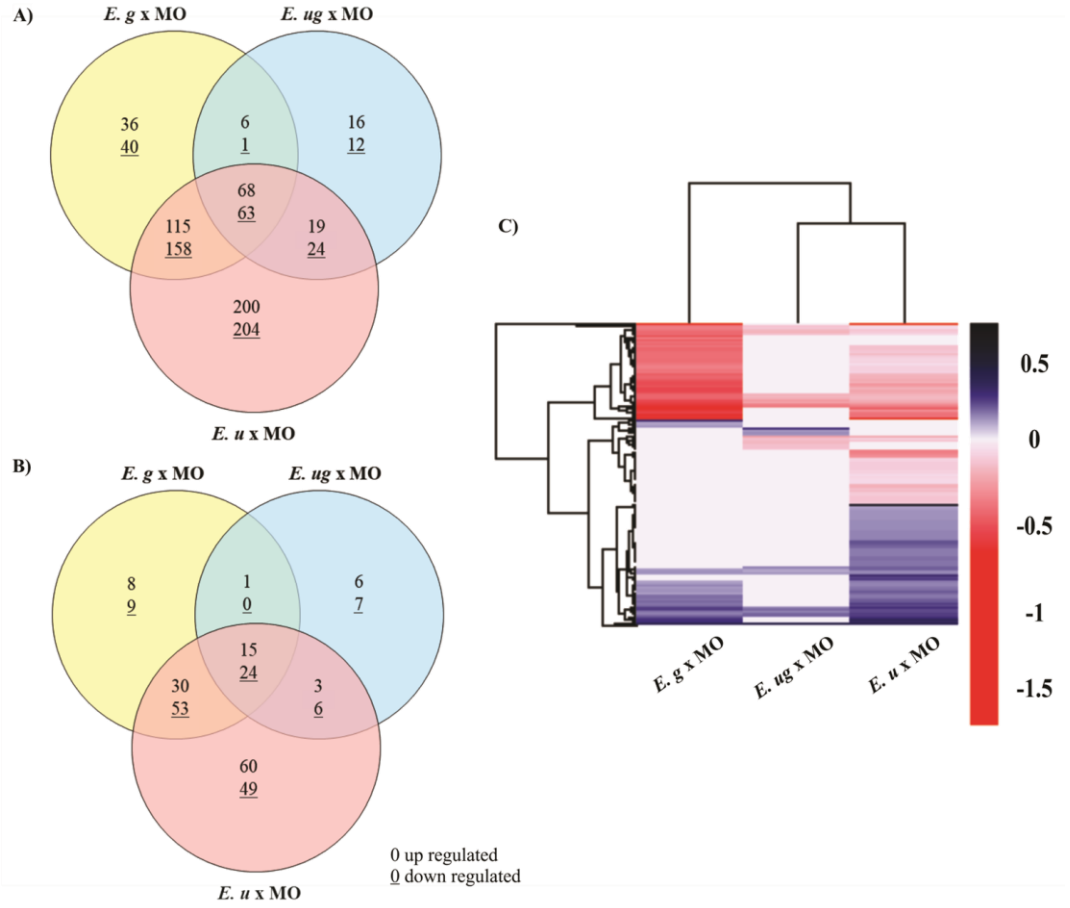

Figure 3. *A. psidii* DEGs in different cuticular waxes sources of *Eucalyptus* spp. Venn diagram (A and B): overlapping areas show the numbers of genes found to been congruently up/down regulated where A) total DEGs (known function, hypothetical function and uncharacterized/NA) and

B) known function DEGs. Heatmap (C): levels of expression are represented as Log2FC of TPM (transcripts per million) where dark blue indicates up-regulated and red signify down-regulated.

GO enrichment analyze

The GO enrichment analyses to biological function were performed for known function DEGs from all comparative analyses. The complete list of GO terms are shown in Appendix A and B. In particular, four GO terms, including proteins related with establishment (GO: 0045184), localization (GO: 0051641), cellular response to stimulus (GO: 0051716) and organelle organization (GO: 0006996), were exclusively enriched amongst DEGs from *E. g* x MO (susceptible) (Figure 4).

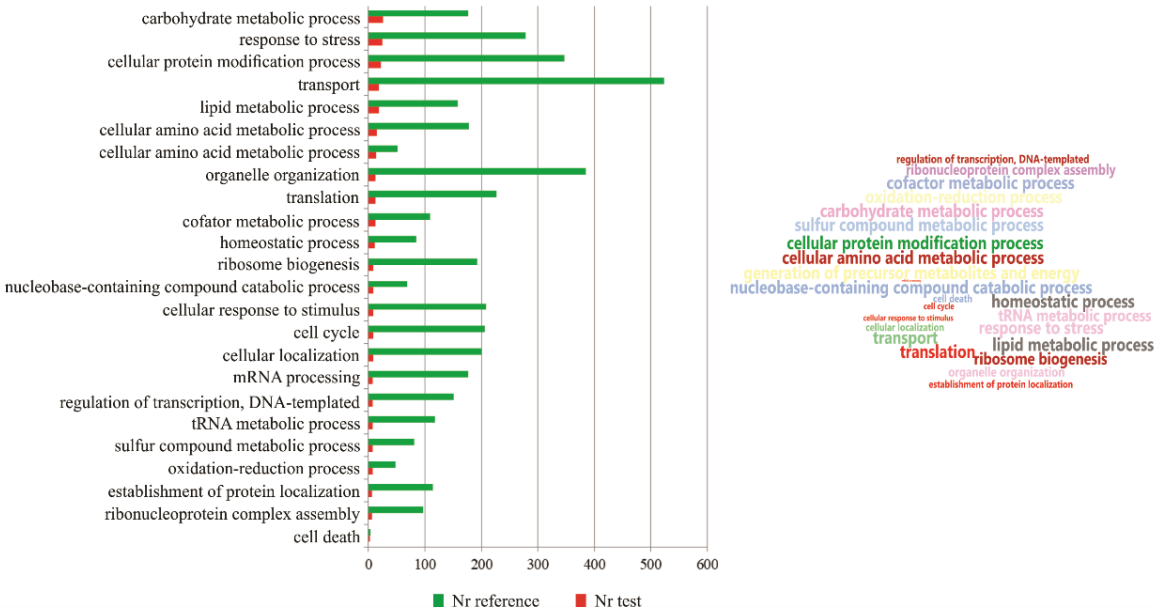

Figure 4. GO enrichment analysis of DEGs from *A. psidii* uredospore according to the *E. grandis* x MO analysis. Only biological process terms were considered in the analysis. It was applied Fisher's Exact Test < 0.05. Legend: Nr reference: DEGs; Nr test: Genome.

From *E. ug* x MO (intermediate) DEGs six GO terms were highlighted: anatomical structure development (GO: 0048856), regulation of gene expression (GO: 0010468), mRNA metabolic process (GO: 0016071), reproduction (GO: 0000003), regulation of cellular process (GO: 0010468) and cellular component organization (GO: 0016043) (Figure 5).

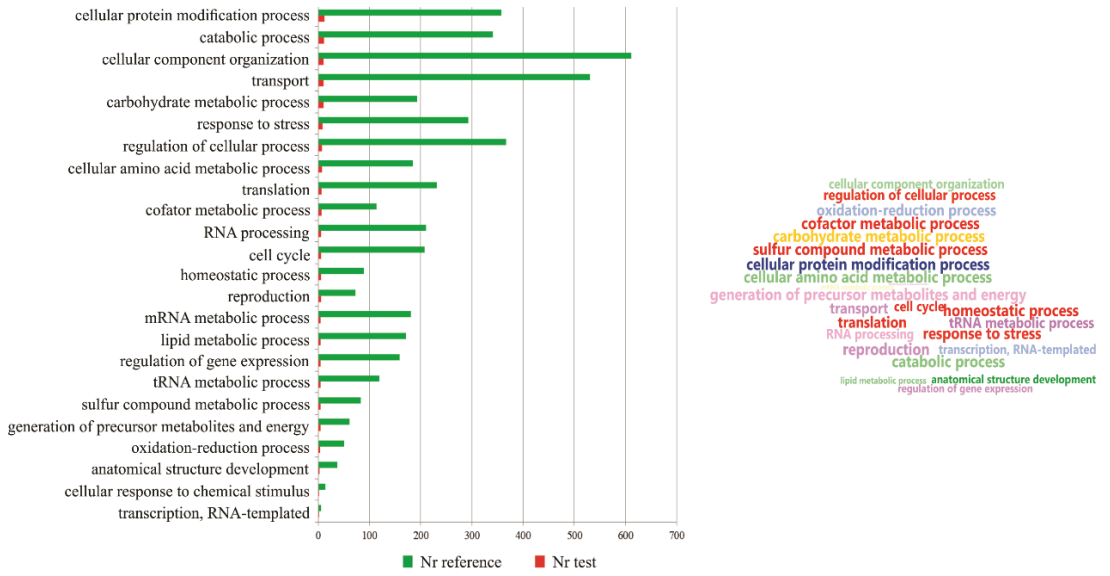

Figure 5. GO enrichment analysis of DEGs from *A. psidii* uredospore according to the *E. urograndis* x MO analysis. Only biological process terms were considered in the analysis. It was applied Fisher's Exact Test < 0.05. Legend: Nr reference: DEGs; Nr test: Genome.

Finally, greater enrichment was found in resistant *E. u* x MO, with exclusive GO terms as reciprocal meiotic recombination (GO: 0007131), cell budding (GO: 0007114), protein maturation (GO: 0051604), amongst others (Figure 6).

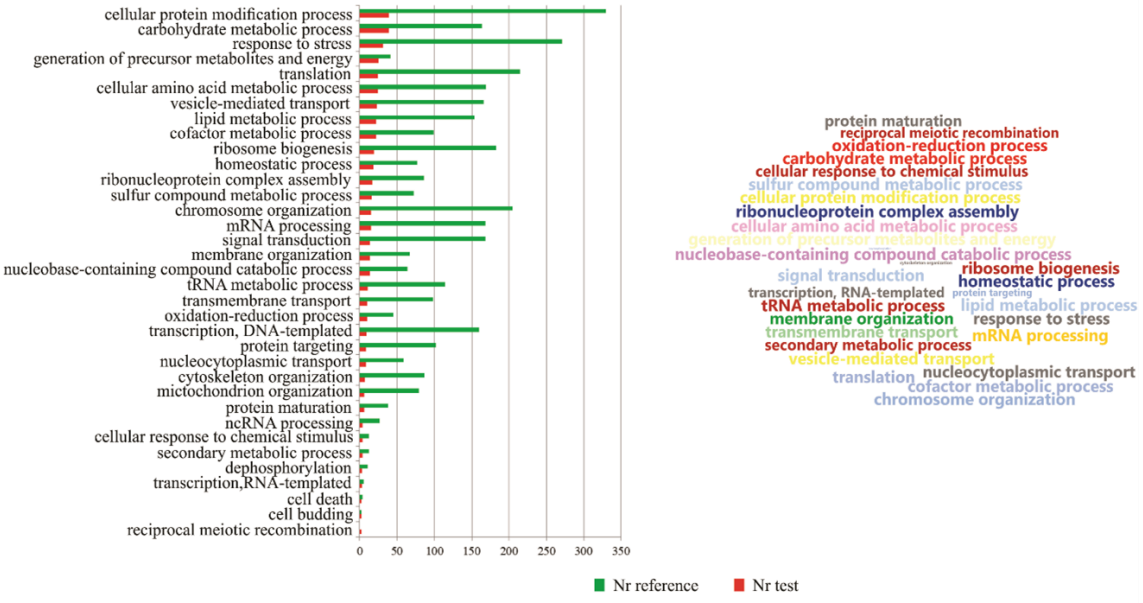

Figure 6. GO enrichment analysis of DEGs from *A. psidii* uredospore according to the *E. urophylla* x MO analysis. Only biological process terms were considered in the analysis. It was applied Fisher's Exact Test < 0.05. Legend: Nr reference: DEGs; Nr test: Genome.

Differential expression of pathogenicity related genes

Concerning the gene expression of *A. psidii* uredospores that was influenced by presence of cuticular waxes from *Eucalyptus* spp., top twenty DEGs with known function are shown in Table 3. The complete list is in Appendix C and D. Ten DEGs were common in three analysis. Few DEGs were shared among *E. g* x MO – *E. ug* x MO or *E. u* x MO – *E. ug* – MO, however, several DEGs were common to *A. psidii* in *E. g* x MO - *E. u* x MO (seven DEGs up and down). In *E. g* x MO and *E. u* x MO, genes encoding to chaperones, PCWDE (Plant Cell Wall Degrading Enzymes) as glycosyltransferases and glycosides hydrolases were up-regulated. *E. g* x MO and *E. u* x MO (resistant) shared DEGs down-regulated to proteins such as cell wall degradation (family 26 glycoside hydrolase and endoglucanase V), peroxidases (catalase), growth and adaptation (malate synthase A and cytochrome P450 monooxygenase) (Table 3).

It was observed that the cuticular waxes from *E. grandis* induced the expression of DEGs which encoding proteins related to growth and colonization of *A. psidii*, for instance, binding proteins (peptidylprolyl isomerase and ribosomal) and cell wall degrading proteins (beta-xylanase). In contrast, *E. grandis* cuticular waxes repressed DEGs that encoding pathogenic proteins such triosephosphate isomerase, family 18 glycoside hydrolase, mitochondrial ATP carrier and glutamine-dependent NAD synthetase. The DEGs up regulated by cuticular wax *E. urograndis* were related to secreted protein, family 4 carbohydrate esterase, DNA repair and recombination and protein kinase with repression of transmembrane transport and glycosyltransferases proteins. Already the cuticular waxes from *E. urophylla* were observed up-regulated DEGs associated to pheromone, cutinases and prefoldin. Finally, DEGs down regulated in presence of cuticular waxes from *E. urophylla* are listed to hydrolases families (family 18 and 23 glycoside hydrolase) and enzyme cofactors (thiamine pyrophosphokinase) (Table 3).

Table 3. Top 40 DEGs from *A. psidii*, up/down regulated, with known function and annotated by Blast2GO. The comparative analyses were *E. g* x MO, *E. ug* x MO and *E. u* x MO.

Function putative (Blast2Go)	***E. g* x MO**		***E. ug* x MO**		***E. u* x MO**	
	FC[1]	***Log2*FC[2]**	**FC[1]**	***Log2*FC[2]**	**FC[1]**	***Log2* FC[2]**
Zinc finger bed domain-containing protein day sleeper	1.25	0.32	1.18	0.23	1.2	0.26
Plasma membrane ATPase	1.19	0.25	1.12	0.16	1.21	0.28
TATA-box-binding protein	1.18	0.24	1.12	0.17	1.19	0.25
AGC NDR kinase	1.14	0.19	1.15	0.2	1.21	0.27
Histone H3	1.14	0.19	1.14	0.2	1.19	0.25
Thiamine thiazole synthase	0.38	-1.7	0.33	-1.59	0.27	-1.87
D-lactaldehyde dehydrogenase	0.62	-0.98	0.63	-0.66	0.62	-0.68
Aminotransferase	0.74	-0.72	0.75	-0.42	0.75	-0.42
Proline iminopeptidase	0.76	-0.68	0.76	-0.39	0.78	-0.35
Glyceraldehyde-3-phosphate dehydrogenase	0.76	-0.68	0.74	-0.43	0.76	-0.39
Molecular chaperone	1.57	0.65	-	-	1.7	0.76
Glutathione peroxidase	1.23	0.29	-	-	1.38	0.47
Family 71 glycosyltransferase	1.23	0.29	-	-	1.26	0.34
Trimethyllysine dioxygenase	1.23	0.29	-	-	1.27	0.34
Family 4 carbohydrate esterase	1.21	0.28	-	-	1.29	0.37
Small nuclear ribonucleo D3	1.18	0.24	-	-	1.23	0.3
Mitochondrial intermediate peptidase mitochondrial precursor	1.16	0.21	-	-	1.23	0.3
Family 26 glycoside hydrolase	0.4	-1.6	-	-	0.37	-1.45
Catalase	0.56	-1.13	-	-	0.55	-0.87
Glutamate decarboxylase	0.68	-0.84	-	-	0.69	-0.53
Malic enzyme	0.74	-0.73	-	-	0.77	-0.38
Glutamate decarboxylase	0.74	-0.72	-	-	0.73	-0.45
Cytochrome P450 monooxygenase	0.75	-0.71	-	-	0.74	-0.44
Carbohydrate-binding module family 12	0.76	-0.69	-	-	0.79	-0.33
Family 15 glycoside hydrolase	1.19	0.25	1.14	0.19	-	-
Serine/threonine protein kinase	1.17	0.23	1.1	0.14	-	-
Phosphoglucomutase	0.79	-0.63	0.83	-0.27	-	-
Family 26 glycoside hydrolase	-	-	1.14	0.19	1.19	0.25
Peptidylprolyl isomerase	1.27	0.34	-	-	-	-

Protein of RNA polymerase III Rpc4 family	1.24	0.31	-	-	-	-
RNA-binding domain protein	1.15	0.2	-	-	-	-
Beta-xylanase	1.14	0.19	-	-	-	-
Serine threonine kinase	1.14	0.19	-	-	-	-
Triosephosphate isomerase	0.76	-0.69	-	-	-	-
Family 18 glycoside hydrolase	0.79	-0.64	-	-	-	-
Mitochondrial ATP carrier	0.8	-0.61	-	-	-	-
Glutamine-dependent NAD() synthetase	0.8	-0.61	-	-	-	-
D-3-phosphoglycerate dehydrogenase	0.8	-0.61	-	-	-	-
Transposable element tc3 transposase	-	-	1.27	0.34	-	-
MFS general substrate transporter	-	-	1.23	0.3	-	-
Golgi SNAP receptor complex member 1	-	-	1.12	0.16	-	-
Ubiquitin-conjugating enzyme E2 N	-	-	1.12	0.16	-	-
Secreted protein	-	-	1.11	0.15	-	-
Family 4 carbohydrate esterase	-	-	1.1	0.14	-	-
DNA repair and recombination RAD54	-	-	1.1	0.13	-	-
Family 90 glycosyltransferase	-	-	1.09	0.13	-	-
GAF domain-like protein	-	-	1.09	0.12	-	-
STE/STE7/MKK protein kinase	-	-	1.09	0.12	-	-
Glycine dehydrogenase subunit 2	-	-	1.09	0.12	-	-
Transmembrane transport	-	-	0.8	-0.31	-	-
Nucleoside diphosphate kinase	-	-	0.81	-0.3	-	-
Pyruvate dehydrogenase kinase	-	-	0.82	-0.29	-	-
Ubiquitin 5	-	-	0.82	-0.29	-	-
60S acidic ribosomal P1	-	-	0.82	-0.28	-	-
MFS general substrate transporter	-	-	0.83	-0.26	-	-
Transaldolase	-	-	0.85	-0.23	-	-
Terpene cyclase/mutase family member	-	-	0.85	-0.23	-	-
Family 22 glycosyltransferase	-	-	0.86	-0.22	-	-
Mannosyltransferase	-	-	0.86	-0.22	-	-
Large subunit ribosomal L6e	-	-	0.86	-0.22	-	-
Carbohydrate kinase	-	-	0.86	-0.22	-	-
Asparagine synthetase	-	-	0.86	-0.21	-	-
Methylthioribose-1-phosphate isomerase	-	-	0.87	-0.2	-	-
Pheromone with four tandem repeats of a	-	-	-	-	1.57	0.65

putative pheromone peptide						
Cutinase	-	-	-	-	1.49	0.57
NADH dehydrogenase (Ubiquinone) Fe-S protein 7	-	-	-	-	1.24	0.32
TatD family	-	-	-	-	1.24	0.31
Prefoldin, alpha subunit	-	-	-	-	1.2	0.26
Splicing factor subunit	-	-	-	-	1.2	0.26
Reverse transcriptase domain protein	-	-	-	-	0.75	-0.41
Family 18 glycoside hydrolase	-	-	-	-	0.75	-0.41
Thiamine pyrophosphokinase	-	-	-	-	0.76	-0.4
Family 23 glycoside hydrolase	-	-	-	-	0.76	-0.4
Glutamate-cysteine ligase catalytic subunit	-	-	-	-	0.78	-0.36
60S acidic ribosomal protein P0	-	-	-	-	0.79	-0.34

* Legend: *q-value** $\leq$ 0.05 (*p-value* ajustado FDR). FC[1]: Fold-Change (FC): mean of TPM (transcripts per kilobase million) obtained by reason: TPM treatment/TPM control; Log2FC[2]: Base log (2) of FC.

Validation of RNA-seq data by quantitative RT-qPCR

DEGs randomly selected were validated by RT-qPCR. Due to low Log2FC values found in the RNASeq only three transcripts were statistically difference by RT-qPCR peptidylprolyl isomerase (up regulated in *E. g* x MO) and aminotransferase (down regulated in *E. ug* x MO and *E. u* x MO). However, all selected DEG showed the same expression perfil in RNASeq and RT-qPCR (Figure 7).

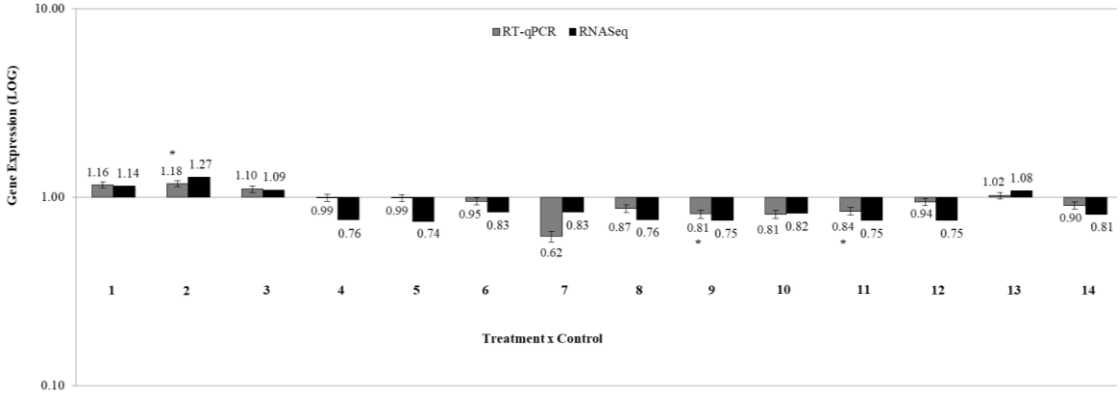

Figure 7. Relative expression of fourteen DEGs by RT-qPCR analysis. Relative gene expression was measured according to the Pfaffl method (PFAFFL, 2001). The statistical difference between the treatment (species) and the control (mineral oil) was calculated by the Pairwise Fixed Reallocation Randomization Test with bootstrap value = 1000. The significant comparison (specie x mineral oil) shows the symbol (*) at p <0.05. Error bars indicate standard error, n= 4. Four biological replicates including two technical replicates each were used for all samples in RT-qPCR analysis.

Grey columns represent relative expression measured by RT-qPCR. Black columns represent corresponding RNASeq data. Legend: *E. g* x MO: 1- family 10 glycoside hydrolase; 2- Peptidylprolyl isomerase; 3- G2 mitotic-specific cyclin 1 2; 4- proline iminopeptidase; 5- aminotransferase; 6- pyruvate dehydrogenase kinase; 7- family 20 glycoside hydrolase. *E. ug* x MO: 8- proline iminopeptidase; 9- aminotransferase; 10- pyruvate dehydrogenase kinase. *E. u* x MO: 11- aminotransferase; 12- family 18 glycoside hydrolase; 13- carboxypeptidase C; and 14- pyruvate dehydrogenase kinase.

Discussion

Cuticular wax is the first barrier that plants use to limit pathogen attack. Prior to engaging fully with plant resistance, fungal pathogens must first adhere to, recognize, respond to, and the grown on or through plant surfaces to initiate infection (Kubicek et al., 2014). In this study, we analyzed the transcriptome changes in *A. psidii* modulated by cuticular waxes from *Eucalyptus* spp. with different degree of resistance/susceptibility.

Initially we observed that the cuticular waxes influenced the germination and differentiation of *A. psidii* uredospores at 18 hours post inoculation (h.p.i.). In the presence of cuticular waxes from *E. grandis* (susceptible) and *E. urograndis* (intermediate), *A. psidii* uredospores formed germ tube and appressorium. It was not observed appressorium in *E. urophyla* and control (mineral oil). It is known that the early infection events, especially by *A. psidii*, include adherence to cuticle and direct germ tube grown on host plant surface with direct penetration, forming appressorium and haustorium. According to Xavier (2001) and Leite (2012) these processes occur until 12 h.p.i. independently of resistant or susceptible host. It is difficult to identify which signals *in planta* corresponding to signals present in our study. However, we observed that chemical signals from cuticular wax had a direct influence on gene expression, i. e. since the first contact pathogen - host, occur the repression/activation of genes related to fungal growth and differentiation (Van der Does and Rep, 2017). Our data corroborate the results from Santos et al (2019) that demonstrated that the cuticular waxes from *Eucalyptus* spp. assume a major role in preformed defense mechanism against *A. psidii*.

By Venn diagram we observed many DEGs were common to the three independent analyses. Interestingly, the analysis *E .u* x MO had the highest amount of exclusive DEGs (up and down regulated). *E. urophylla* is resistant specie to myrtle rust. Probably, during the interaction with this host, *A. psidii* tries to overcome the plant defense system using a larger arsenal of genes. Unfortunately, biotrophic colonization of plant cells is barely explored at the molecular level for either the pathogen or the host, especially in pathosystem *A. psidii* x *Eucalyptus* these studies are still very limited. Coram et al. (2008) showed that the incompatible interaction with *Puccinia striiformis f. sp. tritici* (*Pst*) conferred a greater diversity and number of DEGs, 115 induced by *Pst*-inoculation over

the time course and only one has been repressed. The *Pst*-induced DEGs involved in pathogen defense-related pathways, signal transduction, protein/carbohydrate transport, growth and metabolism.

Overall the GO enrichment was diverse presenting an overview of the pathways that are potentially important for *A. psidii* during the early infection in different *Eucalyptus* species. We observed that in presence of cuticular waxes from *E. grandis*, *A. psidii* has the proteins profile related to establishment, localization, cellular response to stimulus and organelle organization. Differently, cuticular waxes from *E. urograndis* and *E. urophylla* improved the presence DEGs encoding proteins related with metabolic process, cell budding, protein maturation, among others. Coram et al. (2008) obtained similar results with *Puccinia striiformis* Westend. f. sp. *tritici* Eriks (*Pst*) that causes the stripe rust in wheat (*Triticum aestivum* L.). The authors identified DEGs associated with incompatible (Yr5-mediated) and compatible (yr5-mediated) interactions. In the incompatible interaction were identified related DEGs to biological functions such as signal transduction, transport and metabolism; while in the compatible interaction were observed related basal defense processes.

The RNASeq analyses reveled that several DEGs up regulated were common to cuticular waxes *Eucalyptus* spp. regardless the susceptibility or resistance of the host, for instance, zinc finger, proteases, protein transporters, histones and kinases proteins. During infection, fungal pathogens activate virulence mechanisms, such as host adhesion, penetration and growth. Flor-Parra et al. (2006) described the importance of zinc finger proteins in the process appressorium formation and plant penetration by *Ustilago maydis*. According to the authors, this protein has a key role in for fungal pathogenic development. Other study has showed that protein kinases in *Fusarium oxysporum* are required for plant infection and controls process such vegetative hyphal fusion (López-Berges et al., 2010). However, in this research these proteins do not seem to be crucial for the process and establishment of *A. psidii* in *Eucalyptus* spp. The results found by Leite (2012) corroborate with our data, the author observed the process of germination, differentiation and colonization of *A. psidii* in resistant (R3) and susceptible (S4) genotypes of *E. grandis* and noted that there is no difference in process of germination of uredospores, formation of appressory and penetration of *A. psidii* in genotypes R3 and S4 up to 12 h.p.i.; after 12 h.p.i. the defense process begins in plants R3 and in genotype S4 continues the process of colonization by pathogen.

It was observed some DEGs up regulated encoding PCWDE were common between *E. grandis* - susceptible and *E. urophyla* - resistant species with higher Log2FC in *E. u* x MO analysis. Some transcriptome analysis has demonstrated that a large proportion of genes whose expression is up regulated upon host invasion are related to growth encode secreted enzymes, in particular, PCWDE and proteases. In some cases, the PCWDEs are expressed in early/biotrophic phases such as shows the study conducted by Haddadi et al. (2015) The authors observed that during *Leptosphaeria maculans* (hemibiotrophic fungal) x *Brassica napus* interaction, biotrophic phase, the most prevalent PCWDE at early stage of infection were glycoside hydrolases. Interestingly, it was observed that the expression of peroxidases, glycosyltransferases and esterases was higher in presence cuticular waxes from *E.*

urophylla perhaps this contributes to more rapid activation of the plant defense system resulting in the failure of infection by *A. psidii* in this specie.

The presence of *E. grandis* cuticular waxes induced the expression of DEGs encoding proteins such as beta-xylanase, an enzyme involved in cell wall modification/degradation of fungi/plants. These results corroborate the biotrophic lifestyle of *A. psidii* which has a very low penetration rate via stomates (approximately 2%) and penetrate through the cuticle and host epidermis, between the epidermal cell wall of the epidermal cell and after its penetration through the intracellular haustory, extract nutrients from the host cells (Glen et al., 2007; Silva et al., 2017). Ökmen et al. (2018) also found the presence of proteins such as xylanases, glucoses, glucanases, cellulases and galactosidases during the initial phase of infection in *Ustilago hordei*.

The expression of cutinases by *A. psidii* with higher Log2FC in *E. u* X MO suggests that pathogen has try in all ways infect the host tissue, but it is possibly detected by plant defense mechanism. The cutinases are secreted proteins involved in the degradation of the cuticle and Feng et al. (2009) and Weidenbach et al. (2014) demonstrated that germination and development of *Erysiphe necator*, biotrophic fungus causal agent powdery mildew in grapevine, is related to the secretion of fungal lytic enzymes as cutinases, esterases and lipases.

A small amount of DEGs down regulated were common to all analysis *E. g* x MO, *E. ug* x MO and *E. u* x MO. One of those DEGs was the aminotransferase. The repression of this enzyme may coordinate the carbon and nitrogen metabolism, i.e., it is critical nutrient acquisition and metabolism to pathogen (Wang et al., 2016). The aminotransferase repression was greater in *E. g* x MO, this is intriguing, because several studies such as Harata et al. (2016) report that the levels of expression of this enzyme are greater during the biotrophic stage than the development of appressory. In fact, it is supposed that *A. psidii* has a very refined pathogenic gene pool and during interaction with susceptible host (*E. grandis*) the fungus uses other proteins/enzymes than aminotransferase related to adhere, cuticule rupture, penetrate and colonize the host tissue.

The repression of exclusive genes of each analysis revealed proteins releated with *A. psidii* infection process. The pyruvate dehydrogenase kinase (PDK) was down regulated in the analysis *E. ug* x MO. The physiological roles of PDK in phytopathogens are largely unknown. However, Gao et al. (2016) isolated a PDK gene from *Fusarium graminearum*. After the knock-out of this gene, the authors observed several phenotypic phenomenos, such as growth delaying, failure in perithecia and conidia production and decrease pathogenicity of *F. graminearum*.

The cuticular wax from *E. grandis* down-regulated genes that encode pathogenicity proteins such as glycoside hydrolase, mitochondrial ATP carrier and glutamine-dependent NAD() synthetase. It is known that fungi produce a wide range of extracellular enzymes to break down plant cell walls. Among them are the glycoside hydrolases, the largest and most diverse family of extracellular enzymes (Murphy et al., 2011). Tao et al. (2017) investigated the transcriptomes of *Gymnosporangium yamadae* and *G. asiaticum*, causal agent apple rust and pear rust, respectively. The

authors verified that the presence some glycoside hydrolase families involved in fungal pathogenicity. Non-expecting, various DEGs that encode PCWDE were identified, the repression of family 18 glycoside hydrolase does not seem to have significant effect in pathogenicity of *A. psidii* in susceptible host (*E. grandis*).

Despite considerable advances in understanding of pathosystems over the past few years through RNASeq analyses, the understanding concerning the biotrophic early interaction established between *A. psidii* - *Eucalyptus* spp. that cause the myrtle rust is still very limited. To our knowledge, this study is the first reporting at the molecular level of *A. psidii* transcriptome. This provides the basis of hypotheses regarding cuticular waxes as an important source of preformed defense, protecting the host surface as well modulating the gene expression of pathogen during the crucial early interaction.

Supplementary Material

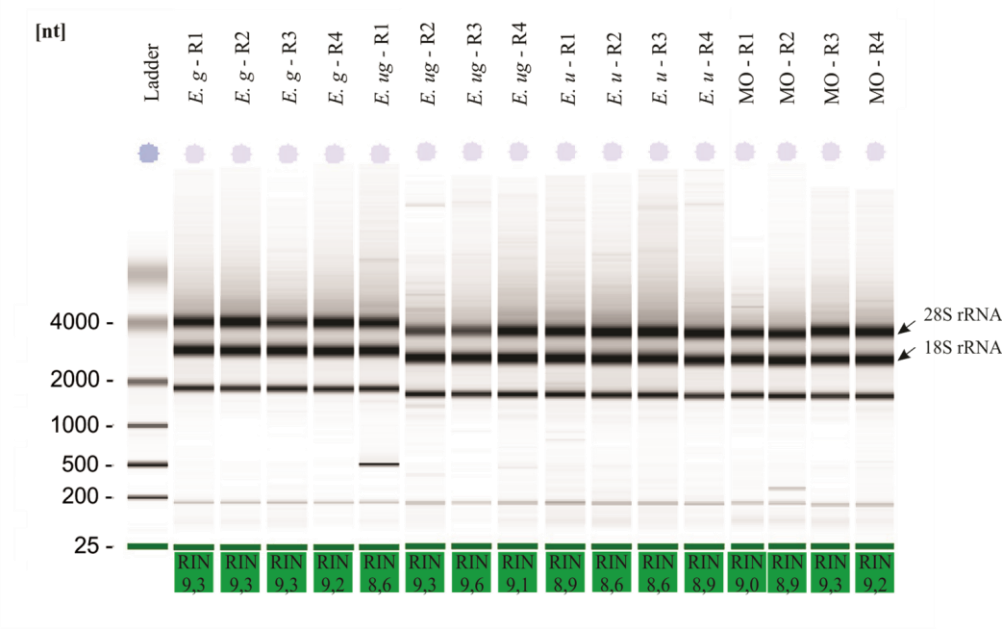

Figure S1. Total RNA of *A. psidii* uredospores (18 h.p.i.) germinated in agar-water solid medium supplemented with different cuticular waxes. Gel source Agilent 2100 Bioanalyzer. Legend: R: biological replicates. The arrows indicate the typical ribosomal subunits of eukaryotes (28S and 18S rRNA).

Table S1. Summary and alignment of paired-end reads with reference genome of *A. psidii* by Kallisto software.

Treatment	Sample	PE	Nº raw reads	Nº pre processed reads	Kallisto Pseudoalignment	
					Number	%
E. grandis	R1	1	20634652	20440960	16665423	81.1
		2	20845236	20647832		
E. grandis	R2	1	21289678	21297624	16973185	80.1
		2	21508258	21081468		
E. grandis	R3	1	20829166	20677078	16663928	80.2
		2	21054678	20898612		
E. grandis	R4	1	18601140	18440194	14829786	79.9
		2	18851134	18686770		
E. urograndis	R1	1	19312150	19136560	14829786	79.8
		2	19528610	19351022		
E. urograndis	R2	1	20167814	20027332	16238675	80.7
		2	20377456	20234206		
E. urograndis	R3	1	21629400	21452734	17426241	80.8
		2	21857782	21676518		
E. urograndis	R4	1	21043608	20744648	16779598	80.5
		2	21278400	20975084		
E. urophylla	R1	1	20760426	20503966	16625484	80.7
		2	20967492	20708578		
E. urophylla	R2	1	20332294	20068836	16307945	80.9
		2	20586982	20318414		
E. urophylla	R3	1	21326566	21055390	16996954	80.3
		2	21555988	21279572		
E. urophylla	R4	1	20679848	18893798	14896484	78.4
		2	20903550	19095514		
Mineral oil	R1	1	20652406	20495790	16739424	81.1
		2	20929846	20770030		
Mineral oil	R2	1	20030326	20252652	16154800	80.7
		2	20490170	19800144		
Mineral oil	R3	1	16547874	16306758	13128779	80.1
		2	16744768	16500018		
Mineral oil	R4	1	20512592	20305314	16458619	80.6
		2	20770724	20559720		

References

Beenken, L. 2017. *Austropuccinia*: A new genus name for the myrtle rust *Puccinia psidii* placed within the redefined family Sphaerophragmiaceae (Pucciniales). Phytotaxa, 297: 53–61. doi: 10.11646/phytotaxa.297.1.5.

Bini, A. P., Quecine, M. C., Silva, T. M., Silva, L. D., Labate, C. A. (2018). Development of a quantitative real-time PCR assay using SYBR Green for early detection and quantification of Austropuccinia psidii in Eucalyptus grandis. Eur. J. Plant Pathol. 150, 735–746. doi: 10.1007/s10658-017-1321-7.

Bini, A. P., Pachon, D. M. R., Almeida, J. R., Franceschini, L. M., Tsui, S., Lopes, M. S., Santos, I. B., Labate, C. A., Quecine, M. C. 2017. Deciphering the biology of *Austropuccinia psidii* from 'omics' approaches. In: 29º Congresso Brasileiro de Microbiologia, 2017, Foz de Iguaçu-PR.

Bini AP (2016). Estudo molecular do desenvolvimento de Puccinia psidii Winter in vitro e no processo de infecção em Eucalyptus grandis. Thesis. University of São Paulo - "Luiz de Queiroz" College of Agriculture, Piracicaba, Brazil.

Bray, N. L., Pimentel, H., Melsted, P., Pachter, L. 2016. Near-optimal probabilistic RNA-seq quantification. Nature Biotechnology, 34: 5: 525-7. doi: 10.1038/nbt.3519.

Bolger, A. M., Lohse, M., Usadel, B. 2014. Trimmomatic: a flexible trimmer for Illumina sequence data. Bioinformatics, 30: 15: 2114-20. doi: 10.1093/bioinformatics/btu170.

Buschhaus, C., Jetter, R. 2011. Composition differences between epicuticular and intracuticular wax substructures: How do plants seal their epidermal surfaces? Journal of Experimental Botany, 62: 841–853. doi: 10.1093/jxb/erq366.

Carnegie, A. J., Lidbetter, J. R., Walker, J., Horwood, M. A., Tesoriero, L., Glen, M., Priest, M. 2010. Uredo rangelii, a taxon in the guava rust complex, newly recorded on Myrtaceae in Australia. Australasian Plant Pathology, 39: 463–466. doi: 10.1071/AP10102.

Carnegie, A. J., Kathuria, A., Pegg, G. S., Entwistle, P., Nagel, M., Giblin, F. R. 2016. Impact of the invasive rust *Puccinia psidii* (myrtle rust) on native Myrtaceae in natural ecosystems in Australia. Biological invasions, 18: 127–144. doi: 10.1007/s10530-015-0996-y.

Coram, T. E., Wang, M., Chen, Z. 2008. Transcriptome analysis of the wheat Puccinia striiformis f. sp. tritici interaction. Molecular Plant Pathology, 9: 2: 157-169. doi: 10.1111/j.1364-3703.2007.00453.x.

Conesa, A., Madrigal, P., Tarazona, S., Gomez-Cabrero, D., Cervera, A., McPherson, A., Szczesniak, M. W., Gaffney, D. J., Elo, L. L., Zhang, X., Mortazavi, A. 2016. A survey of best practices for RNA-Seq data analysis. Genome Biology, 17: 13: 1-13. doi: 10.1186/s13059-016-0881-8.

Conesa, A., Gotz, S., Garcia-Gomez, J. M., Terol. J., Talon, M., Robles, M. 2005. Blast2GO: a universal tool for annotation, visualization and analysis in functional genomics research. Bioinformatics, 21: 3674–3676. doi: 10.1093/bioinformatics/bti610.

De Carvalho, M. C., Costa, N. L., Darben, L. M., Polizel-Podanosqui, A. M., Lopes-Caitar, V. S., Qi, M., Rocha, C. S., Carazzolle, M. F., Kuwahara, M. K., Pereira, G. A., Abdelnoor, R. V., Whitham, S. A., Marcelino-Guimarães, F. C. 2017. Prediction of the in planta *Phakopora pachyrhizi* secretome and potential effector families. Molecular Plant Pathology, 18: 3: 363-377. doi: 10.1111/mpp.12405.

Du Plessis, E., McTaggart, A. R., Granados, G. M., Wingfield, M. J., Roux, J., Pegg, G. S., Ali, M. I. M., Makinson, J., Purcell, M. 2017. First Report of Myrtle Rust Caused by Austropuccinia psidii on Rhodomyrtus tomentosa (Myrtaceae) from Singapore. Plant Disease, 101: 9: 1676. doi: 10.1094/PDIS-04-17-0530-PDN.

Feng, J., Wang, F., Liu, G., Greenshields, D., Shen, W., Kaminskyj, S., Hughes, G. R., Peng, Y., Selvaraj, G. Zou, J., Wei, Y. 2009. Analysis of Blumeria graminis secreted lipase reveals the importance of host epicuticular wax components for fungal adhesion and development. Molecular Microbe Interaction, 22: 1601-1610. doi: 10.1094/MPMI-22-12-1601.

Flor-Parra, I., Vranes, M., Kämper, J., Pèrez-Martin, J. 2006. Biz1, a Zinc Finger Protein Required for Plant Invasion by Ustilago maydis, Regulates the Levels of a Mitotic Cyclin. The Plant Cell, 18: 2369–2387. doi: 10.1105/tpc.106.042754.

Gao, T., Chen, J., Shi, Z. 2016. Fusarium graminearum pyruvate dehydrogenase kinase 1 (FgPDK1) is critical for conidiation, mycelium growth, and pathogenicity. Plos One, 11: 6: e0158077. doi: 10.1371/journal.pone.0158077.

Garnica, D. P., Upadhyaya, N. M., Dodds, P. N., Rathjen, J. P. 2013. Strategies for wheat stripe rust pathogenicity identified by transcriptome sequencing. Plos One, 8: 6: 1-17. doi: 10.1371/journal.pone.0067150.

Glen, M., Alfenas, A. C., Zauza, E. A. V., Wingfield, M. J., Mohammed, C.2007. Puccinia psidii: A threat to the Australian environment and economy—A review. Australasian Plant Pathology, 36: 1–16. doi: 10.1071/AP06088.

Granados, G. M., McTaggart, A. R., Barnes, I., Rodas, C. A., Roux, J., Wingfield, M. J. 2017. The pandemic biotype of *Austropuccinia ps*idii discovered in South America. Australasian Plant Pathology, 46: 267–275. doi: 10.1007/s13313-017-0488-x.

Haas, B. J., Papanicolaou, A., Yassour, M., Grabherr, M., Blood, P. D., Bowden, J., Couger, M. B., Eccles, D., Li, B., Lieber, M., Macmanes, M. D., Ott, M., Orvis, J., Pochet, N., Strozzi, F., Weeks, N., Westerman, R., William, T., Dewey, C. N., Henschel, R., Leduc, R. D., Friedman, N., Regev, A. 2013. De novo transcript sequence

reconstruction from RNA-Seq: reference generation and analysis with Trinity. Nature Protocols, 8: 8: 1-43. doi: 10.1038/nprot.2013.084.

Haddadi, P., Ma, L., Wang, H., Borhan, M. H. 2015. Genome-wide transcriptomic analyses provide insights into the lifestyle transition and effector repertoire of Leptosphaeria maculans during the colonization of Brassica napus seedlings. Molecular Plant Pathology, 17: 8: 1196-1210. doi: 10.1111/mpp.12356.

Harata, K., Nishiuchi, T., Kubo, Y. 2016. Colletotrichum orbiculare WHI2, a Yeast Stress-Response Regulator Homolog, Controls the Biotrophic Stage of Hemibiotrophic Infection through TOR Signaling. Molecular Plant-Microbe Interactions, 29: 6: 468-483. doi: 10.1094/MPMI-02-16-0030-R.

Hayden, K. J., Garvelotto, M., Knaus, B. J., Cronn, R. C., Rai, H., Wright, J. W. 2014. Dual RNA-seq of the plant pathogen Phytophthora ramorum and its tonoak host. Tree Genetics and Genomes, 10: 3: 489-502. doi: 10.1007/s11295-014-0698-0.

Joffily, J. 1944. Eucalyptus Rust. Bragantia, 4, 475-487. doi: 10.1590/S0006-87051944000300001.

Kawanishi, T., Uemastu, S., Kakishima, M., Kagiwada, S., Hamamoto, H., Horie, H., & Namba, S. 2009. First report of rust disease on ohia and the causal fungus, Puccinia psidii, in Japan. Journal of General Plant Pathology, 75: 428–431. doi: 10.1007/s10327-009-0202-0.

Kern, F. D., Toro, R. A. 1935. Notes on some fungi from Colombia. Mycologia, 27: 615–617. doi: 10.1080/00275514.1927.12020553.

Kubicek, C. P., Starr, T. L., Glass, N. L. 2014. Plant cell wall-degrading enzymes and their secretion in plant-pathogenic fungi. Annual Review of Phytopathology, 52: 427-451. doi: 10.1146/annurev-phyto-102313-045831.

Lanver, D., Berndt, P., Tollot, M., Naik, V., Vranes, M., Warmann, T., Munch, K., Rossel, N., Kahmann, R. 2014. Plant surface cues prime Ustilago maydis for biotrophic development. Plos Pathogens, 10: 7: 1-14. doi: 10.1371/journal.ppat.1004272.

Leite TF (2012). Estabelecimento de um patossistema modelo e análise da interação molecular planta-patógeno entre Eucalyptus grandis e Puccinia psidii Winter por meio da técnica de Rna-seq. Thesis. . University of São Paulo - “Luiz de Queiroz” College of Agriculture, Piracicaba, Brazil.

López-Berges, M. S., Rispail, N., Prados-Rosales, R. C., Di Pietro, A. 2010. A Nitrogen Response Pathway Regulates Virulence Functions in Fusarium oxysporum via the Protein Kinase TOR and the bZIP Protein MeaB. Plant Cell, 22: 7: 2459-75. doi: 10.1105/tpc.110.075937.

MacLachlan, J. D. 1938. A rust of the pimento tree in Jamaica, B.W.I. Phytopathology, 28: 157–170.

McTaggart, A. R., Roux, J., Granados, G. M., Gafur, A., Tarrigan, M., Santhakumar, P., Wingfield, M. J. 2016. Rust (*Puccinia psidii*) recorded in Indonesia poses a threat to forests and forestry in South-East Asia. Australasian Plant Pathology, 45: 83–89. doi: 10.1007/s13313-015-0386-z.

Mohali, S. R., Aime, M. C. 2016. First report of *Puccinia psidii* (myrtle rust) on *Syzygium jambos* in Venezuela. New Disease Reports, 34: 18. doi: 10.5197/j.2044-0588.2016.034.018.

Murphy, C., Powlowski, J., Wu, M., Butler, G., Tsang, A. 2011. Curation of characterized glycoside hydrolases of fungal origin. Database, 2011: bar020. doi: 10.1093/database.

Ökmen, B., Mathow, D., Hof, A., Lahrmann, U., Abmann, D., Doehlemann, G. 2018. Mining the effector repertoire of the biotrophic fungal pathogen Ustilago hordei during host and non-host infection. Molecular Plant Pahtology, 19: 12: 2603-2622. doi: 10.1111/mpp.12732.

Pfaffl, M. W., Horgan, G. W., Dempfle, L. 2002. Relative expression software tool (REST©) for group-wise comparison and statistical analysis of relative expression results in real-time PCR. Nucleic Acids Research, 30: 9: e36.

Pfaffl, M. W. 2001. A new mathematical model for relative quantification in real-time RT-PCR. Nucleic Acids Research, 29: 9: e45. doi.org/10.1093/nar/29.9.e45.

Pegg, G., Taylor, T., Entwistle, P., Guymer, G., Giblin, F., Carnegie, A. 2017. Impact of *Austropuccinia psidii* (myrtle rust) on Myrtaceae-rich wet sclerophyll forests in south east Queensland. Plos One, 12: e0188058. doi: 10.1371/journal.pone.0188058.

Pegg, G. S., Giblin, F. R., McTaggart, A. R., Guymer, G. P., Taylor, H., Ireland, K. B., Shivas, R. G., Perry, S. 2014. *Puccinia psidii* in Queensland, Australia: disease symptoms, distribution and impact. Plant Pathology, 63: 1005–1021. doi: 10.1111/ppa.12173.

Pérez, C. A., Wingfield, M. J., Altier, N. A., Simeto, S., & Blanchette, R. A. 2011. *Puccinia psidii* infecting cultivated *Eucalyptus* and native myrtaceae in Uruguay. Mycological Progress, 10: 273–282. doi: 10.1007/s11557-010-0698-x.

Pimentel, H., Bray, N. L., Puente, S., Melsted, P., Pachter, L. 2017. Differential analysis of RNA-seq incorporating quantification uncertainty. Nature Methods, 14: 7: 687-390. doi: 10.1038/nmeth.4324.

Quecine, M. C., Bini, A. P., Romagnoli, E. R., Andreote, F. D., Moon, D. H., Labate, C. A. 2014. Genetic variability in *Puccinia psidii* populations as revealed by PCR-DGGE and T-RFLP markers. Plant disease, 98: 1: 16- 23. doi: 10.1094/PDIS-03-13-0332-RE.

Ramakers, C., Ruijter, J. M., Deprez, R. H., Moorman, A. F. 2003. Assumption-free analysis of quantitative real-time polymerase chain reaction (PCR) data. Neuroscience Letters, 13: 339: 1: 62-6. doi: 10.1016/S0304-3940(02)01423-4.

Rampant, P. F., Lesur, I., Boussardon, C., Bitton, F., Martin-Magniett, M. L., Bodenes, C., Le Provost, G., Berges, H., Fluch, S., Kremer, A., Plomion, C. 2011. Analysis of BAC end sequences in oak, a keystone forest tree species, providing insight into the composition of its genome. BMC Genomics, 12:292. doi: 10.1186/1471-2164-12-292.

Roux, J., Greyling, I., Coutinho, T. A., Verleur, M., & Wingfield, M. J. (2013). The Myrtle rust pathogen, Puccinia psidii, discovered in Africa. IMA Fungus, 4: 155–159. doi: 10.5598/imafungus.2013.04.01.14.

Roy, B. A., Alenxander, H. M., Davidson, J., Campbell, F. T., Burdon, J. J., Sniezko, R., Brasier, C. 2014. Increasing forest loss worldwide from invasive pests requires new trade regulations. Frontiers in Ecology and the Environment, 12: 457–465. doi: 10.1890/130240.

Rossman, A. Y. 2009. The impact of invasive fungi on agricultural ecosystems in the United States. Biological Invasions, 11: 97–107. doi: 10.1007/s10530-008-9322-2.

Ruijter, J. M., Ramakers, C., Hoogaars, W. M., Karlen,Y., Bakker, O., Van den Hoff, M. J., Moorman, A. F. 2009. Amplification efficiency: linking baseline and bias in the analysis of quantitative PCR data. Nucleic Acids Reasearch, 37: 6: e45. doi: 10.1093/nar/gkp045.

Silva, R. R., Silva, A. C., Rodella, R. A., Serrão, J. E., Zanuncio, J. C., Furtado, E. L. 2017. Pre-infection stages of Austropuccinia psidii in the epidermis of Eucalyptus hybrid leaves with diferente resistance levels. Forests, 8: 362. doi:10.3390/f8100362.

Silveira, R. L. V. A. Higashi, E. N. 2003. Aspectos nutricionais envolvidos na ocorrência de doenças com ênfase para o eucalipto. Circular Técnica, Instituto de Pesquisa e Estudos Florestais, 200, 1-13.

Stewart, J. E., Ross-Davis, A. L., Graça, R. N., Alfenas, A. C., Peever, T. L., Hanna, J. W., Uchida, J. Y, Hauff, R. S., Kadooka, C. Y., Kim, M. S., Cannon, P. G., Namba, S., Simeto, S., Pérez, C. A., Rayamajhi, M. B., Lodge, D. J., Arquedas, M., Medel-Ortiz, R., Lópes-Ramirez, M. A., Tennant, P., Glen, M., Machado, P. S., McTaggart, A. R., Carnegie, A. J., Klopfenstein, N. B. 2018. Genetic diversity of the myrtle rust pathogen (*Austropuccinia psidii*) in the Americas and Hawaii: Global implications for invasive threat assessments. Forest Pathology, 48: 1: 1-13. doi: 10.1111/efp.12378.

Takahashi SS (2002). Ferrugem do eucalipto: Índice de infecção, análise temporal e estimativas de danos relacionados à intensidade da doença no campo. Dissertation, School of São Paulo State University Julio de Mesquita Filho, Botucatu, Brazil.

Taniguti, L. M., Schaker, P. D. C., Benevenuto, J., Peters, L. P., Carvalho, G., Palhares, A., Quecine, M. C., Nunes, F. R. S., Kmit, M . C. P., Wai, A., Hausner, G., Aitken, K. S., Berkman, P. J., Fraser, J. A., Moolhuijzen, P. M., Coutinho, L. L., Creste, S., Vieira, M. L. C., Kitajima, J. P., Monteiro-Vitorello, C. B. 2015. Complete genome sequence of Sporisorium scitamineum and biotrophic interaction transcriptome with sugarcane. Plos One, 10: 6: e0129318. doi:10.1371/journal.pone.0129318.

Tao, S. Q., Cao, B., Tian, C. M., Liang, Y. M. 2017. Comparative transcriptome analysis and identification of candidate effectors in two related rust species (Gymnosporangium yamadae and Gymnosporangium asiaticum). BMC Genomics, 18: 654. doi: 10.1186/s12864-017-4059-x.

Tommerup, I. C., Alfenas, A. C., & Old, K. M. 2003. Guava rust in Brazil ‐ a threat to *Eucalyptus* and other Myrtaceae. New Zealand Journal of Forestry Science, 33: 420–428.

Uchida, J., Zhong, S., Killgore, E. 2006. First report of a rust disease on Ohia caused by *Puccinia psidii* in Hawaii. Plant Disease, 90: 4: 524. doi: 10.1094/PD-90-0524C.

Van Der Does, H. C., Rep, M. 2017. Adaptation to the host environment by plant-pathogenic fungi. Annual Review of Phytopathology, 15: 31: 1-24. doi: 10.1146/annurev-phyto-080516-035551.

Wang, Z., Gerstein, M, Snyder, M. 2009. RNA-Seq: a revolutionary tool for transcriptomics. Nature Reviews Genetics, 10: 1-7. doi: 10.1038/nrg2484.

Wang, L., Wang, S., Li, W. 2012. RSeQC: quality control of RNA-seq experiments. Bioinformatics, 28: 16: 2184-5. doi: 10.1093/bioinformatics/bts356.

Wang, R., Zhang, M., Liu, H., Xu, J., He, F., Zhang, X., Dong, S., Dou, D. 2016. PsAAT3, an oomycete-specific aspartate aminotransferase, is required for full pathogenicity of the oomycete pathogen Phytophthora sojae. Fungal Biology, 120: 4: 620-630. doi: 10.1016/j.funbio.2016.01.005.

Weidenbach, D., Jansen, M., Franke, R. B., Hensel, G., Weissgerber, W., Ulferts, S., Jansen, I., Schreiber, L., Korzun, V., Pontzen, R., Kumlehn, J., Pillen, K., Schaffrath, U. 2014. Evolutionary conserved function of barley and Arabidopsis 3-ketoacyl-CoA synthases in providing wax signals for germination of powdery mildew fungi. Plant Physiology, 166: 1621-1633. doi: 10.1104/pp.114.246348.

Winter, G. 1884. Repertorium. Rabenhorstii fungi europaei et extraeuraopaei. Cent. XXXI et XXXII. Hedwigia 23:164–172.

Xavier, A. A., Alfenas, A. C., Matsuoka, K., Hodges, C. S. 2001. Infection of resistant and susceptible Eucalyptus grandis genotypes by urediniospores of Puccinia psidii. Australas. Plant Pathol. 30: 277-281, doi: 10.1071/AP01038.

Zhao, S., Fung-Leung, W. P., Bittner, A., Ngo, K., Liu, X. 2014. Comparison of RNA-Seq and microarray in transcriptome profiling of activated T cells. Plos One, 9: 1: 1-13. doi: 10.1371/journal.pone.0078644.

Zhuang, J. Y., Wei, S. X. 2011. Additional materials for the rust flora of Hainan Province, China. Mycosystema, 30, 853–860.

4. ADDITIONAL INFORMATION

Additional information 1. Trimmomatic:

T2R1:

TrimmomaticPE: Started with arguments: -threads 10 -phred33 /media/hd_externo_3/genoma_carol/Rna_Seq_Isaneli/Amostras/T2R1/T2R1_S1_L001_R1_001.fastq.gz /media/hd_externo_3/genoma_carol/Rna_Seq_Isaneli/Amostras/T2R1/T2R1_S1_L001_R2_001.fastq.gz T2R1_S1_L001_R1_001_forward_paired.fq.gz T2R1_S1_L001_R1_001_forward_unpaired.fq.gz T2R1_S1_L001_R2_001_reverse_paired.fq.gz T2R1_S1_L001_R2_001_reverse_unpaired.fq.gz ILLUMINACLIP:/media/hd_externo_3/genoma_carol/Trimmomatic-0.36/adapters/TruSeq3-PE.fa:2:30:10:5:true MAXINFO:60:0.85 MINLEN:60
Using PrefixPair: 'TACACTCTTTCCCTACACGACGCTCTTCCGATCT' and 'GTGACTGGAGTTCAGACGTGTGCTCTTCCGATCT'
ILLUMINACLIP: Using 1 prefix pairs, 0 forward/reverse sequences, 0 forward only sequences, 0 reverse only sequences
Input Read Pairs: 10317326 Both Surviving: 10310152 (99.93%) Forward Only Surviving: 0 (0.00%) Reverse Only Surviving: 326 (0.00%) Dropped: 6848 (0.07%)
TrimmomaticPE: Completed successfully
TrimmomaticPE: Started with arguments: -threads 10 -phred33 /media/hd_externo_3/genoma_carol/Rna_Seq_Isaneli/Amostras/T2R1/T2R1_S1_L002_R1_001.fastq.gz /media/hd_externo_3/genoma_carol/Rna_Seq_Isaneli/Amostras/T2R1/T2R1_S1_L002_R2_001.fastq.gz T2R1_S1_L002_R1_001_forward_paired.fq.gz T2R1_S1_L002_R1_001_forward_unpaired.fq.gz T2R1_S1_L002_R2_001_reverse_paired.fq.gz T2R1_S1_L002_R2_001_reverse_unpaired.fq.gz ILLUMINACLIP:/media/hd_externo_3/genoma_carol/Trimmomatic-0.36/adapters/TruSeq3-PE.fa:2:30:10:5:true MAXINFO:60:0.85 MINLEN:60
Using PrefixPair: 'TACACTCTTTCCCTACACGACGCTCTTCCGATCT' and 'GTGACTGGAGTTCAGACGTGTGCTCTTCCGATCT'
ILLUMINACLIP: Using 1 prefix pairs, 0 forward/reverse sequences, 0 forward only sequences, 0 reverse only sequences
Input Read Pairs: 10422618 Both Surviving: 10414586 (99.92%) Forward Only Surviving: 1201 (0.01%) Reverse Only Surviving: 0 (0.00%) Dropped: 6831 (0.07%)
TrimmomaticPE: Completed successfully

T2R2:

TrimmomaticPE: Started with arguments: -threads 10 -phred33 T2R2_S2_L001_R1_001.fastq.gz T2R2_S2_L001_R2_001.fastq.gz T2R2_S2_L001_R1_001_forward_paired.fq.gz T2R2_S2_L001_R1_001_forward_unpaired.fq.gz T2R2_S2_L001_R2_001_reverse_paired.fq.gz T2R2_S2_L001_R2_001_reverse_unpaired.fq.gz ILLUMINACLIP:/media/hd_externo_3/genoma_carol/Trimmomatic-0.36/adapters/TruSeq3-PE.fa:2:30:10:5:true MAXINFO:60:0.85 MINLEN:60
Using PrefixPair: 'TACACTCTTTCCCTACACGACGCTCTTCCGATCT' and 'GTGACTGGAGTTCAGACGTGTGCTCTTCCGATCT'
ILLUMINACLIP: Using 1 prefix pairs, 0 forward/reverse sequences, 0 forward only sequences, 0 reverse only sequences
TrimmomaticPE: Started with arguments: -threads 10 -phred33 T2R2_S2_L002_R1_001.fastq.gz T2R2_S2_L002_R2_001.fastq.gz T2R2_S2_L002_R1_001_forward_paired.fq.gz T2R2_S2_L002_R1_001_forward_unpaired.fq.gz T2R2_S2_L002_R2_001_reverse_paired.fq.gz T2R2_S2_L002_R2_001_reverse_unpaired.fq.gz ILLUMINACLIP:/media/hd_externo_3/genoma_carol/Trimmomatic-0.36/adapters/TruSeq3-PE.fa:2:30:10:5:true MAXINFO:60:0.85 MINLEN:60
Using PrefixPair: 'TACACTCTTTCCCTACACGACGCTCTTCCGATCT' and 'GTGACTGGAGTTCAGACGTGTGCTCTTCCGATCT'
ILLUMINACLIP: Using 1 prefix pairs, 0 forward/reverse sequences, 0 forward only sequences, 0 reverse only sequences
Input Read Pairs: 10644839 Both Surviving: 10632281 (99.88%) Forward Only Surviving: 0 (0.00%) Reverse Only Surviving: 313 (0.00%) Dropped: 12245 (0.12%)
TrimmomaticPE: Completed successfully

Input Read Pairs: 10754129 Both Surviving: 10740740 (99.88%) Forward Only Surviving: 1285 (0.01%) Reverse Only Surviving: 0 (0.00%) Dropped: 12104 (0.11%)
TrimmomaticPE: Completed successfully

T2R3:
TrimmomaticPE: Started with arguments: -threads 10 -phred33 T2R3_S3_L001_R1_001.fastq.gz T2R3_S3_L001_R2_001.fastq.gz T2R3_S3_L001_R1_001_forward_paired.fq.gz T2R3_S3_L001_R1_001_forward_unpaired.fq.gz T2R3_S3_L001_R2_001_reverse_paired.fq.gz T2R3_S3_L001_R2_001_reverse_unpaired.fq.gz
ILLUMINACLIP:/media/hd_externo_3/genoma_carol/Trimmomatic-0.36/adapters/TruSeq3-PE.fa:2:30:10:5:true MAXINFO:60:0.85 MINLEN:60
Using PrefixPair: 'TACACTCTTTCCCTACACGACGCTCTTCCGATCT' and 'GTGACTGGAGTTCAGACGTGTGCTCTTCCGATCT'
ILLUMINACLIP: Using 1 prefix pairs, 0 forward/reverse sequences, 0 forward only sequences, 0 reverse only sequences
TrimmomaticPE: Started with arguments: -threads 10 -phred33 T2R3_S3_L002_R1_001.fastq.gz T2R3_S3_L002_R2_001.fastq.gz T2R3_S3_L002_R1_001_forward_paired.fq.gz T2R3_S3_L002_R1_001_forward_unpaired.fq.gz T2R3_S3_L002_R2_001_reverse_paired.fq.gz T2R3_S3_L002_R2_001_reverse_unpaired.fq.gz
ILLUMINACLIP:/media/hd_externo_3/genoma_carol/Trimmomatic-0.36/adapters/TruSeq3-PE.fa:2:30:10:5:true MAXINFO:60:0.85 MINLEN:60
Using PrefixPair: 'TACACTCTTTCCCTACACGACGCTCTTCCGATCT' and 'GTGACTGGAGTTCAGACGTGTGCTCTTCCGATCT'
ILLUMINACLIP: Using 1 prefix pairs, 0 forward/reverse sequences, 0 forward only sequences, 0 reverse only sequences
Input Read Pairs: 10414583 Both Surviving: 10406560 (99.92%) Forward Only Surviving: 0 (0.00%) Reverse Only Surviving: 332 (0.00%) Dropped: 7691 (0.07%)
TrimmomaticPE: Completed successfully
Input Read Pairs: 10527339 Both Surviving: 10518171 (99.91%) Forward Only Surviving: 1219 (0.01%) Reverse Only Surviving: 0 (0.00%) Dropped: 7949 (0.08%)
TrimmomaticPE: Completed successfully

T2R4:
TrimmomaticPE: Started with arguments: -threads 10 -phred33 T2R4_S4_L001_R1_001.fastq.gz T2R4_S4_L001_R2_001.fastq.gz T2R4_S4_L001_R1_001_forward_paired.fq.gz T2R4_S4_L001_R1_001_forward_unpaired.fq.gz T2R4_S4_L001_R2_001_reverse_paired.fq.gz T2R4_S4_L001_R2_001_reverse_unpaired.fq.gz
ILLUMINACLIP:/media/hd_externo_3/genoma_carol/Trimmomatic-0.36/adapters/TruSeq3-PE.fa:2:30:10:5:true MAXINFO:60:0.85 MINLEN:60
Using PrefixPair: 'TACACTCTTTCCCTACACGACGCTCTTCCGATCT' and 'GTGACTGGAGTTCAGACGTGTGCTCTTCCGATCT'
ILLUMINACLIP: Using 1 prefix pairs, 0 forward/reverse sequences, 0 forward only sequences, 0 reverse only sequences
TrimmomaticPE: Started with arguments: -threads 10 -phred33 T2R4_S4_L002_R1_001.fastq.gz T2R4_S4_L002_R2_001.fastq.gz T2R4_S4_L002_R1_001_forward_paired.fq.gz T2R4_S4_L002_R1_001_forward_unpaired.fq.gz T2R4_S4_L002_R2_001_reverse_paired.fq.gz T2R4_S4_L002_R2_001_reverse_unpaired.fq.gz
ILLUMINACLIP:/media/hd_externo_3/genoma_carol/Trimmomatic-0.36/adapters/TruSeq3-PE.fa:2:30:10:5:true MAXINFO:60:0.85 MINLEN:60
Using PrefixPair: 'TACACTCTTTCCCTACACGACGCTCTTCCGATCT' and 'GTGACTGGAGTTCAGACGTGTGCTCTTCCGATCT'
ILLUMINACLIP: Using 1 prefix pairs, 0 forward/reverse sequences, 0 forward only sequences, 0 reverse only sequences
Input Read Pairs: 9300570 Both Surviving: 9293293 (99.92%) Forward Only Surviving: 0 (0.00%) Reverse Only Surviving: 296 (0.00%) Dropped: 6981 (0.08%)
TrimmomaticPE: Completed successfully
Input Read Pairs: 9425567 Both Surviving: 9417466 (99.91%) Forward Only Surviving: 1116 (0.01%) Reverse Only Surviving: 0 (0.00%) Dropped: 6985 (0.07%)
TrimmomaticPE: Completed successfully

T3R1:

TrimmomaticPE: Started with arguments: -threads 10 -phred33 T3R1_S5_L001_R1_001.fastq.gz T3R1_S5_L001_R2_001.fastq.gz T3R1_S5_L001_R1_001_forward_paired.fq.gz T3R1_S5_L001_R1_001_forward_unpaired.fq.gz T3R1_S5_L001_R2_001_reverse_paired.fq.gz T3R1_S5_L001_R2_001_reverse_unpaired.fq.gz ILLUMINACLIP:/media/hd_externo_3/genoma_carol/Trimmomatic-0.36/adapters/TruSeq3-PE.fa:2:30:10:5:true MAXINFO:60:0.85 MINLEN:60

TrimmomaticPE: Started with arguments: -threads 10 -phred33 T3R1_S5_L002_R1_001.fastq.gz T3R1_S5_L002_R2_001.fastq.gz T3R1_S5_L002_R1_001_forward_paired.fq.gz T3R1_S5_L002_R1_001_forward_unpaired.fq.gz T3R1_S5_L002_R2_001_reverse_paired.fq.gz T3R1_S5_L002_R2_001_reverse_unpaired.fq.gz ILLUMINACLIP:/media/hd_externo_3/genoma_carol/Trimmomatic-0.36/adapters/TruSeq3-PE.fa:2:30:10:5:true MAXINFO:60:0.85 MINLEN:60

Using PrefixPair: 'TACACTCTTTCCCTACACGACGCTCTTCCGATCT' and 'GTGACTGGAGTTCAGACGTGTGCTCTTCCGATCT'

ILLUMINACLIP: Using 1 prefix pairs, 0 forward/reverse sequences, 0 forward only sequences, 0 reverse only sequences

Using PrefixPair: 'TACACTCTTTCCCTACACGACGCTCTTCCGATCT' and 'GTGACTGGAGTTCAGACGTGTGCTCTTCCGATCT'

ILLUMINACLIP: Using 1 prefix pairs, 0 forward/reverse sequences, 0 forward only sequences, 0 reverse only sequences

Input Read Pairs: 9764305 Both Surviving: 9756662 (99.92%) Forward Only Surviving: 1179 (0.01%) Reverse Only Surviving: 0 (0.00%) Dropped: 6464 (0.07%)

TrimmomaticPE: Completed successfully

Input Read Pairs: 9656075 Both Surviving: 9649276 (99.93%) Forward Only Surviving: 0 (0.00%) Reverse Only Surviving: 282 (0.00%) Dropped: 6517 (0.07%)

TrimmomaticPE: Completed successfully

T3R2:

TrimmomaticPE: Started with arguments: -threads 10 -phred33 T3R2_S6_L002_R1_001.fastq.gz T3R2_S6_L002_R2_001.fastq.gz T3R2_S6_L002_R1_001_forward_paired.fq.gz T3R2_S6_L002_R1_001_forward_unpaired.fq.gz T3R2_S6_L002_R2_001_reverse_paired.fq.gz T3R2_S6_L002_R2_001_reverse_unpaired.fq.gz ILLUMINACLIP:/media/hd_externo_3/genoma_carol/Trimmomatic-0.36/adapters/TruSeq3-PE.fa:2:30:10:5:true MAXINFO:60:0.85 MINLEN:60

Using PrefixPair: 'TACACTCTTTCCCTACACGACGCTCTTCCGATCT' and 'GTGACTGGAGTTCAGACGTGTGCTCTTCCGATCT'

ILLUMINACLIP: Using 1 prefix pairs, 0 forward/reverse sequences, 0 forward only sequences, 0 reverse only sequences

TrimmomaticPE: Started with arguments: -threads 10 -phred33 T3R2_S6_L001_R1_001.fastq.gz T3R2_S6_L001_R2_001.fastq.gz T3R2_S6_L001_R1_001_forward_paired.fq.gz T3R2_S6_L001_R1_001_forward_unpaired.fq.gz T3R2_S6_L001_R2_001_reverse_paired.fq.gz T3R2_S6_L001_R2_001_reverse_unpaired.fq.gz ILLUMINACLIP:/media/hd_externo_3/genoma_carol/Trimmomatic-0.36/adapters/TruSeq3-PE.fa:2:30:10:5:true MAXINFO:60:0.85 MINLEN:60

Using PrefixPair: 'TACACTCTTTCCCTACACGACGCTCTTCCGATCT' and 'GTGACTGGAGTTCAGACGTGTGCTCTTCCGATCT'

ILLUMINACLIP: Using 1 prefix pairs, 0 forward/reverse sequences, 0 forward only sequences, 0 reverse only sequences

Input Read Pairs: 10083907 Both Surviving: 10077537 (99.94%) Forward Only Surviving: 0 (0.00%) Reverse Only Surviving: 320 (0.00%) Dropped: 6050 (0.06%)

TrimmomaticPE: Completed successfully

Input Read Pairs: 10188728 Both Surviving: 10181493 (99.93%) Forward Only Surviving: 1173 (0.01%) Reverse Only Surviving: 0 (0.00%) Dropped: 6062 (0.06%)

TrimmomaticPE: Completed successfully

T3R3:

TrimmomaticPE: Started with arguments: -threads 10 -phred33 T3R3_S7_L001_R1_001.fastq.gz T3R3_S7_L001_R2_001.fastq.gz T3R3_S7_L001_R1_001_forward_paired.fq.gz T3R3_S7_L001_R1_001_forward_unpaired.fq.gz T3R3_S7_L001_R2_001_reverse_paired.fq.gz

T3R3_S7_L001_R2_001_reverse_unpaired.fq.gz
ILLUMINACLIP:/media/hd_externo_3/genoma_carol/Trimmomatic-0.36/adapters/TruSeq3-PE.fa:2:30:10:5:true MAXINFO:60:0.85 MINLEN:60
Using PrefixPair: 'TACACTCTTTCCCTACACGACGCTCTTCCGATCT' and 'GTGACTGGAGTTCAGACGTGTGCTCTTCCGATCT'
ILLUMINACLIP: Using 1 prefix pairs, 0 forward/reverse sequences, 0 forward only sequences, 0 reverse only sequences
TrimmomaticPE: Started with arguments: -threads 10 -phred33 T3R3_S7_L002_R1_001.fastq.gz T3R3_S7_L002_R2_001.fastq.gz T3R3_S7_L002_R1_001_forward_paired.fq.gz T3R3_S7_L002_R1_001_forward_unpaired.fq.gz T3R3_S7_L002_R2_001_reverse_paired.fq.gz T3R3_S7_L002_R2_001_reverse_unpaired.fq.gz
ILLUMINACLIP:/media/hd_externo_3/genoma_carol/Trimmomatic-0.36/adapters/TruSeq3-PE.fa:2:30:10:5:true MAXINFO:60:0.85 MINLEN:60
Using PrefixPair: 'TACACTCTTTCCCTACACGACGCTCTTCCGATCT' and 'GTGACTGGAGTTCAGACGTGTGCTCTTCCGATCT'
ILLUMINACLIP: Using 1 prefix pairs, 0 forward/reverse sequences, 0 forward only sequences, 0 reverse only sequences
Input Read Pairs: 10928891 Both Surviving: 10920390 (99.92%) Forward Only Surviving: 1269 (0.01%) Reverse Only Surviving: 0 (0.00%) Dropped: 7232 (0.07%)
TrimmomaticPE: Completed successfully
Input Read Pairs: 10814700 Both Surviving: 10807270 (99.93%) Forward Only Surviving: 0 (0.00%) Reverse Only Surviving: 334 (0.00%) Dropped: 7096 (0.07%)
TrimmomaticPE: Completed successfully

T3R4:
TrimmomaticPE: Started with arguments: -threads 10 -phred33 T3R4_S8_L001_R1_001.fastq.gz T3R4_S8_L001_R2_001.fastq.gz T3R4_S8_L001_R1_001_forward_paired.fq.gz T3R4_S8_L001_R1_001_forward_unpaired.fq.gz T3R4_S8_L001_R2_001_reverse_paired.fq.gz T3R4_S8_L001_R2_001_reverse_unpaired.fq.gz
ILLUMINACLIP:/media/hd_externo_3/genoma_carol/Trimmomatic-0.36/adapters/TruSeq3-PE.fa:2:30:10:5:true MAXINFO:60:0.85 MINLEN:60
Using PrefixPair: 'TACACTCTTTCCCTACACGACGCTCTTCCGATCT' and 'GTGACTGGAGTTCAGACGTGTGCTCTTCCGATCT'
ILLUMINACLIP: Using 1 prefix pairs, 0 forward/reverse sequences, 0 forward only sequences, 0 reverse only sequences
TrimmomaticPE: Started with arguments: -threads 10 -phred33 T3R4_S8_L002_R1_001.fastq.gz T3R4_S8_L002_R2_001.fastq.gz T3R4_S8_L002_R1_001_forward_paired.fq.gz T3R4_S8_L002_R1_001_forward_unpaired.fq.gz T3R4_S8_L002_R2_001_reverse_paired.fq.gz T3R4_S8_L002_R2_001_reverse_unpaired.fq.gz
ILLUMINACLIP:/media/hd_externo_3/genoma_carol/Trimmomatic-0.36/adapters/TruSeq3-PE.fa:2:30:10:5:true MAXINFO:60:0.85 MINLEN:60
Using PrefixPair: 'TACACTCTTTCCCTACACGACGCTCTTCCGATCT' and 'GTGACTGGAGTTCAGACGTGTGCTCTTCCGATCT'
ILLUMINACLIP: Using 1 prefix pairs, 0 forward/reverse sequences, 0 forward only sequences, 0 reverse only sequences
Input Read Pairs: 10521804 Both Surviving: 10514977 (99.94%) Forward Only Surviving: 0 (0.00%) Reverse Only Surviving: 302 (0.00%) Dropped: 6525 (0.06%)
TrimmomaticPE: Completed successfully
Input Read Pairs: 10639200 Both Surviving: 10631430 (99.93%) Forward Only Surviving: 1278 (0.01%) Reverse Only Surviving: 0 (0.00%) Dropped: 6492 (0.06%)
TrimmomaticPE: Completed successfully

T4R1:
TrimmomaticPE: Started with arguments: -threads 10 -phred33 T4R1_S9_L001_R1_001.fastq.gz T4R1_S9_L001_R2_001.fastq.gz T4R1_S9_L001_R1_001_forward_paired.fq.gz T4R1_S9_L001_R1_001_forward_unpaired.fq.gz T4R1_S9_L001_R2_001_reverse_paired.fq.gz T4R1_S9_L001_R2_001_reverse_unpaired.fq.gz
ILLUMINACLIP:/media/hd_externo_3/genoma_carol/Trimmomatic-0.36/adapters/TruSeq3-PE.fa:2:30:10:5:true MAXINFO:60:0.85 MINLEN:60

TrimmomaticPE: Started with arguments: -threads 10 -phred33 T4R1_S9_L002_R1_001.fastq.gz T4R1_S9_L002_R2_001.fastq.gz T4R1_S9_L002_R1_001_forward_paired.fq.gz T4R1_S9_L002_R1_001_forward_unpaired.fq.gz T4R1_S9_L002_R2_001_reverse_paired.fq.gz T4R1_S9_L002_R2_001_reverse_unpaired.fq.gz ILLUMINACLIP:/media/hd_externo_3/genoma_carol/Trimmomatic-0.36/adapters/TruSeq3-PE.fa:2:30:10:5:true MAXINFO:60:0.85 MINLEN:60
Using PrefixPair: 'TACACTCTTTCCCTACACGACGCTCTTCCGATCT' and 'GTGACTGGAGTTCAGACGTGTGCTCTTCCGATCT'
ILLUMINACLIP: Using 1 prefix pairs, 0 forward/reverse sequences, 0 forward only sequences, 0 reverse only sequences
Using PrefixPair: 'TACACTCTTTCCCTACACGACGCTCTTCCGATCT' and 'GTGACTGGAGTTCAGACGTGTGCTCTTCCGATCT'
ILLUMINACLIP: Using 1 prefix pairs, 0 forward/reverse sequences, 0 forward only sequences, 0 reverse only sequences
Input Read Pairs: 10380213 Both Surviving: 10373677 (99.94%) Forward Only Surviving: 0 (0.00%) Reverse Only Surviving: 354 (0.00%) Dropped: 6182 (0.06%)
TrimmomaticPE: Completed successfully
Input Read Pairs: 10483746 Both Surviving: 10476494 (99.93%) Forward Only Surviving: 1204 (0.01%) Reverse Only Surviving: 0 (0.00%) Dropped: 6048 (0.06%)
TrimmomaticPE: Completed successfully

T4R2:
TrimmomaticPE: Started with arguments: -threads 10 -phred33 T4R2_S10_L001_R1_001.fastq.gz T4R2_S10_L001_R2_001.fastq.gz T4R2_S10_L001_R1_001_forward_paired.fq.gz T4R2_S10_L001_R1_001_forward_unpaired.fq.gz T4R2_S10_L001_R2_001_reverse_paired.fq.gz T4R2_S10_L001_R2_001_reverse_unpaired.fq.gz ILLUMINACLIP:/media/hd_externo_3/genoma_carol/Trimmomatic-0.36/adapters/TruSeq3-PE.fa:2:30:10:5:true MAXINFO:60:0.85 MINLEN:60
Using PrefixPair: 'TACACTCTTTCCCTACACGACGCTCTTCCGATCT' and 'GTGACTGGAGTTCAGACGTGTGCTCTTCCGATCT'
ILLUMINACLIP: Using 1 prefix pairs, 0 forward/reverse sequences, 0 forward only sequences, 0 reverse only sequences
TrimmomaticPE: Started with arguments: -threads 10 -phred33 T4R2_S10_L002_R1_001.fastq.gz T4R2_S10_L002_R2_001.fastq.gz T4R2_S10_L002_R1_001_forward_paired.fq.gz T4R2_S10_L002_R1_001_forward_unpaired.fq.gz T4R2_S10_L002_R2_001_reverse_paired.fq.gz T4R2_S10_L002_R2_001_reverse_unpaired.fq.gz ILLUMINACLIP:/media/hd_externo_3/genoma_carol/Trimmomatic-0.36/adapters/TruSeq3-PE.fa:2:30:10:5:true MAXINFO:60:0.85 MINLEN:60
Using PrefixPair: 'TACACTCTTTCCCTACACGACGCTCTTCCGATCT' and 'GTGACTGGAGTTCAGACGTGTGCTCTTCCGATCT'
ILLUMINACLIP: Using 1 prefix pairs, 0 forward/reverse sequences, 0 forward only sequences, 0 reverse only sequences
Input Read Pairs: 10166147 Both Surviving: 10160002 (99.94%) Forward Only Surviving: 0 (0.00%) Reverse Only Surviving: 359 (0.00%) Dropped: 5786 (0.06%)
TrimmomaticPE: Completed successfully
Input Read Pairs: 10293491 Both Surviving: 10286382 (99.93%) Forward Only Surviving: 1205 (0.01%) Reverse Only Surviving: 0 (0.00%) Dropped: 5904 (0.06%)
TrimmomaticPE: Completed successfully

T4R3:
TrimmomaticPE: Started with arguments: -threads 10 -phred33 T4R3_S11_L001_R1_001.fastq.gz T4R3_S11_L001_R2_001.fastq.gz T4R3_S11_L001_R1_001_forward_paired.fq.gz T4R3_S11_L001_R1_001_forward_unpaired.fq.gz T4R3_S11_L001_R2_001_reverse_paired.fq.gz T4R3_S11_L001_R2_001_reverse_unpaired.fq.gz ILLUMINACLIP:/media/hd_externo_3/genoma_carol/Trimmomatic-0.36/adapters/TruSeq3-PE.fa:2:30:10:5:true MAXINFO:60:0.85 MINLEN:60
Using PrefixPair: 'TACACTCTTTCCCTACACGACGCTCTTCCGATCT' and 'GTGACTGGAGTTCAGACGTGTGCTCTTCCGATCT'
ILLUMINACLIP: Using 1 prefix pairs, 0 forward/reverse sequences, 0 forward only sequences, 0 reverse only sequences

TrimmomaticPE: Started with arguments: -threads 10 -phred33 T4R3_S11_L002_R1_001.fastq.gz T4R3_S11_L002_R2_001.fastq.gz T4R3_S11_L002_R1_001_forward_paired.fq.gz T4R3_S11_L002_R1_001_forward_unpaired.fq.gz T4R3_S11_L002_R2_001_reverse_paired.fq.gz T4R3_S11_L002_R2_001_reverse_unpaired.fq.gz ILLUMINACLIP:/media/hd_externo_3/genoma_carol/Trimmomatic-0.36/adapters/TruSeq3-PE.fa:2:30:10:5:true MAXINFO:60:0.85 MINLEN:60
Using PrefixPair: 'TACACTCTTTCCCTACACGACGCTCTTCCGATCT' and 'GTGACTGGAGTTCAGACGTGTGCTCTTCCGATCT'
ILLUMINACLIP: Using 1 prefix pairs, 0 forward/reverse sequences, 0 forward only sequences, 0 reverse only sequences
Input Read Pairs: 10777994 Both Surviving: 10770450 (99.93%) Forward Only Surviving: 1267 (0.01%) Reverse Only Surviving: 0 (0.00%) Dropped: 6277 (0.06%)
TrimmomaticPE: Completed successfully
Input Read Pairs: 10663283 Both Surviving: 10656780 (99.94%) Forward Only Surviving: 0 (0.00%) Reverse Only Surviving: 342 (0.00%) Dropped: 6161 (0.06%)
TrimmomaticPE: Completed successfully

T4R4:
TrimmomaticPE: Started with arguments: -threads 10 -phred33 T4R4_S12_L001_R1_001.fastq.gz T4R4_S12_L001_R2_001.fastq.gz T4R4_S12_L001_R1_001_forward_paired.fq.gz T4R4_S12_L001_R1_001_forward_unpaired.fq.gz T4R4_S12_L001_R2_001_reverse_paired.fq.gz T4R4_S12_L001_R2_001_reverse_unpaired.fq.gz ILLUMINACLIP:/media/hd_externo_3/genoma_carol/Trimmomatic-0.36/adapters/TruSeq3-PE.fa:2:30:10:5:true MAXINFO:60:0.85 MINLEN:60
Using PrefixPair: 'TACACTCTTTCCCTACACGACGCTCTTCCGATCT' and 'GTGACTGGAGTTCAGACGTGTGCTCTTCCGATCT'
ILLUMINACLIP: Using 1 prefix pairs, 0 forward/reverse sequences, 0 forward only sequences, 0 reverse only sequences
TrimmomaticPE: Started with arguments: -threads 10 -phred33 T4R4_S12_L002_R1_001.fastq.gz T4R4_S12_L002_R2_001.fastq.gz T4R4_S12_L002_R1_001_forward_paired.fq.gz T4R4_S12_L002_R1_001_forward_unpaired.fq.gz T4R4_S12_L002_R2_001_reverse_paired.fq.gz T4R4_S12_L002_R2_001_reverse_unpaired.fq.gz ILLUMINACLIP:/media/hd_externo_3/genoma_carol/Trimmomatic-0.36/adapters/TruSeq3-PE.fa:2:30:10:5:true MAXINFO:60:0.85 MINLEN:60
Using PrefixPair: 'TACACTCTTTCCCTACACGACGCTCTTCCGATCT' and 'GTGACTGGAGTTCAGACGTGTGCTCTTCCGATCT'
ILLUMINACLIP: Using 1 prefix pairs, 0 forward/reverse sequences, 0 forward only sequences, 0 reverse only sequences
Input Read Pairs: 10339924 Both Surviving: 10333373 (99.94%) Forward Only Surviving: 0 (0.00%) Reverse Only Surviving: 327 (0.00%) Dropped: 6224 (0.06%)
TrimmomaticPE: Completed successfully
Input Read Pairs: 10451775 Both Surviving: 10444507 (99.93%) Forward Only Surviving: 1180 (0.01%) Reverse Only Surviving: 0 (0.00%) Dropped: 6088 (0.06%)
TrimmomaticPE: Completed successfully

T5R1:
TrimmomaticPE: Started with arguments: -threads 10 -phred33 T5R1_S13_L001_R1_001.fastq.gz -threads T5R1_S13_L001_R2_001.fastq.gz 10 T5R1_S13_L001_R1_001_forward_paired.fq.gz -phred33 T5R1_S13_L001_R1_001_forward_unpaired.fq.gz T5R1_S13_L002_R1_001.fastq.gz T5R1_S13_L001_R2_001_reverse_paired.fq.gz T5R1_S13_L002_R2_001.fastq.gz T5R1_S13_L001_R2_001_reverse_unpaired.fq.gz T5R1_S13_L002_R1_001_forward_paired.fq.gz ILLUMINACLIP:/media/hd_externo_3/genoma_carol/Trimmomatic-0.36/adapters/TruSeq3-PE.fa:2:30:10:5:true T5R1_S13_L002_R1_001_forward_unpaired.fq.gz MAXINFO:60:0.85 T5R1_S13_L002_R2_001_reverse_paired.fq.gz MINLEN:60 T5R1_S13_L002_R2_001_reverse_unpaired.fq.gz ILLUMINACLIP:/media/hd_externo_3/genoma_carol/Trimmomatic-0.36/adapters/TruSeq3-PE.fa:2:30:10:5:true MAXINFO:60:0.85 MINLEN:60
Using PrefixPair: 'TACACTCTTTCCCTACACGACGCTCTTCCGATCT' and 'GTGACTGGAGTTCAGACGTGTGCTCTTCCGATCT'
Using PrefixPair: 'TACACTCTTTCCCTACACGACGCTCTTCCGATCT' and 'GTGACTGGAGTTCAGACGTGTGCTCTTCCGATCT'

ILLUMINACLIP: Using 1 prefix pairs, 0 forward/reverse sequences, 0 forward only sequences, 0 reverse only sequences
ILLUMINACLIP: Using 1 prefix pairs, 0 forward/reverse sequences, 0 forward only sequences, 0 reverse only sequences
Input Read Pairs: 10326203 Both Surviving: 10320105 (99.94%) Forward Only Surviving: 0 (0.00%) Reverse Only Surviving: 358 (0.00%) Dropped: 5740 (0.06%)
TrimmomaticPE: Completed successfully
Input Read Pairs: 10464923 Both Surviving: 10457915 (99.93%) Forward Only Surviving: 1279 (0.01%) Reverse Only Surviving: 0 (0.00%) Dropped: 5729 (0.05%)
TrimmomaticPE: Completed successfully

T5R2:
TrimmomaticPE: Started with arguments: -threads 10 -phred33 T5R2_S14_L001_R1_001.fastq.gz -phred33 T5R2_S14_L001_R2_001.fastq.gz T5R2_S14_L002_R1_001.fastq.gz T5R2_S14_L001_R1_001_forward_paired.fq.gz T5R2_S14_L002_R2_001.fastq.gz T5R2_S14_L001_R1_001_forward_unpaired.fq.gz T5R2_S14_L002_R1_001_forward_paired.fq.gz T5R2_S14_L001_R2_001_reverse_paired.fq.gz T5R2_S14_L002_R1_001_forward_unpaired.fq.gz T5R2_S14_L001_R2_001_reverse_unpaired.fq.gz T5R2_S14_L002_R2_001_reverse_paired.fq.gz ILLUMINACLIP:/media/hd_externo_3/genoma_carol/Trimmomatic-0.36/adapters/TruSeq3-PE.fa:2:30:10:5:true T5R2_S14_L002_R2_001_reverse_unpaired.fq.gz MAXINFO:60:0.85 ILLUMINACLIP:/media/hd_externo_3/genoma_carol/Trimmomatic-0.36/adapters/TruSeq3-PE.fa:2:30:10:5:true MINLEN:60 MAXINFO:60:0.85
MINLEN:60
Using PrefixPair: 'TACACTCTTTCCCTACACGACGCTCTTCCGATCT' and 'GTGACTGGAGTTCAGACGTGTGCTCTTCCGATCT'
Using PrefixPair: 'TACACTCTTTCCCTACACGACGCTCTTCCGATCT' and 'GTGACTGGAGTTCAGACGTGTGCTCTTCCGATCT'
ILLUMINACLIP: Using 1 prefix pairs, 0 forward/reverse sequences, 0 forward only sequences, 0 reverse only sequences
ILLUMINACLIP: Using 1 prefix pairs, 0 forward/reverse sequences, 0 forward only sequences, 0 reverse only sequences
Input Read Pairs: 10245085 Both Surviving: 10234986 (99.90%) Forward Only Surviving: 1177 (0.01%) Reverse Only Surviving: 0 (0.00%) Dropped: 8922 (0.09%)
TrimmomaticPE: Completed successfully
Input Read Pairs: 10015163 Both Surviving: 10006042 (99.91%) Forward Only Surviving: 0 (0.00%) Reverse Only Surviving: 290 (0.00%) Dropped: 8831 (0.09%)
TrimmomaticPE: Completed successfully

T5R3:
TrimmomaticPE: Started with arguments: -threads 10 -phred33 T5R3_S15_L002_R1_001.fastq.gz T5R3_S15_L002_R2_001.fastq.gz T5R3_S15_L002_R1_001_forward_paired.fq.gz T5R3_S15_L002_R1_001_forward_unpaired.fq.gz T5R3_S15_L002_R2_001_reverse_paired.fq.gz T5R3_S15_L002_R2_001_reverse_unpaired.fq.gz
ILLUMINACLIP:/media/hd_externo_3/genoma_carol/Trimmomatic-0.36/adapters/TruSeq3-PE.fa:2:30:10:5:true MAXINFO:60:0.85 MINLEN:60
Using PrefixPair: 'TACACTCTTTCCCTACACGACGCTCTTCCGATCT' and 'GTGACTGGAGTTCAGACGTGTGCTCTTCCGATCT'
ILLUMINACLIP: Using 1 prefix pairs, 0 forward/reverse sequences, 0 forward only sequences, 0 reverse only sequences
TrimmomaticPE: Started with arguments: -threads 10 -phred33 T5R3_S15_L001_R1_001.fastq.gz T5R3_S15_L001_R2_001.fastq.gz T5R3_S15_L001_R1_001_forward_paired.fq.gz T5R3_S15_L001_R1_001_forward_unpaired.fq.gz T5R3_S15_L001_R2_001_reverse_paired.fq.gz T5R3_S15_L001_R2_001_reverse_unpaired.fq.gz
ILLUMINACLIP:/media/hd_externo_3/genoma_carol/Trimmomatic-0.36/adapters/TruSeq3-PE.fa:2:30:10:5:true MAXINFO:60:0.85 MINLEN:60
Using PrefixPair: 'TACACTCTTTCCCTACACGACGCTCTTCCGATCT' and 'GTGACTGGAGTTCAGACGTGTGCTCTTCCGATCT'
ILLUMINACLIP: Using 1 prefix pairs, 0 forward/reverse sequences, 0 forward only sequences, 0 reverse only sequences

Input Read Pairs: 8273937 Both Surviving: 8268057 (99.93%) Forward Only Surviving: 0 (0.00%) Reverse Only Surviving: 242 (0.00%) Dropped: 5638 (0.07%)
TrimmomaticPE: Completed successfully
Input Read Pairs: 8372384 Both Surviving: 8365525 (99.92%) Forward Only Surviving: 1007 (0.01%) Reverse Only Surviving: 0 (0.00%) Dropped: 5852 (0.07%)
TrimmomaticPE: Completed successfully

T5R4:
TrimmomaticPE: Started with arguments: -threads 10 -phred33 T5R4_S16_L002_R1_001.fastq.gz T5R4_S16_L001_R1_001.fastq.gz T5R4_S16_L002_R2_001.fastq.gz T5R4_S16_L001_R2_001.fastq.gz T5R4_S16_L002_R1_001_forward_paired.fq.gz T5R4_S16_L001_R1_001_forward_paired.fq.gz T5R4_S16_L002_R1_001_forward_unpaired.fq.gz T5R4_S16_L002_R2_001_reverse_paired.fq.gz T5R4_S16_L001_R1_001_forward_unpaired.fq.gz T5R4_S16_L002_R2_001_reverse_unpaired.fq.gz T5R4_S16_L001_R2_001_reverse_paired.fq.gz
ILLUMINACLIP:/media/hd_externo_3/genoma_carol/Trimmomatic-0.36/adapters/TruSeq3-PE.fa:2:30:10:5:true T5R4_S16_L001_R2_001_reverse_unpaired.fq.gz MAXINFO:60:0.85 MINLEN:60 ILLUMINACLIP:/media/hd_externo_3/genoma_carol/Trimmomatic-0.36/adapters/TruSeq3-PE.fa:2:30:10:5:true
MAXINFO:60:0.85 MINLEN:60
Using PrefixPair: 'TACACTCTTTCCCTACACGACGCTCTTCCGATCT' and 'GTGACTGGAGTTCAGACGTGTGCTCTTCCGATCT'
Using PrefixPair: 'TACACTCTTTCCCTACACGACGCTCTTCCGATCT' and 'GTGACTGGAGTTCAGACGTGTGCTCTTCCGATCT'
ILLUMINACLIP: Using 1 prefix pairs, 0 forward/reverse sequences, 0 forward only sequences, 0 reverse only sequences
ILLUMINACLIP: Using 1 prefix pairs, 0 forward/reverse sequences, 0 forward only sequences, 0 reverse only sequences
Input Read Pairs: 10385362 Both Surviving: 10377986 (99.93%) Forward Only Surviving: 1175 (0.01%) Reverse Only Surviving: 0 (0.00%) Dropped: 6201 (0.06%)
TrimmomaticPE: Completed successfully
Input Read Pairs: 10256296 Both Surviving: 10249748 (99.94%) Forward Only Surviving: 0 (0.00%) Reverse Only Surviving: 316 (0.00%) Dropped: 6232 (0.06%)
TrimmomaticPE: Completed successfully

Additional information 2. Kallisto

T2R1:
{ "n_targets": 47121,
"n_bootstraps": 100,
"n_processed": 20539218,
"n_pseudoaligned": 16665423,
"n_unique": 16645662,
"p_pseudoaligned": 81.1,
"p_unique": 81.0,
"kallisto_version": "0.44.0",
"index_version": 10,
"start_time": "Mon May 21 11:14:55 2018",
"call": "kallisto quant -i /data/kishi/esalq/livia/Referencia_Kallisto/transcripts_clean_assembly_unique_2_MASKED_EVM.idx -o /data/kishi/esalq/livia/Quant/T2R1/ --bias -b 100 --seed=42 --rf-stranded -t 10 /data/kishi/esalq/livia/Amostras/T2R1/T2R1_NON_Egrandis_NON_AP.fastq.1.gz /data/kishi/esalq/livia/Amostras/T2R1/T2R1_NON_Egrandis_NON_AP.fastq.2.gz"}

T2R2:
{ "n_targets": 47121,
"n_bootstraps": 100,
"n_processed": 21188029,
"n_pseudoaligned": 16973185,
"n_unique": 16953042,
"p_pseudoaligned": 80.1,

"p_unique": 80.0,
"kallisto_version": "0.44.0",
"index_version": 10,
"start_time": "Mon May 21 11:17:40 2018",
"call": "kallisto quant -i /data/kishi/esalq/livia/Referencia_Kallisto/transcripts_clean_assembly_unique_2_MASKED_EVM.idx -o /data/kishi/esalq/livia/Quant/T2R2/ --bias -b 100 --seed=42 --rf-stranded -t 10 /data/kishi/esalq/livia/Amostras/T2R2/T2R2_NON_Egrandis_NON_AP.fastq.1.gz /data/kishi/esalq/livia/Amostras/T2R2/T2R2_NON_Egrandis_NON_AP.fastq.2.gz"}

T2R3

{ "n_targets": 47121,
"n_bootstraps": 100,
"n_processed": 20786079,
"n_pseudoaligned": 16663928,
"n_unique": 16642640,
"p_pseudoaligned": 80.2,
"p_unique": 80.1,
"kallisto_version": "0.44.0",
"index_version": 10,
"start_time": "Fri May 25 14:48:41 2018",
"call": "kallisto quant -i /data/kishi/esalq/livia/Referencia_Kallisto/transcripts_clean_assembly_unique_2_MASKED_EVM.idx -o /data/kishi/esalq/livia/Quant_sem_pseudobam/T2R3/ --bias -b 100 --seed=42 --rf-stranded -t 10 /data/kishi/esalq/livia/Amostras/T2R3/T2R3_NON_Egrandis_NON_AP.fastq.1.gz /data/kishi/esalq/livia/Amostras/T2R3/T2R3_NON_Egrandis_NON_AP.fastq.2.gz"}

T2R4

{ "n_targets": 47121,
"n_bootstraps": 100,
"n_processed": 18560818,
"n_pseudoaligned": 14829786,
"n_unique": 14811315,
"p_pseudoaligned": 79.9,
"p_unique": 79.8,
"kallisto_version": "0.44.0",
"index_version": 10,
"start_time": "Mon May 21 11:20:25 2018",
"call": "kallisto quant -i /data/kishi/esalq/livia/Referencia_Kallisto/transcripts_clean_assembly_unique_2_MASKED_EVM.idx -o /data/kishi/esalq/livia/Quant/T2R4/ --bias -b 100 --seed=42 --rf-stranded -t 10 /data/kishi/esalq/livia/Amostras/T2R4/T2R4_NON_Egrandis_NON_AP.fastq.1.gz /data/kishi/esalq/livia/Amostras/T2R4/T2R4_NON_Egrandis_NON_AP.fastq.2.gz"}

T3R1

{ "n_targets": 47121,
"n_bootstraps": 100,
"n_processed": 18560818,
"n_pseudoaligned": 14829786,
"n_unique": 14811315,
"p_pseudoaligned": 79.9,
"p_unique": 79.8,
"kallisto_version": "0.44.0",
"index_version": 10,
"start_time": "Mon May 21 11:20:25 2018",
"call": "kallisto quant -i /data/kishi/esalq/livia/Referencia_Kallisto/transcripts_clean_assembly_unique_2_MASKED_EVM.idx -o /data/kishi/esalq/livia/Quant/ T3R1/ --bias -b 100 --seed=42 --rf-stranded -t 10 /data/kishi/esalq/livia/Amostras/T3R1/T2R4_NON_Egrandis_NON_AP.fastq.1.gz /data/kishi/esalq/livia/Amostras/ T3R1/T2R4_NON_Egrandis_NON_AP.fastq.2.gz"}

T3R2

{ "n_targets": 47121,
"n_bootstraps": 100,
"n_processed": 20128367,
"n_pseudoaligned": 16238675,
"n_unique": 16218694,
"p_pseudoaligned": 80.7,
"p_unique": 80.6,
"kallisto_version": "0.44.0",
"index_version": 10,
"start_time": "Mon May 21 11:25:20 2018",
"call": "kallisto quant -i /data/kishi/esalq/livia/Referencia_Kallisto/transcripts_clean_assembly_unique_2_MASKED_EVM.idx -o /data/kishi/esalq/livia/Quant/T3R2/ --bias -b 100 --seed=42 --rf-stranded -t 10 /data/kishi/esalq/livia/Amostras/T3R2/T3R2_NON_Egrandis_NON_AP.fastq.1.gz /data/kishi/esalq/livia/Amostras/T3R2/T3R2_NON_Egrandis_NON_AP.fastq.2.gz"}

T3R3

{ "n_targets": 47121,
"n_bootstraps": 100,
"n_processed": 21563132,
"n_pseudoaligned": 17426241,
"n_unique": 17405915,
"p_pseudoaligned": 80.8,
"p_unique": 80.7,
"kallisto_version": "0.44.0",
"index_version": 10,
"start_time": "Mon May 21 11:28:03 2018",
"call": "kallisto quant -i /data/kishi/esalq/livia/Referencia_Kallisto/transcripts_clean_assembly_unique_2_MASKED_EVM.idx -o /data/kishi/esalq/livia/Quant/T3R3/ --bias -b 100 --seed=42 --rf-stranded -t 10 /data/kishi/esalq/livia/Amostras/T3R3/T3R3_NON_Egrandis_NON_AP.fastq.1.gz /data/kishi/esalq/livia/Amostras/T3R3/T3R3_NON_Egrandis_NON_AP.fastq.2.gz"}

T3R4

{ "n_targets": 47121,
"n_bootstraps": 100,
"n_processed": 20847885,
"n_pseudoaligned": 16779598,
"n_unique": 16760856,
"p_pseudoaligned": 80.5,
"p_unique": 80.4,
"kallisto_version": "0.44.0",
"index_version": 10,
"start_time": "Mon May 21 11:30:49 2018",
"call": "kallisto quant -i /data/kishi/esalq/livia/Referencia_Kallisto/transcripts_clean_assembly_unique_2_MASKED_EVM.idx -o /data/kishi/esalq/livia/Quant/T3R4/ --bias -b 100 --seed=42 --rf-stranded -t 10 /data/kishi/esalq/livia/Amostras/T3R4/T3R4_NON_Egrandis_NON_AP.fastq.1.gz /data/kishi/esalq/livia/Amostras/T3R4/T3R4_NON_Egrandis_NON_AP.fastq.2.gz"}

T4R1

{ "n_targets": 47121,
"n_bootstraps": 100,
"n_processed": 20604850,
"n_pseudoaligned": 16625484,
"n_unique": 16605010,
"p_pseudoaligned": 80.7,
"p_unique": 80.6,
"kallisto_version": "0.44.0",

"index_version": 10,
"start_time": "Mon May 21 11:33:32 2018",
"call": "kallisto quant -i /data/kishi/esalq/livia/Referencia_Kallisto/transcripts_clean_assembly_unique_2_MASKED_EVM.idx -o /data/kishi/esalq/livia/Quant/T4R1/ --bias -b 100 --seed=42 --rf-stranded -t 10 /data/kishi/esalq/livia/Amostras/T4R1/T4R1_NON_Egrandis_NON_AP.fastq.1.gz /data/kishi/esalq/livia/Amostras/T4R1/T4R1_NON_Egrandis_NON_AP.fastq.2.gz"}

T4R2

{ "n_targets": 47121,
"n_bootstraps": 100,
"n_processed": 20166155,
"n_pseudoaligned": 16307945,
"n_unique": 16289176,
"p_pseudoaligned": 80.9,
"p_unique": 80.8,
"kallisto_version": "0.44.0",
"index_version": 10,
"start_time": "Mon May 21 11:36:13 2018",
"call": "kallisto quant -i /data/kishi/esalq/livia/Referencia_Kallisto/transcripts_clean_assembly_unique_2_MASKED_EVM.idx -o /data/kishi/esalq/livia/Quant/T4R2/ --bias -b 100 --seed=42 --rf-stranded -t 10 /data/kishi/esalq/livia/Amostras/T4R2/T4R2_NON_Egrandis_NON_AP.fastq.1.gz /data/kishi/esalq/livia/Amostras/T4R2/T4R2_NON_Egrandis_NON_AP.fastq.2.gz"}

T4R13

{ "n_targets": 47121,
"n_bootstraps": 100,
"n_processed": 21165512,
"n_pseudoaligned": 16996954,
"n_unique": 16976524,
"p_pseudoaligned": 80.3,
"p_unique": 80.2,
"kallisto_version": "0.44.0",
"index_version": 10,
"start_time": "Mon May 21 11:38:48 2018",
"call": "kallisto quant -i /data/kishi/esalq/livia/Referencia_Kallisto/transcripts_clean_assembly_unique_2_MASKED_EVM.idx -o /data/kishi/esalq/livia/Quant/T4R3/ --bias -b 100 --seed=42 --rf-stranded -t 10 /data/kishi/esalq/livia/Amostras/T4R3/T4R3_NON_Egrandis_NON_AP.fastq.1.gz /data/kishi/esalq/livia/Amostras/T4R3/T4R3_NON_Egrandis_NON_AP.fastq.2.gz"}

T4R4

{ "n_targets": 47121,
"n_bootstraps": 100,
"n_processed": 18992953,
"n_pseudoaligned": 14896484,
"n_unique": 14878864,
"p_pseudoaligned": 78.4,
"p_unique": 78.3,
"kallisto_version": "0.44.0",
"index_version": 10,
"start_time": "Mon May 21 11:41:39 2018",
"call": "kallisto quant -i /data/kishi/esalq/livia/Referencia_Kallisto/transcripts_clean_assembly_unique_2_MASKED_EVM.idx -o /data/kishi/esalq/livia/Quant/T4R4/ --bias -b 100 --seed=42 --rf-stranded -t 10 /data/kishi/esalq/livia/Amostras/T4R4/T4R4_NON_Egrandis_NON_AP.fastq.1.gz /data/kishi/esalq/livia/Amostras/T4R4/T4R4_NON_Egrandis_NON_AP.fastq.2.gz"}

T5R1

{ "n_targets": 47121,
"n_bootstraps": 100,
"n_processed": 20631130,
"n_pseudoaligned": 16739424,
"n_unique": 16722429,
"p_pseudoaligned": 81.1,
"p_unique": 81.1,
"kallisto_version": "0.44.0",
"index_version": 10,
"start_time": "Mon May 21 11:44:17 2018",
"call": "kallisto quant -i /data/kishi/esalq/livia/Referencia_Kallisto/transcripts_clean_assembly_unique_2_MASKED_EVM.idx -o /data/kishi/esalq/livia/Quant/T5R1/ --bias -b 100 --seed=42 --rf-stranded -t 10 /data/kishi/esalq/livia/Amostras/T5R1/T5R1_NON_Egrandis_NON_AP.fastq.1.gz /data/kishi/esalq/livia/Amostras/T5R1/T5R1_NON_Egrandis_NON_AP.fastq.2.gz"}

T5R2

{ "n_targets": 47121,
"n_bootstraps": 100,
"n_processed": 20024580,
"n_pseudoaligned": 16154800,
"n_unique": 16137635,
"p_pseudoaligned": 80.7,
"p_unique": 80.6,
"kallisto_version": "0.44.0",
"index_version": 10,
"start_time": "Mon May 21 11:47:00 2018",
"call": "kallisto quant -i /data/kishi/esalq/livia/Referencia_Kallisto/transcripts_clean_assembly_unique_2_MASKED_EVM.idx -o /data/kishi/esalq/livia/Quant/T5R2/ --bias -b 100 --seed=42 --rf-stranded -t 10 /data/kishi/esalq/livia/Amostras/T5R2/T5R2_NON_Egrandis_NON_AP.fastq.1.gz /data/kishi/esalq/livia/Amostras/T5R2/T5R2_NON_Egrandis_NON_AP.fastq.2.gz"}

T5R3

{ "n_targets": 47121,
"n_bootstraps": 100,
"n_processed": 16381503,
"n_pseudoaligned": 13128779,
"n_unique": 13114835,
"p_pseudoaligned": 80.1,
"p_unique": 80.1,
"kallisto_version": "0.44.0",
"index_version": 10,
"start_time": "Mon May 21 11:49:34 2018",
"call": "kallisto quant -i /data/kishi/esalq/livia/Referencia_Kallisto/transcripts_clean_assembly_unique_2_MASKED_EVM.idx -o /data/kishi/esalq/livia/Quant/T5R3/ --bias -b 100 --seed=42 --rf-stranded -t 10 /data/kishi/esalq/livia/Amostras/T5R3/T5R3_NON_Egrandis_NON_AP.fastq.1.gz /data/kishi/esalq/livia/Amostras/T5R3/T5R3_NON_Egrandis_NON_AP.fastq.2.gz"}

T5R4

{ "n_targets": 47121,
"n_bootstraps": 100,
"n_processed": 20429631,
"n_pseudoaligned": 16458619,
"n_unique": 16441350,
"p_pseudoaligned": 80.6,
"p_unique": 80.5,
"kallisto_version": "0.44.0",
"index_version": 10,

"start_time": "Mon May 21 11:51:46 2018",
"call": "kallisto quant -i /data/kishi/esalq/livia/Referencia_Kallisto/transcripts_clean_assembly_unique_2_MASKED_EVM.idx -o /data/kishi/esalq/livia/Quant/T5R4/ --bias -b 100 --seed=42 --rf-stranded -t 10 /data/kishi/esalq/livia/Amostras/T5R4/T5R4_NON_Egrandis_NON_AP.fastq.1.gz /data/kishi/esalq/livia/Amostras/T5R4/T5R4_NON_Egrandis_NON_AP.fastq.2.gz"}

Additional information 3. Sleuth

T2 (*E. grandis*) x T5 (Óleo Mineral)

```
> library("sleuth")
> sample_id <- dir(file.path("C:/Users/Isaneli/Documents/RNASeq_Ceras_Isaneli", "Results_T2_T5"))
> sample_id
[1] "T2R1" "T2R2" "T2R3" "T2R4" "T5R1" "T5R2" "T5R3" "T5R4"
> kal_dirs <- file.path("C:/Users/Isaneli/Documents/RNASeq_Ceras_Isaneli", "Results_T2_T5", sample_id)
> kal_dirs
[1] "C:/Users/Isaneli/Documents/RNASeq_Ceras_Isaneli/Results_T2_T5/T2R1"
[2] "C:/Users/Isaneli/Documents/RNASeq_Ceras_Isaneli/Results_T2_T5/T2R2"
[3] "C:/Users/Isaneli/Documents/RNASeq_Ceras_Isaneli/Results_T2_T5/T2R3"
[4] "C:/Users/Isaneli/Documents/RNASeq_Ceras_Isaneli/Results_T2_T5/T2R4"
[5] "C:/Users/Isaneli/Documents/RNASeq_Ceras_Isaneli/Results_T2_T5/T5R1"
[6] "C:/Users/Isaneli/Documents/RNASeq_Ceras_Isaneli/Results_T2_T5/T5R2"
[7] "C:/Users/Isaneli/Documents/RNASeq_Ceras_Isaneli/Results_T2_T5/T5R3"
[8] "C:/Users/Isaneli/Documents/RNASeq_Ceras_Isaneli/Results_T2_T5/T5R4"
> s2c <- read.table(file.path("C:/Users/Isaneli/Documents/RNASeq_Ceras_Isaneli", "metadata", "hiseq_info_T2_T5.txt"), header = TRUE, stringsAsFactors=FALSE)
> s2c <- mutate(s2c, path = kal_dirs)
> print(s2c)
  sample    condition                                                path
1   T5R1 MinOil_18hpi C:/Users/Isaneli/Documents/RNASeq_Ceras_Isaneli/Results_T2_T5/T2R1
2   T5R2 MinOil_18hpi C:/Users/Isaneli/Documents/RNASeq_Ceras_Isaneli/Results_T2_T5/T2R2
3   T5R3 MinOil_18hpi C:/Users/Isaneli/Documents/RNASeq_Ceras_Isaneli/Results_T2_T5/T2R3
4   T5R4 MinOil_18hpi C:/Users/Isaneli/Documents/RNASeq_Ceras_Isaneli/Results_T2_T5/T2R4
5   T2R1    E.g_18hpi C:/Users/Isaneli/Documents/RNASeq_Ceras_Isaneli/Results_T2_T5/T5R1
6   T2R2    E.g_18hpi C:/Users/Isaneli/Documents/RNASeq_Ceras_Isaneli/Results_T2_T5/T5R2
7   T2R3    E.g_18hpi C:/Users/Isaneli/Documents/RNASeq_Ceras_Isaneli/Results_T2_T5/T5R3
8   T2R4    E.g_18hpi C:/Users/Isaneli/Documents/RNASeq_Ceras_Isaneli/Results_T2_T5/T5R4
> so <- sleuth_prep(s2c, extra_bootstrap_summary = TRUE,read_bootstrap_tpm=TRUE)
reading in kallisto results
dropping unused factor levels
.....
normalizing est_counts
7873 targets passed the filter
normalizing tpm
merging in metadata
summarizing bootstraps
.....
Warning message:
In check_num_cores(num_cores) :
  It appears that you are running Sleuth from within Rstudio.
Because of concerns with forking processes from a GUI, 'num_cores' is being set to 1.
If you wish to take advantage of multiple cores, please consider running sleuth from the command line.
> so <- sleuth_fit(so, ~condition, 'full')
fitting measurement error models
shrinkage estimation
computing variance of betas
> so <- sleuth_fit(so, ~1, 'reduced')
fitting measurement error models
shrinkage estimation
computing variance of betas
```

```
> so <- sleuth_lrt(so, 'reduced', 'full')
> models(so)
[  full  ]
formula:  ~condition
coefficients:
        (Intercept)
        conditionMinOil_18hpi
[  reduced  ]
formula:  ~1
coefficients:
        (Intercept)
> sleuth_table <- sleuth_results(so, 'reduced:full', 'lrt', show_all = FALSE)
> sleuth_significant <- dplyr::filter(sleuth_table, qval <= 0.05)
> head(sleuth_significant)
                          target_id test_stat         pval        qval       rss   sigma_sq
1 evm.model.NODE_43908_length_4518_cov_0.233834.1   26.98466 2.050764e-07 0.001613951 0.10646587
0.01493982
2 evm.model.NODE_10252_length_10043_cov_2.06676.2   21.54072 3.463946e-06 0.005480271 0.07893387
0.01105647
3 evm.model.NODE_23724_length_6470_cov_0.662936.1   21.22156 4.091353e-06 0.005480271 0.19634616
0.02736270
4 evm.model.NODE_3177_length_17556_cov_0.617419.1   21.18135 4.178098e-06 0.005480271 0.07950002
0.01105554
5 evm.model.NODE_6962_length_12091_cov_0.682464.1   21.34336 3.839484e-06 0.005480271 0.10776661
0.01470563
6 evm.model.NODE_9355_length_10503_cov_0.577872.2   21.62603 3.313249e-06 0.005480271 0.23237961
0.03317514
     tech_var  mean_obs    var_obs sigma_sq_pmax smooth_sigma_sq final_sigma_sq degrees_free
1 0.0002695878  8.299428 0.01520941    0.01493982     0.001228025     0.01493982           1
2 0.0002197949  8.184488 0.01127627    0.01105647     0.001211168     0.01105647           1
3 0.0006867464  7.464197 0.02804945    0.02736270     0.001168420     0.02736270           1
4 0.0003016026  8.129152 0.01135715    0.01105554     0.001202853     0.01105554           1
5 0.0006896015  7.226988 0.01539523    0.01470563     0.001227305     0.01470563           1
6 0.0000219502 10.765217 0.03319709    0.03317514     0.001447251     0.03317514           1
> write.csv(sleuth_table, file =
"C:/Users/Isaneli/Documents/RNASeq_Ceras_Isaneli/sleuth_table_LRT_t2_t5.txt",row.names=FALSE,quote=F
ALSE)
> write.csv(sleuth_significant, file =
"C:/Users/Isaneli/Documents/RNASeq_Ceras_Isaneli/sleuth_significant_LRT_t2_t5.txt",row.names=FALSE,qu
ote=FALSE)
> conditionE.g_18hpi<-s2c$sample[s2c$condition=="E.g_18hpi"]
> conditionMinOil_18hpi<-s2c$sample[s2c$condition=="MinOil_18hpi"]
> E.g_18hpiraw<-subset(so$obs_raw,so$obs_raw$sample %in% conditionE.g_18hpi)
> MinOil_18hpiraw<-subset(so$obs_raw,so$obs_raw$sample %in% conditionMinOil_18hpi)
> E.g_18hpimeans<-aggregate(tpm~target_id,data=E.g_18hpiraw,FUN=function(x) c(mean=mean(x)))
> colnames(E.g_18hpimeans)<-c("target_id","tpm_E.g_18hpi")
> MinOil_18hpimeans<-aggregate(tpm~target_id,data=MinOil_18hpiraw,FUN=function(x) c(mean=mean(x)))
> colnames(MinOil_18hpimeans)<-c("target_id","tpm_MinOil_18hpi")
> merged_means<-merge(MinOil_18hpimeans,E.g_18hpimeans,by=c("target_id"))
> sleuth_table_wTPM<-left_join(sleuth_table,merged_means)
Joining, by = "target_id"
> write.csv(sleuth_table_wTPM, file =
"C:/Users/Isaneli/Documents/RNASeq_Ceras_Isaneli/sleuth_table_LRT_Up_Down_t2_t5.txt")
> sleuth_significant_wTPM<-left_join(sleuth_significant,merged_means)
Joining, by = "target_id"
> head(sleuth_significant_wTPM)
                          target_id test_stat         pval        qval       rss   sigma_sq
1 evm.model.NODE_43908_length_4518_cov_0.233834.1   26.98466 2.050764e-07 0.001613951 0.10646587
0.01493982
```

2 evm.model.NODE_10252_length_10043_cov_2.06676.2 21.54072 3.463946e-06 0.005480271 0.07893387 0.01105647
3 evm.model.NODE_23724_length_6470_cov_0.662936.1 21.22156 4.091353e-06 0.005480271 0.19634616 0.02736270
4 evm.model.NODE_3177_length_17556_cov_0.617419.1 21.18135 4.178098e-06 0.005480271 0.07950002 0.01105554
5 evm.model.NODE_6962_length_12091_cov_0.682464.1 21.34336 3.839484e-06 0.005480271 0.10776661 0.01470563
6 evm.model.NODE_9355_length_10503_cov_0.577872.2 21.62603 3.313249e-06 0.005480271 0.23237961 0.03317514

	tech_var	mean_obs	var_obs	sigma_sq_pmax	smooth_sigma_sq	final_sigma_sq	degrees_free	tpm_MinOil_18hpi
1	0.0002695878	8.299428	0.01520941	0.01493982	0.001228025	0.01493982	1	83.47899
2	0.0002197949	8.184488	0.01127627	0.01105647	0.001211168	0.01105647	1	49.88632
3	0.0006867464	7.464197	0.02804945	0.02736270	0.001168420	0.02736270	1	41.18123
4	0.0003016026	8.129152	0.01135715	0.01105554	0.001202853	0.01105554	1	110.67542
5	0.0006896015	7.226988	0.01539523	0.01470563	0.001227305	0.01470563	1	15.97967
6	0.0000219502	10.765217	0.03319709	0.03317514	0.001447251	0.03317514	1	4138.79054

	tpm_E.g_18hpi
1	104.88933
2	40.79216
3	55.30778
4	91.40494
5	19.95806
6	2903.12998

> write.csv(sleuth_significant_wTPM, file = "C:/Users/Isaneli/Documents/RNASeq_Ceras_Isaneli/sleuth_significant_LRT_Up_Down_t2_t5.txt")
> sleuth_live(so)
Loading required package: shiny

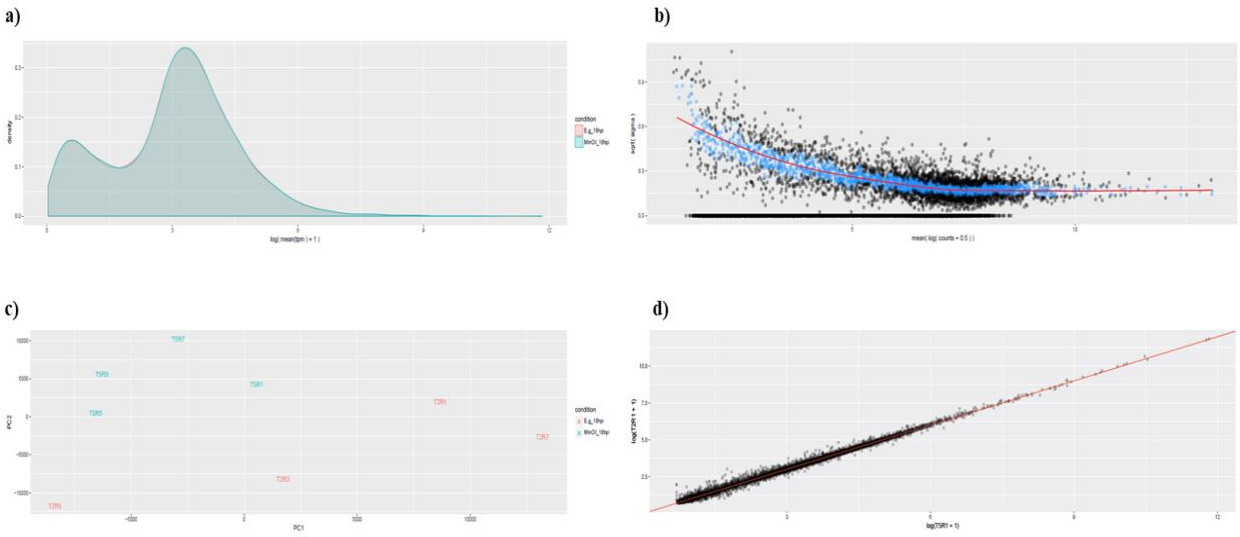

Figure 1. Plots of the group comparison *E. g* x MO obtained by Sleuth package (software R). Legend: a) Density x log mean tpm; b) Scatter x log counts; c) PCA (Principal Component Analysis); d) Mean variance.

T3 (*E. urograndis*) x T5 (Óleo Mineral)

> library("sleuth")
> sample_id <- dir(file.path("C:/Users/Isaneli/Documents/RNASeq_Ceras_Isaneli", "Results_T3_T5"))
> sample_id
[1] "T3R1" "T3R2" "T3R3" "T3R4" "T5R1" "T5R2" "T5R3" "T5R4"
> kal_dirs <- file.path("C:/Users/Isaneli/Documents/RNASeq_Ceras_Isaneli", "Results_T3_T5", sample_id)
> kal_dirs
[1] "C:/Users/Isaneli/Documents/RNASeq_Ceras_Isaneli/Results_T3_T5/T3R1"
[2] "C:/Users/Isaneli/Documents/RNASeq_Ceras_Isaneli/Results_T3_T5/T3R2"

```
[3] "C:/Users/Isaneli/Documents/RNASeq_Ceras_Isaneli/Results_T3_T5/T3R3"
[4] "C:/Users/Isaneli/Documents/RNASeq_Ceras_Isaneli/Results_T3_T5/T3R4"
[5] "C:/Users/Isaneli/Documents/RNASeq_Ceras_Isaneli/Results_T3_T5/T5R1"
[6] "C:/Users/Isaneli/Documents/RNASeq_Ceras_Isaneli/Results_T3_T5/T5R2"
[7] "C:/Users/Isaneli/Documents/RNASeq_Ceras_Isaneli/Results_T3_T5/T5R3"
[8] "C:/Users/Isaneli/Documents/RNASeq_Ceras_Isaneli/Results_T3_T5/T5R4"
> s2c <- read.table(file.path("C:/Users/Isaneli/Documents/RNASeq_Ceras_Isaneli", "metadata",
"hiseq_info_T3_T5.txt"), header = TRUE, stringsAsFactors=FALSE)
> s2c <- mutate(s2c, path = kal_dirs)
> print(s2c)
  sample    condition                                                    path
1   T5R1 MinOil_18hpi C:/Users/Isaneli/Documents/RNASeq_Ceras_Isaneli/Results_T3_T5/T3R1
2   T5R2 MinOil_18hpi C:/Users/Isaneli/Documents/RNASeq_Ceras_Isaneli/Results_T3_T5/T3R2
3   T5R3 MinOil_18hpi C:/Users/Isaneli/Documents/RNASeq_Ceras_Isaneli/Results_T3_T5/T3R3
4   T5R4 MinOil_18hpi C:/Users/Isaneli/Documents/RNASeq_Ceras_Isaneli/Results_T3_T5/T3R4
5   T3R1   E.ug_18hpi C:/Users/Isaneli/Documents/RNASeq_Ceras_Isaneli/Results_T3_T5/T5R1
6   T3R2   E.ug_18hpi C:/Users/Isaneli/Documents/RNASeq_Ceras_Isaneli/Results_T3_T5/T5R2
7   T3R3   E.ug_18hpi C:/Users/Isaneli/Documents/RNASeq_Ceras_Isaneli/Results_T3_T5/T5R3
8   T3R4   E.ug_18hpi C:/Users/Isaneli/Documents/RNASeq_Ceras_Isaneli/Results_T3_T5/T5R4
> so <- sleuth_prep(s2c, extra_bootstrap_summary = TRUE,read_bootstrap_tpm=TRUE)
reading in kallisto results
dropping unused factor levels
........
normalizing est_counts
7880 targets passed the filter
normalizing tpm
merging in metadata
summarizing bootstraps
........
Warning message:
In check_num_cores(num_cores) :
  It appears that you are running Sleuth from within Rstudio.
Because of concerns with forking processes from a GUI, 'num_cores' is being set to 1.
If you wish to take advantage of multiple cores, please consider running sleuth from the command line.
> so <- sleuth_fit(so, ~condition, 'full')
fitting measurement error models
shrinkage estimation
computing variance of betas
> so <- sleuth_fit(so, ~1, 'reduced')
fitting measurement error models
shrinkage estimation
computing variance of betas
> so <- sleuth_lrt(so, 'reduced', 'full')
> models(so)
[  full  ]
formula:  ~condition
coefficients:
            (Intercept)
            conditionMinOil_18hpi
[  reduced  ]
formula:  ~1
coefficients:
            (Intercept)
> sleuth_table <- sleuth_results(so, 'reduced:full', 'lrt', show_all = FALSE)
> sleuth_significant <- dplyr::filter(sleuth_table, qval <= 0.05)
> head(sleuth_significant)
                                    target_id test_stat         pval       qval        rss    sigma_sq     tech_var
1  evm.model.NODE_10275_length_10031_cov_0.514788.1    16.33395  5.310389e-05  0.02300443  0.05836949
0.007727069 0.0006114301
```

```
2   evm.model.NODE_1196_length_26518_cov_0.691183.1   17.65393  2.649674e-05  0.02300443  0.23910332
0.031362620 0.0027949965
3   evm.model.NODE_14940_length_8316_cov_0.216754.1   16.30579  5.389900e-05  0.02300443  0.34478909
0.047664757 0.0015908270
4   evm.model.NODE_18318_length_7503_cov_0.718818.1   17.47585  2.909810e-05  0.02300443  0.18907231
0.026871580 0.0001387510
5    evm.model.NODE_18723_length_7409_cov_1.43408.1   16.81547  4.119611e-05  0.02300443  0.08068591
0.011403442 0.0001231166
6   evm.model.NODE_19667_length_7209_cov_0.602205.1   15.73068  7.302994e-05  0.02300443  0.40999002
0.055163129 0.0034068741
  mean_obs     var_obs sigma_sq_pmax smooth_sigma_sq final_sigma_sq degrees_free
1 7.379187 0.008338499   0.007727069     0.001135206    0.007727069           1
2 5.888970 0.034157616   0.031362620     0.003094948    0.031362620           1
3 6.340229 0.049255584   0.047664757     0.002174424    0.047664757           1
4 8.887587 0.027010331   0.026871580     0.001322927    0.026871580           1
5 9.088151 0.011526559   0.011403442     0.001360196    0.011403442           1
6 5.650189 0.058570003   0.055163129     0.003726229    0.055163129           1
> write.csv(sleuth_table, file =
"C:/Users/Isaneli/Documents/RNASeq_Ceras_Isaneli/sleuth_table_LRT_t3_t5.txt",row.names=FALSE,quote=F
ALSE)
> write.csv(sleuth_significant, file =
"C:/Users/Isaneli/Documents/RNASeq_Ceras_Isaneli/sleuth_significant_LRT_t3_t5.txt",row.names=FALSE,qu
ote=FALSE)
> conditionE.ug_18hpi<-s2c$sample[s2c$condition=="E.ug_18hpi"]
> conditionMinOil_18hpi<-s2c$sample[s2c$condition=="MinOil_18hpi"]
> E.ug_18hpiraw<-subset(so$obs_raw,so$obs_raw$sample %in% conditionE.ug_18hpi)
> MinOil_18hpiraw<-subset(so$obs_raw,so$obs_raw$sample %in% conditionMinOil_18hpi)
> E.ug_18hpimeans<-aggregate(tpm~target_id,data=E.ug_18hpiraw,FUN=function(x) c(mean=mean(x)))
> colnames(E.ug_18hpimeans)<-c("target_id","tpm_E.ug_18hpi")
> MinOil_18hpimeans<-aggregate(tpm~target_id,data=MinOil_18hpiraw,FUN=function(x) c(mean=mean(x)))
> colnames(MinOil_18hpimeans)<-c("target_id","tpm_MinOil_18hpi")
> merged_means<-merge(MinOil_18hpimeans,E.ug_18hpimeans,by=c("target_id"))
> sleuth_table_wTPM<-left_join(sleuth_table,merged_means)
Joining, by = "target_id"
> write.csv(sleuth_table_wTPM, file =
"C:/Users/Isaneli/Documents/RNASeq_Ceras_Isaneli/sleuth_table_LRT_Up_Down_t3_t5.txt")
> sleuth_significant_wTPM<-left_join(sleuth_significant,merged_means)
Joining, by = "target_id"
> head(sleuth_significant_wTPM)
                                  target_id test_stat        pval       qval       rss    sigma_sq     tech_var
1  evm.model.NODE_10275_length_10031_cov_0.514788.1   16.33395  5.310389e-05  0.02300443  0.05836949
0.007727069 0.0006114301
2   evm.model.NODE_1196_length_26518_cov_0.691183.1   17.65393  2.649674e-05  0.02300443  0.23910332
0.031362620 0.0027949965
3   evm.model.NODE_14940_length_8316_cov_0.216754.1   16.30579  5.389900e-05  0.02300443  0.34478909
0.047664757 0.0015908270
4   evm.model.NODE_18318_length_7503_cov_0.718818.1   17.47585  2.909810e-05  0.02300443  0.18907231
0.026871580 0.0001387510
5    evm.model.NODE_18723_length_7409_cov_1.43408.1   16.81547  4.119611e-05  0.02300443  0.08068591
0.011403442 0.0001231166
6   evm.model.NODE_19667_length_7209_cov_0.602205.1   15.73068  7.302994e-05  0.02300443  0.40999002
0.055163129 0.0034068741
  mean_obs        var_obs  sigma_sq_pmax  smooth_sigma_sq  final_sigma_sq  degrees_free  tpm_MinOil_18hpi
tpm_E.ug_18hpi
1 7.379187 0.008338499   0.007727069     0.001135206    0.007727069           1       26.746650      31.196401
2 5.888970 0.034157616   0.031362620     0.003094948    0.031362620           1        2.997258       4.132133
3 6.340229 0.049255584   0.047664757     0.002174424    0.047664757           1        9.355905      13.611354
4 8.887587 0.027010331   0.026871580     0.001322927    0.026871580           1      238.439815     176.498278
5 9.088151 0.011526559   0.011403442     0.001360196    0.011403442           1      748.264112     903.116732
6 5.650189 0.058570003   0.055163129     0.003726229    0.055163129           1        3.593609       5.406146
```

> write.csv(sleuth_significant_wTPM, file = "C:/Users/Isaneli/Documents/RNASeq_Ceras_Isaneli/sleuth_significant_LRT_Up_Down_t3_t5.txt")
> sleuth_live(so)
Loading required package: shiny

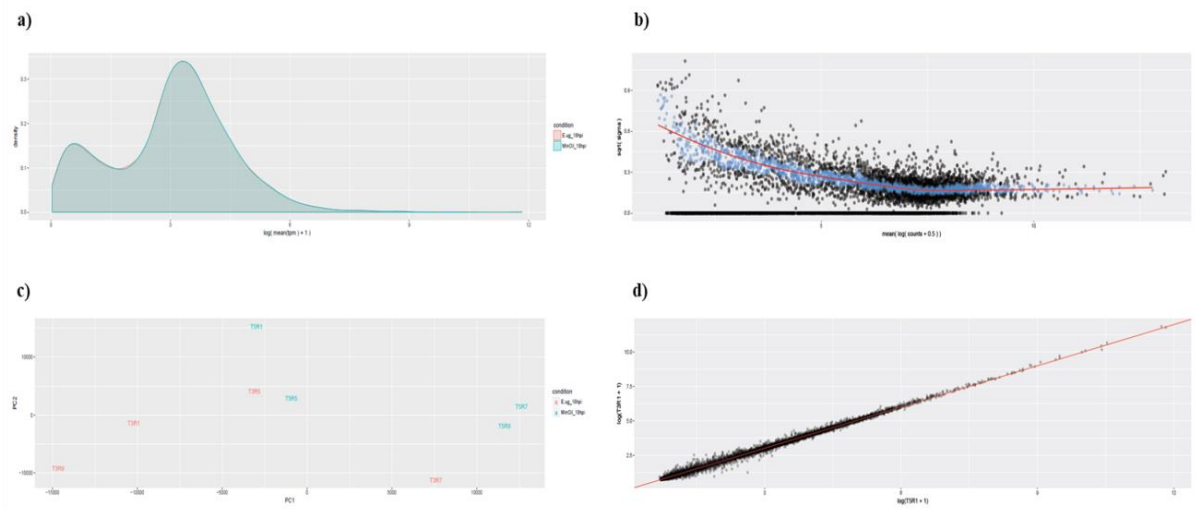

Figure 2. Plots of the group comparison *E. ug* x MO obtained by Sleuth package (software R). Legend: a) Density x log mean tpm; b) Scatter x log counts; c) PCA (Principal Component Analysis); d) Mean variance.

T4 (*E. urophylla*) x T5 (Óleo Mineral)

```
> library("sleuth")
> sample_id <- dir(file.path("C:/Users/Isaneli/Documents/RNASeq_Ceras_Isaneli", "Results_T4_T5"))
> sample_id
[1] "T4R1" "T4R2" "T4R3" "T4R4" "T5R1" "T5R2" "T5R3" "T5R4"
> kal_dirs <- file.path("C:/Users/Isaneli/Documents/RNASeq_Ceras_Isaneli", "Results_T4_T5", sample_id)
> kal_dirs
[1] "C:/Users/Isaneli/Documents/RNASeq_Ceras_Isaneli/Results_T4_T5/T4R1"
[2] "C:/Users/Isaneli/Documents/RNASeq_Ceras_Isaneli/Results_T4_T5/T4R2"
[3] "C:/Users/Isaneli/Documents/RNASeq_Ceras_Isaneli/Results_T4_T5/T4R3"
[4] "C:/Users/Isaneli/Documents/RNASeq_Ceras_Isaneli/Results_T4_T5/T4R4"
[5] "C:/Users/Isaneli/Documents/RNASeq_Ceras_Isaneli/Results_T4_T5/T5R1"
[6] "C:/Users/Isaneli/Documents/RNASeq_Ceras_Isaneli/Results_T4_T5/T5R2"
[7] "C:/Users/Isaneli/Documents/RNASeq_Ceras_Isaneli/Results_T4_T5/T5R3"
[8] "C:/Users/Isaneli/Documents/RNASeq_Ceras_Isaneli/Results_T4_T5/T5R4"
> s2c <- read.table(file.path("C:/Users/Isaneli/Documents/RNASeq_Ceras_Isaneli", "metadata", "hiseq_info_T4_T5.txt"), header = TRUE, stringsAsFactors=FALSE)
> s2c <- mutate(s2c, path = kal_dirs)
> print(s2c)
  sample    condition                                                path
1   T5R1 MinOil_18hpi C:/Users/Isaneli/Documents/RNASeq_Ceras_Isaneli/Results_T4_T5/T4R1
2   T5R2 MinOil_18hpi C:/Users/Isaneli/Documents/RNASeq_Ceras_Isaneli/Results_T4_T5/T4R2
3   T5R3 MinOil_18hpi C:/Users/Isaneli/Documents/RNASeq_Ceras_Isaneli/Results_T4_T5/T4R3
4   T5R4 MinOil_18hpi C:/Users/Isaneli/Documents/RNASeq_Ceras_Isaneli/Results_T4_T5/T4R4
5   T4R1    E.u_18hpi C:/Users/Isaneli/Documents/RNASeq_Ceras_Isaneli/Results_T4_T5/T5R1
6   T4R2    E.u_18hpi C:/Users/Isaneli/Documents/RNASeq_Ceras_Isaneli/Results_T4_T5/T5R2
7   T4R3    E.u_18hpi C:/Users/Isaneli/Documents/RNASeq_Ceras_Isaneli/Results_T4_T5/T5R3
8   T4R4    E.u_18hpi C:/Users/Isaneli/Documents/RNASeq_Ceras_Isaneli/Results_T4_T5/T5R4
> so <- sleuth_prep(s2c, extra_bootstrap_summary = TRUE,read_bootstrap_tpm=TRUE)
reading in kallisto results
dropping unused factor levels
.....
normalizing est_counts
7886 targets passed the filter
normalizing tpm
merging in metadata
```

```
summarizing bootstraps
........
Warning message:
In check_num_cores(num_cores) :
  It appears that you are running Sleuth from within Rstudio.
Because of concerns with forking processes from a GUI, 'num_cores' is being set to 1.
If you wish to take advantage of multiple cores, please consider running sleuth from the command line.
> so <- sleuth_fit(so, ~condition, 'full')
fitting measurement error models
shrinkage estimation
computing variance of betas
> so <- sleuth_fit(so, ~1, 'reduced')
fitting measurement error models
shrinkage estimation
computing variance of betas
> so <- sleuth_lrt(so, 'reduced', 'full')
> models(so)
[  full  ]
formula:  ~condition
coefficients:
            (Intercept)
            conditionMinOil_18hpi
[  reduced  ]
formula:  ~1
coefficients:
            (Intercept)
> sleuth_table <- sleuth_results(so, 'reduced:full', 'lrt', show_all = FALSE)
> sleuth_significant <- dplyr::filter(sleuth_table, qval <= 0.05)
> head(sleuth_significant)
                                    target_id test_stat         pval        qval        rss    sigma_sq     tech_var
1       evm.model.NODE_31350_length_5584_cov_1.512.1    27.57918  1.507931e-07  0.001188551  0.25047772
0.035054583 7.279478e-04
2    evm.model.NODE_10599_length_9875_cov_1.37372.2    23.39981  1.315915e-06  0.003206790  0.06014302
0.008494097 9.776215e-05
3  evm.model.NODE_3723_length_16235_cov_0.318518.1    23.18810  1.469033e-06  0.003206790  0.07707003
0.010762708 2.472955e-04
4    evm.model.NODE_6068_length_12929_cov_1.05014.1    22.99126  1.627399e-06  0.003206790  0.22963360
0.032767494 3.730609e-05
5  evm.model.NODE_10557_length_9889_cov_0.437097.1    20.35697  6.425858e-06  0.003731145  0.10804704
0.015153059 2.822319e-04
6  evm.model.NODE_13115_length_8884_cov_0.522782.1    20.18465  7.031490e-06  0.003731145  0.14789533
0.020302451 8.254528e-04
   mean_obs    var_obs sigma_sq_pmax smooth_sigma_sq final_sigma_sq degrees_free
1  7.241281 0.03578253   0.035054583     0.001203751    0.035054583           1
2  9.191288 0.00859186   0.008494097     0.001241634    0.008494097           1
3  8.322833 0.01101000   0.010762708     0.001142749    0.010762708           1
4 10.168286 0.03280480   0.032767494     0.001357412    0.032767494           1
5  8.233254 0.01543529   0.015153059     0.001132656    0.015153059           1
6  7.217466 0.02112790   0.020302451     0.001216176    0.020302451           1
>                                    write.csv(sleuth_table,                                    file                                    =
"C:/Users/Isaneli/Documents/RNASeq_Ceras_Isaneli/sleuth_table_LRT_t4_t5.txt",row.names=FALSE,quote=F
ALSE)
>                                    write.csv(sleuth_significant,                                    file                                    =
"C:/Users/Isaneli/Documents/RNASeq_Ceras_Isaneli/sleuth_significant_LRT_t4_t5.txt",row.names=FALSE,qu
ote=FALSE)
> conditionE.u_18hpi<-s2c$sample[s2c$condition=="E.u_18hpi"]
> conditionMinOil_18hpi<-s2c$sample[s2c$condition=="MinOil_18hpi"]
> E.u_18hpiraw<-subset(so$obs_raw,so$obs_raw$sample %in% conditionE.u_18hpi)
> MinOil_18hpiraw<-subset(so$obs_raw,so$obs_raw$sample %in% conditionMinOil_18hpi)
> E.u_18hpimeans<-aggregate(tpm~target_id,data=E.u_18hpiraw,FUN=function(x) c(mean=mean(x)))
```

```
> colnames(E.u_18hpimeans)<-c("target_id","tpm_E.u_18hpi")
> MinOil_18hpimeans<-aggregate(tpm~target_id,data=MinOil_18hpiraw,FUN=function(x) c(mean=mean(x)))
> colnames(MinOil_18hpimeans)<-c("target_id","tpm_MinOil_18hpi")
> merged_means<-merge(MinOil_18hpimeans,E.u_18hpimeans,by=c("target_id"))
> sleuth_table_wTPM<-left_join(sleuth_table,merged_means)
Joining, by = "target_id"
> write.csv(sleuth_table_wTPM, file =
"C:/Users/Isaneli/Documents/RNASeq_Ceras_Isaneli/sleuth_table_LRT_Up_Down_t4_t5.txt")
> sleuth_significant_wTPM<-left_join(sleuth_significant,merged_means)
Joining, by = "target_id"
> head(sleuth_significant_wTPM)
                    target_id test_stat       pval       qval       rss   sigma_sq    tech_var
1     evm.model.NODE_31350_length_5584_cov_1.512.1   27.57918  1.507931e-07  0.001188551  0.25047772
0.035054583 7.279478e-04
2   evm.model.NODE_10599_length_9875_cov_1.37372.2   23.39981  1.315915e-06  0.003206790  0.06014302
0.008494097 9.776215e-05
3  evm.model.NODE_3723_length_16235_cov_0.318518.1   23.18810  1.469033e-06  0.003206790  0.07707003
0.010762708 2.472955e-04
4   evm.model.NODE_6068_length_12929_cov_1.05014.1   22.99126  1.627399e-06  0.003206790  0.22963360
0.032767494 3.730609e-05
5  evm.model.NODE_10557_length_9889_cov_0.437097.1   20.35697  6.425858e-06  0.003731145  0.10804704
0.015153059 2.822319e-04
6  evm.model.NODE_13115_length_8884_cov_0.522782.1   20.18465  7.031490e-06  0.003731145  0.14789533
0.020302451 8.254528e-04
  mean_obs      var_obs  sigma_sq_pmax  smooth_sigma_sq  final_sigma_sq  degrees_free  tpm_MinOil_18hpi
tpm_E.u_18hpi
1  7.241281 0.03578253   0.035054583    0.001203751    0.035054583          1       36.39531     26.27869
2  9.191288 0.00859186   0.008494097    0.001241634    0.008494097          1       90.51022    109.91867
3  8.322833 0.01101000   0.010762708    0.001142749    0.010762708          1      357.38154    299.94850
4 10.168286 0.03280480   0.032767494    0.001357412    0.032767494          1     5737.57040   4212.38903
5  8.233254 0.01543529   0.015153059    0.001132656    0.015153059          1      102.00573     82.96785
6  7.217466 0.02112790   0.020302451    0.001216176    0.020302451          1      104.27297    138.43211
> write.csv(sleuth_significant_wTPM, file =
"C:/Users/Isaneli/Documents/RNASeq_Ceras_Isaneli/sleuth_significant_LRT_Up_Down_t4_t5.txt")
> sleuth_live(so)
```

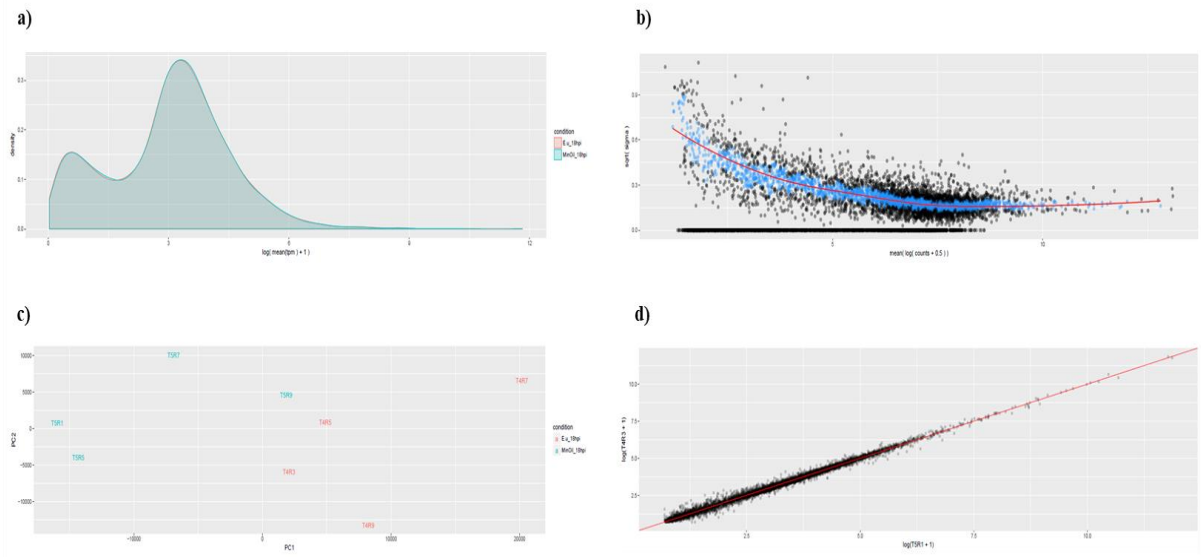

Figure 3. Plots of the group comparison *E. u* x MO obtained by Sleuth package (software R). Legend: a) Density x log mean tpm; b) Scatter x log counts; c) PCA (Principal Component Analysis); d) Mean variance.

5. APPENDIX

Appendix A. GO terms of biological processes from *A. psidii* DEGs, up regulated and annotated by Blast2GO. The comparative analyses were: *E. g* x MO, *E. ug* x MO and *E. u* x MO.

GO Termos	GO ID	GO related transcripts					
		***E. g* x MO**		***E. ug* x MO**		***E. u* x MO**	
		Nº	**%**	**Nº**	**%**	**Nº**	**%**
cell communication	GO:0007154	-	-	2	1.83	-	-
cell cycle	GO:0007049	-	-	2	1.83	-	-
chromosome organization	GO:0051276	-	-	2	1.83	-	-
DNA metabolic process	GO:0006259	-	-	2	1.83	-	-
generation of precursor metabolites and energy	GO:0006091	-	-	2	1.83	-	-
lipid metabolic process	GO:0006629	-	-	2	1.83	-	-
nuclear transport	GO:0051169	-	-	2	1.83	-	-
nucleocytoplasmic transport	GO:0006913	-	-	2	1.83	-	-
Reproduction	GO:0000003	-	-	2	1.83	-	-
ribosome biogenesis	GO:0042254	-	-	2	1.83	-	-
signal transduction	GO:0007165	-	-	2	1.83	-	-
Signaling	GO:0023052	-	-	2	1.83	-	-
cellular amino acid metabolic process	GO:0006520	-	-	3	2.75	-	-
cofactor metabolic process	GO:0051186	-	-	3	2.75	-	-
ncRNA metabolic process	GO:0034660	-	-	3	2.75	-	-
tRNA metabolic process	GO:0006399	-	-	3	2.75	-	-
sulfur compound metabolic process	GO:0006790	-	-	3	2.75	-	-
vesicle-mediated transport	GO:0016192	-	-	3	2.75	-	-
carbohydrate metabolic process	GO:0005975	-	-	4	3.67	-	-
homeostatic process	GO:0042592	-	-	4	3.67	-	-
regulation of biological quality	GO:0065008	-	-	4	3.67	-	-
intracellular protein transport	GO:0006886	-	-	-	-	15	3.73
cellular protein-containing complex assembly	GO:0034622	-	-	-	-	15	3.73
organic substance catabolic process	GO:1901575	-	-	-	-	15	3.73
peptide metabolic process	GO:0006518	-	-	-	-	15	3.73
protein-containing complex assembly	GO:0065003	-	-	-	-	15	3.73
protein-containing complex subunit organization	GO:0065003	-	-	-	-	15	3.73
establishment of protein localization	GO:0045184	-	-	-	-	16	3.98
cellular amide metabolic process	GO:0043603	-	-	-	-	16	3.98
carbohydrate derivative metabolic process	GO:1901135	-	-	-	-	16	3.98
amide transport	GO:0042886	-	-	-	-	16	3.98
nitrogen compound transport	GO:0071705	-	-	-	-	16	3.98
peptide transport	GO:0015833	-	-	-	-	16	3.98
protein transport	GO:0015031	-	-	-	-	16	3.98
regulation of biosynthetic process	GO:0009889	-	-	-	-	16	3.98

regulation of cellular biosynthetic process	GO:0031326	-	-	-	-	16	3.98
regulation of cellular macromolecule biosynthetic process	GO:2000112	-	-	-	-	16	3.98
regulation of macromolecule biosynthetic process	GO:0010556	-	-	-	-	16	3.98
RNA processing	GO:0006396	-	-	-	-	16	3.98
transmembrane transport	GO:0055085	-	-	-	-	16	3.98
nucleic acid-templated transcription	GO:0097659	-	-	-	-	17	4.23
regulation of gene expression	GO:0010468	-	-	-	-	17	4.23
RNA biosynthetic process	GO:0032774	-	-	-	-	17	4.23
transcription, DNA-templated	GO:0006351	-	-	-	-	17	4.23
organic substance transport	GO:0071702	-	-	-	-	18	4.48
regulation of cellular metabolic process	GO:0031323	-	-	-	-	18	4.48
regulation of nitrogen compound metabolic process	GO:0051171	-	-	-	-	18	4.48
regulation of primary metabolic process	GO:0080090	-	-	-	-	18	4.48
oxidation-reduction process	GO:0055114	-	-	-	-	20	4.98
regulation of macromolecule metabolic process	GO:0060255	-	-	-	-	20	4.98
regulation of metabolic process	GO:0019222	-	-	-	-	20	4.98
cellular macromolecule localization	GO:0070727	-	-	-	-	21	5.22
cellular protein localization	GO:0034613	-	-	-	-	21	5.22
phosphate-containing compound metabolic process	GO:0006796	-	-	-	-	22	5.47
macromolecule localization	GO:0033036	-	-	-	-	23	5.72
nucleobase-containing compound biosynthetic process	GO:0034654	-	-	-	-	23	5.72
phosphorus metabolic process	GO:0006793	-	-	-	-	23	5.72
protein localization	GO:0008104	-	-	-	-	23	5.72
heterocycle biosynthetic process	GO:0018130	-	-	-	-	26	6.47
organic cyclic compound biosynthetic process	GO:1901362	-	-	-	-	26	6.47
aromatic compound biosynthetic process	GO:0019438	-	-	-	-	27	6.72
cellular macromolecule biosynthetic process	GO:0034645	-	-	-	-	35	8.71
macromolecule biosynthetic process	GO:0009059	-	-	-	-	36	8.96
organonitrogen compound biosynthetic process	GO:1901566	-	-	-	-	36	8.96
cellular nitrogen compound biosynthetic process	GO:0044271	-	-	-	-	39	9.70
organic substance biosynthetic process	GO:1901576	-	-	-	-	52	12.94
cellular biosynthetic process	GO:0044249	-	-	-	-	53	13.18
cellular catabolic process	GO:0044248	-	-	2	1.83	15	3.73
carboxylic acid metabolic process	GO:0019752	-	-	3	2.75	16	3.98
organic acid metabolic process	GO:0006082	-	-	3	2.75	17	4.23
oxoacid metabolic process	GO:0043436	-	-	3	2.75	17	4.23
cellular response to stimulus	GO:0051716	-	-	2	1.83	20	4.98
establishment of localization in cell	GO:0051649	-	-	2	1.83	20	4.98

intracellular transport	GO:0046907	-	-	2	1.83	20	4.98
cellular component assembly	GO:0022607	-	-	3	2.75	21	5.22
cellular localization	GO:0051641	-	-	2	1.83	24	5.97
organelle organization	GO:0006996	-	-	2	1.83	28	6.97
regulation of cellular process	GO:0050794	-	-	2	1.83	28	6.97
regulation of biological process	GO:0050789	-	-	2	1.83	29	7.21
RNA metabolic process	GO:0016070	-	-	3	2.75	34	8.46
gene expression	GO:0010467	11	4.91	-	-	48	11.94
ribonucleoprotein complex biogenesis	GO:0022613	8	3.57	2	1.83	15	3.73
response to stress	GO:0006950	11	4.91	2	1.83	15	3.73
catabolic process	GO:0009056	9	4.02	5	4.59	17	4.23
cellular protein modification process	GO:0006464	11	4.91	4	3.67	17	4.23
protein modification process	GO:0036211	11	4.91	4	3.67	17	4.23
macromolecule modification	GO:0043412	11	4.91	4	3.67	20	4.98
response to stimulus	GO:0050896	14	6.25	5	4.59	23	5.72
cellular component biogenesis	GO:0044085	8	3.57	3	2.75	30	7.46
small molecule metabolic process	GO:0044281	14	6.25	6	5.50	29	7.21
establishment of localization	GO:0051234	7	3.13	4	3.67	36	8.96
Transport	GO:0006810	7	3.13	4	3.67	36	8.96
cellular protein metabolic process	GO:0044267	16	7.14	4	3.67	36	8.96
cellular component organization	GO:0071840	9	4.02	5	4.59	39	9.70
biological regulation	GO:0065007	10	4.46	6	5.50	38	9.45
nucleic acid metabolic process	GO:0090304	10	4.46	5	4.59	40	9.95
localization	GO:0051179	7	3.13	4	3.67	41	10.20
protein metabolic process	GO:0019538	17	7.59	5	4.59	43	10.70
cellular component organization or biogenesis	GO:0071840	12	5.36	5	4.59	48	11.94
nucleobase-containing compound metabolic process	GO:0006139	13	5.80	6	5.50	51	12.69
heterocycle metabolic process	GO:0046483	13	5.80	6	5.50	54	13.43
organic cyclic compound metabolic process	GO:1901360	13	5.80	6	5.50	54	13.43
cellular aromatic compound metabolic process	GO:0006725	13	5.80	6	5.50	55	13.68
cellular macromolecule metabolic process	GO:0044260	19	8.48	5	4.59	59	14.68
organonitrogen compound metabolic process	GO:1901564	22	9.82	8	7.34	64	15.92
biosynthetic process	GO:0009058	25	11.16	8	7.34	55	13.68
macromolecule metabolic process	GO:0043170	25	11.16	8	7.34	77	19.15
cellular nitrogen compound metabolic process	GO:0034641	30	13.39	10	9.17	65	16.17
primary metabolic process	GO:0044238	39	17.41	16	14.68	105	26.12
organic substance metabolic process	GO:0071704	39	17.41	16	14.68	111	27.61
cellular metabolic process	GO:0044237	40	17.86	15	13.76	105	26.12
nitrogen compound metabolic process	GO:0006807	41	18.30	15	13.76	98	24.38
cellular process	GO:0009987	44	19.64	17	15.60	126	31.34
metabolic process	GO:0008152	54	24.11	21	19.27	128	31.84

Appendix B. GO terms of biological processes from *A. psidii* DEGs, down regulated and annotated by Blast2GO. The comparative analyses were: *E. g* x MO, *E. ug* x MO and *E. u* x MO.

GO Termos	GO ID	GO related transcripts					
		***E. g* x MO**		***E. ug* x MO**		***E. u* x MO**	
		Nº	**%**	**Nº**	**%**	**Nº**	**%**
RNA metabolic process	GO:0016070	-	-	4	4.0	-	-
cofactor metabolic process	GO:0051186	-	-	4	4.0	-	-
carboxylic acid metabolic process	GO:0019752	-	-	5	5.0	-	-
cellular amino acid metabolic process	GO:0006520	-	-	5	5.0	-	-
organic acid metabolic process	GO:0006082	-	-	5	5.0	-	-
oxoacid metabolic process	GO:0043436	-	-	5	5.0	-	-
amide biosynthetic process	GO:0043604	-	-	7	7.0	-	-
cellular amide metabolic process	GO:0043603	-	-	7	7.0	-	-
cellular biosynthetic process	GO:0044249	-	-	7	7.0	-	-
cellular macromolecule biosynthetic process	GO:0034645	-	-	7	7.0	-	-
cellular nitrogen compound biosynthetic process	GO:0044271	-	-	7	7.0	-	-
macromolecule biosynthetic process	GO:0009059	-	-	7	7.0	-	-
organic substance biosynthetic process	GO:1901576	-	-	7	7.0	-	-
organonitrogen compound biosynthetic process	GO:1901566	-	-	7	7.0	-	-
peptide biosynthetic process	GO:0043043	-	-	7	7.0	-	-
peptide metabolic process	GO:0006518	-	-	7	7.0	-	-
biological regulation	GO:0065007	-	-	8	8.0	-	-
translation	GO:0006412	-	-	7	7.0	-	-
protein-containing complex assembly	GO:0065003	-	-	-	-	18	4.01
protein-containing complex subunit organization	GO:0043933	-	-	-	-	18	4.01
cellular component assembly	GO:0022607	-	-	-	-	20	4.45
cellular component biogenesis	GO:0044085	-	-	-	-	22	4.90
establishment of localization	GO:0051234	-	-	5	5.0	24	4.45
localization	GO:0051179	-	-	5	5.0	24	5.35
transport	GO:0006810	-	-	5	5.0	24	5.35
response to stress	GO:0006950	11	4.18	5	5.0	-	-
protein modification process	GO:0036211	12	4.56	7	7.0	20	3.79
macromolecule modification	GO:0043412	20	7.60	7	7.0	20	4.45
response to stimulus	GO:0050896	11	4.18	5	5.0	17	4.45
gene expression	GO:0010467	10	3.80	10	10.0	21	4.68
cellular aromatic compound metabolic process	GO:0006725	15	5.70	6	6.0	22	4.90
heterocycle metabolic process	GO:0046483	15	5.70	6	6.0	22	4.90
nucleobase-containing compound metabolic process	GO:0006139	15	5.70	6	6.0	22	4.90
cellular protein modification process	GO:0006464	20	7.60	7	7.0	20	4.90
organic cyclic compound metabolic process	GO:1901360	15	5.70	6	6.0	22	5.35
cellular component organization	GO:0016043	11	4.18	4	4.0	27	6.01
carbohydrate metabolic process	GO:0005975	20	7.60	6	6.0	28	6.24

cellular component organization or biogenesis	GO:0071840	12	4.56	4	4.0	29	6.46
catabolic process	GO:0009056	21	7.98	5	5.0	31	6.90
nucleic acid metabolic process	GO:0090304	11	4.18	5	5.0	35	7.80
cellular protein metabolic process	GO:0044267	15	5.70	12	12.0	32	7.13
protein metabolic process	GO:0019538	15	5.70	12	12.0	34	7.57
cellular macromolecule metabolic process	GO:0044260	18	6.84	12	12.0	36	8.02
organonitrogen compound metabolic process	GO:1901564	23	8.75	17	17.0	45	10.02
macromolecule metabolic process	GO:0043170	24	9.13	15	15.0	44	9.80
biosynthetic process	GO:0009058	35	13.31	24	24.0	58	12.92
cellular nitrogen compound metabolic process	GO:0034641	39	14.83	22	22.0	59	13.14
small molecule metabolic process	GO:0044281	42	15.97	14	14.0	51	11.36
nitrogen compound metabolic process	GO:0006807	49	18.63	27	27.0	79	17.59
cellular metabolic process	GO:0044237	58	22.05	28	28.0	87	19.38
organic substance metabolic process	GO:0071704	62	23.57	28	28.0	93	20.71
primary metabolic process	GO:0044238	62	23.57	28	28.0	93	20.71
cellular process	GO:0009987	62	23.57	31	31.0	105	23.39
metabolic process	GO:0008152	84	31.94	33	33.0	123	27.39

Appendix C. Up-regulated DEGs from *A. psidii* annotated by Blast2GO. The comparative analyses were: *E. g* x MO, *E. ug* x MO and *E. u* x MO.

Description/Função putativa	***E. g* x MO**			***E. ug* x MO**			***E. u* x MO**		
	qval*	**FC[1]**	**Log2 FC[2]**	**qval***	**FC[1]**	**Log2 FC[2]**	**qval***	**FC[1]**	**Log2 FC[2]**
Zinc metalloprotease	0.01	1.34	0.42	0.02	1.38	0.46	0.05	1.34	0.42
Zinc finger bed domain-containing protein daysleeper (Quercus suber)	0.01	1.25	0.32	0.02	1.18	0.23	0.01	1.2	0.26
Plasma membrane ATPase	0.01	1.19	0.25	0.05	1.12	0.16	0.01	1.21	0.28
Family 15 glycoside hydrolase	0.01	1.19	0.25	0.03	1.14	0.19	0.01	1.17	0.23
TATA-box-binding protein	0.01	1.18	0.24	0.05	1.12	0.17	0.01	1.19	0.25
Serine/threonine protein kinase	0.01	1.17	0.23	0.04	1.1	0.14	0.01	1.17	0.23
AGC NDR kinase	0.01	1.14	0.19	0.03	1.15	0.2	0.01	1.21	0.27
Histone H3	0.01	1.14	0.19	0.02	1.14	0.2	0.01	1.19	0.25
Secreted protein	0.01	1.13	0.17	0.03	1.11	0.15	0.01	1.17	0.23
Family 26 glycoside hydrolase	0.03	1.11	0.15	0.03	1.14	0.19	0.01	1.19	0.25
Family 90 glycosyltransferase	0.03	1.1	0.13	0.04	1.09	0.13	0.02	1.11	0.15
Extracellular metalloproteinase	0.01	1.09	0.13	0.04	1.07	0.1	0.01	1.1	0.14
STE/STE7/MKK protein kinase	0.03	1.09	0.13	0.05	1.09	0.12	0.04	1.1	0.14
Bleomycin hydrolase	0.03	1.08	0.12	0.05	1.08	0.11	0.01	1.15	0.2
Vacuolar transporter chaperone 1	0.02	1.08	0.11	0.05	1.07	0.1	0.01	1.13	0.18
Molecular chaperone	0.05	1.57	0.65	-	-	-	0.02	1.7	0.76
Glutathione peroxidase	0.05	1.23	0.29	-	-	-	0.02	1.38	0.47
Family 71 glycosyltransferase	0.01	1.23	0.29	-	-	-	0.02	1.26	0.34
Trimethyllysine dioxygenase	0.01	1.23	0.29	-	-	-	0.01	1.27	0.34

Family 4 carbohydrate esterase	0.01	1.21	0.28	-	-	-	0.01	1.29	0.37
Small nuclear ribonucleo D3	0.02	1.18	0.24	-	-	-	0.02	1.23	0.3
Mitochondrial intermediate peptidase mitochondrial precursor	0.02	1.16	0.21	-	-	-	0.03	1.23	0.3
Serine threonine kinase	0.02	1.14	0.19	-	-	-	0.05	1.12	0.17
Beta-xylanase	0.01	1.14	0.19	-	-	-	0.02	1.16	0.21
Magnesium-dependent phosphatase-1	0.04	1.14	0.18	-	-	-	0.03	1.18	0.23
Orotidine 5 -phosphate decarboxylase	0.04	1.13	0.18	-	-	-	0.04	1.12	0.16
Anthranilate phosphoribosyltransferase	0.02	1.13	0.18	-	-	-	0.02	1.13	0.17
Isoleucyl-tRNA synthetase	0.03	1.13	0.18	-	-	-	0.03	1.17	0.23
Adenosinetriphosphatase	0.01	1.13	0.17	-	-	-	0.01	1.15	0.2
Ribosomal protein L15	0.01	1.13	0.17	-	-	-	0.01	1.19	0.25
Polyubiquitin 11	0.03	1.12	0.16	-	-	-	0.01	1.14	0.19
DNA-directed RNA polymerase II subunit rpb7	0.04	1.11	0.15	-	-	-	0.05	1.13	0.18
Ubiquitin conjugating enzyme family	0.02	1.11	0.15	-	-	-	0.04	1.11	0.15
GDP-mannose 4,6 dehydratase	0.02	1.1	0.14	-	-	-	0.02	1.1	0.14
Pyridoxamine 5 -phosphate oxidase	0.02	1.1	0.13	-	-	-	0.01	1.16	0.21
SPX SLC13_permease	0.02	1.1	0.13	-	-	-	0.03	1.14	0.18
Serine/threonine protein kinase	0.03	1.09	0.13	-	-	-	0.01	1.12	0.17
Calcium-transporting ATPase	0.02	1.09	0.12	-	-	-	0.01	1.13	0.17
Serine/threonine protein kinase	0.02	1.09	0.12	-	-	-	0.01	1.11	0.15
G2 mitotic-specific cyclin 1 2	0.03	1.09	0.12	-	-	-	0.02	1.12	0.17
X-Pro aminopeptidase	0.02	1.09	0.12	-	-	-	0.02	1.1	0.14
Alpha-1,2-Mannosidase	0.03	1.08	0.11	-	-	-	0.02	1.14	0.19
Squalene monooxygenase	0.04	1.08	0.11	-	-	-	0.02	1.11	0.16
Acyl-coenzyme A oxidase	0.03	1.08	0.11	-	-	-	0.02	1.12	0.16
Secreted protein	0.04	1.06	0.09	-	-	-	0.01	1.15	0.2
Ubiquitin-conjugating enzyme E2 N	0.02	1.11	0.15	0.04	1.12	0.16	-	-	-
Golgi SNAP receptor complex member 1	-	-	-	0.03	1.12	0.16	0.01	1.15	0.2
GAF domain-like protein	-	-	-	0.04	1.09	0.12	0.01	1.13	0.18
Peptidylprolyl isomerase	0.01	1.27	0.34	-	-	-	-	-	-
Protein of RNA polymerase III Rpc4 family	0.03	1.24	0.31	-	-	-	-	-	-
RNA-binding domain protein	0.04	1.15	0.2	-	-	-	-	-	-
CTP synthase	0.03	1.11	0.15	-	-	-	-	-	-
Sphinganine-1-phosphate aldolase	0.04	1.1	0.13	-	-	-	-	-	-
Oligopeptide transporter	0.05	1.08	0.11	-	-	-	-	-	
60S ribosomal L10	0.02	1.08	0.11	-	-	-	-	-	-
Transposable element tc3 transposase	-	-	-	0.05	1.27	0.34	-	-	-
MFS general substrate transporter	-	-	-	0.05	1.23	0.3	-	-	-
Family 4 carbohydrate esterase	-	-	-	0.05	1.1	0.14	-	-	-
DNA repair and recombination RAD54	-	-	-	0.04	1.1	0.13	-	-	-
Glycine dehydrogenase subunit 2	-	-	-	0.05	1.09	0.12	-	-	-

E3 ubiquitin-protein ligase	-	-	-	0.05	1.08	0.11	-	-	-
Pheromone with four tandem repeats of a putative pheromone peptide	-	-	-	-	-	-	0.02	1.57	0.65
Cutinase	-	-	-	-	-	-	0.03	1.49	0.57
NADH dehydrogenase (Ubiquinone) Fe-S protein 7	-	-	-	-	-	-	0.01	1.24	0.32
TatD family	-	-	-	-	-	-	0.01	1.24	0.31
Prefoldin, alpha subunit	-	-	-	-	-	-	0.01	1.2	0.26
Splicing factor subunit	-	-	-	-	-	-	0.05	1.2	0.26
Mitochondrial inner membrane protease ATP23	-	-	-	-	-	-	0.01	1.18	0.24
Protein DOM34 homolog	-	-	-	-	-	-	0.02	1.17	0.22
DNA-directed RNA Polymerase II subunit F	-	-	-	-	-	-	0.05	1.17	0.22
MFS PHS inorganic phosphate transporter	-	-	-	-	-	-	0.01	1.16	0.22
Family 20 glycoside hydrolase	-	-	-	-	-	-	0.04	1.16	0.21
Synaptobrevin like YKT6	-	-	-	-	-	-	0.03	1.15	0.2
Ribosome biogenesis protein RLP24	-	-	-	-	-	-	0.03	1.15	0.2
NADH dehydrogenase [ubiquinone] flavoprotein 1, mitochondrial	-	-	-	-	-	-	0.02	1.14	0.19
GTP-binding rhoA	-	-	-	-	-	-	0.01	1.14	0.18
Malate dehydrogenase	-	-	-	-	-	-	0.02	1.13	0.18
AB-hydrolase associated lipase	-	-	-	-	-	-	0.04	1.13	0.18
Fe-S cluster assembly DRE2	-	-	-	-	-	-	0.02	1.13	0.18
Multi-copper oxidase laccase	-	-	-	-	-	-	0.01	1.13	0.17
DNA primase	-	-	-	-	-	-	0.02	1.13	0.17
Ras-like protein Rab7	-	-	-	-	-	-	0.03	1.12	0.17
D-3-phosphoglycerate dehydrogenase	-	-	-	-	-	-	0.02	1.12	0.17
NADH dehydrogenase (quinone) G subunit	-	-	-	-	-	-	0.03	1.12	0.17
Nuclear transcription factor beta	-	-	-	-	-	-	0.02	1.12	0.16
Tubulin beta chain	-	-	-	-	-	-	0.03	1.12	0.16
3-keto sterol reductase	-	-	-	-	-	-	0.04	1.12	0.16
Peptidylprolyl isomerase	-	-	-	-	-	-	0.04	1.12	0.16
Glutamate-5-semialdehyde dehydrogenase	-	-	-	-	-	-	0.01	1.12	0.16
AGC AKT kinase	-	-	-	-	-	-	0.05	1.11	0.16
Alanyl-tRNA synthetase	-	-	-	-	-	-	0.03	1.11	0.16
Cysteine synthase	-	-	-	-	-	-	0.01	1.11	0.16
Translation initiation factor eIF-3 subunit 9	-	-	-	-	-	-	0.04	1.11	0.15
Cytochrome c oxidase subunit IV	-	-	-	-	-	-	0.04	1.11	0.15
Exosome complex component RRP45	-	-	-	-	-	-	0.04	1.11	0.15
DNA-directed RNA polymerase II subunit RPB2	-	-	-	-	-	-	0.02	1.11	0.15
Phospholipid-transporting ATPase	-	-	-	-	-	-	0.05	1.11	0.15
DNA damage-inducible 1	-	-	-	-	-	-	0.05	1.11	0.15
Mitochondrial dicarboxylate carrier	-	-	-	-	-	-	0.03	1.11	0.15
Family 63 glycoside hydrolase	-	-	-	-	-	-	0.04	1.11	0.15

Cytochrome P450 monooxygenase	-	-	-	-	-	-	0.03	1.11	0.14
Dual specificity phosphatase	-	-	-	-	-	-	0.01	1.1	0.14
Autophagy-related protein 18	-	-	-	-	-	-	0.05	1.1	0.14
UDP-glucose 4-epimerase	-	-	-	-	-	-	0.03	1.1	0.14
GTP cyclohydrolase II	-	-	-	-	-	-	0.03	1.1	0.14
Oxoglutarate dehydrogenase (succinyl-transferring) E1 component	-	-	-	-	-	-	0.05	1.1	0.14
ATP synthase gamma subunit	-	-	-	-	-	-	0.04	1.1	0.14
Esterase lipase	-	-	-	-	-	-	0.02	1.1	0.14
Histone chaperone ASF1	-	-	-	-	-	-	0.04	1.1	0.14
Transposase-like protein	-	-	-	-	-	-	0.05	1.1	0.14
Aspartyl-tRNA synthetase	-	-	-	-	-	-	0.05	1.1	0.13
Vacuolar calcium ion transporter	-	-	-	-	-	-	0.02	1.1	0.13
DNA replication licensing factor MCM7	-	-	-	-	-	-	0.04	1.1	0.13
Peroxisomal biogenesis factor 2	-	-	-	-	-	-	0.04	1.09	0.13
Chitin synthase	-	-	-	-	-	-	0.03	1.09	0.13
14-3-3 family protein	-	-	-	-	-	-	0.03	1.09	0.13
Succinate--CoA ligase [ADP-forming] subunit beta, mitochondrial	-	-	-	-	-	-	0.05	1.09	0.13
Cystathionine beta-lyase	-	-	-	-	-	-	0.04	1.09	0.13
V-type proton ATPase subunit a	-	-	-	-	-	-	0.03	1.09	0.12
Family 31 glycoside hydrolase	-	-	-	-	-	-	0.04	1.09	0.12
Acyl- dehydrogenase	-	-	-	-	-	-	0.04	1.08	0.11
Carboxypeptidase	-	-	-	-	-	-	0.03	1.08	0.11

Legend: *q-value** $\leq$ 0.05 (*p-value* ajustado FDR). FC[1]: Fold-Change (FC): mean of TPM (transcripts per kilobase million) obtained by reason: TPM treatment/TPM control; Log2FC[2]: Base log (2) of FC.

Appendix D. Down-regulated DEGs from *A. psidii* annotated by Blast2GO. The comparative analyses were: *E. g* x MO, *E. ug* x MO and *E. u* x MO.

Description/Função putativa (Blast2Go)	***E. g* x MO**			***E. ug* x MO**			***E. u* x MO**		
	qval*	**FC[1]**	***Log2* FC[2]**	**qval***	**FC[1]**	***Log2* FC[2]**	**qval***	**FC[1]**	***Log2* FC[2]**
Thiamine thiazole synthase	0.01	0.38	-1.7	0.03	0.33	-1.59	0	0.27	-1.87
D-lactaldehyde dehydrogenase	0.01	0.62	-0.98	0.03	0.63	-0.66	0.01	0.62	-0.68
Aminotransferase	0.01	0.74	-0.72	0.05	0.75	-0.42	0.01	0.75	-0.42
Proline iminopeptidase	0.01	0.76	-0.68	0.04	0.76	-0.39	0.01	0.78	-0.35
Glyceraldehyde-3-phosphate dehydrogenase	0.01	0.76	-0.68	0.02	0.74	-0.43	0	0.76	-0.39
Phosphoglucomutase	0.01	0.79	-0.63	0.03	0.83	-0.27	0	0.84	-0.26
Nucleoside diphosphate kinase	0.01	0.81	-0.59	0.03	0.81	-0.3	0.01	0.85	-0.23
Pyruvate dehydrogenase kinase	0.01	0.83	-0.57	0.03	0.82	-0.29	0	0.81	-0.31
Transmembrane transport	0.02	0.83	-0.57	0.04	0.8	-0.31	0.02	0.87	-0.2
Carbohydrate kinase	0.01	0.84	-0.54	0.05	0.86	-0.22	0.01	0.87	-0.2
Large subunit ribosomal L6e	0.03	0.86	-0.51	0.03	0.86	-0.22	0.01	0.89	-0.16
Mannosyltransferase	0.01	0.87	-0.5	0.03	0.86	-0.22	0.01	0.86	-0.21
Terpene cyclase/mutase family member	0.01	0.87	-0.5	0.03	0.85	-0.23	0	0.88	-0.19

Transaldolase	0.01	0.87	-0.49	0.05	0.85	-0.23	0.01	0.88	-0.18
Family 5 glycoside hydrolase	0.01	0.87	-0.49	0.02	0.87	-0.2	0	0.88	-0.19
Asparagine synthetase	0.02	0.88	-0.48	0.03	0.86	-0.21	0.02	0.91	-0.13
Phosphoribosylamine-glycine ligase	0.03	0.88	-0.47	0.04	0.88	-0.18	0.03	0.93	-0.1
MC family mitochondrial carrier	0.01	0.88	-0.47	0.03	0.89	-0.17	0.01	0.94	-0.09
Homoserine O-acetyltransferase	0.02	0.9	-0.44	0.03	0.87	-0.19	0.01	0.9	-0.15
Family 4 carbohydrate esterase	0.02	0.91	-0.43	0.05	0.89	-0.17	0.01	0.9	-0.16
Superoxide dismutase	0.01	0.91	-0.42	0.04	0.9	-0.16	0.01	0.94	-0.09
Family 59 glycosyltransferase	0.04	0.91	-0.42	0.02	0.87	-0.2	0.02	0.91	-0.14
Palmitoyl- thioesterase precursor	0.02	0.92	-0.4	0.04	0.92	-0.13	0.03	0.96	-0.07
Glutamate 5-kinase	0.03	0.93	-0.4	0.03	0.91	-0.14	0.04	0.95	-0.07
Family 26 glycoside hydrolase	0.01	0.4	-1.6	-	-	-	0.01	0.37	-1.45
Catalase	0.01	0.56	-1.13	-	-	-	0	0.55	-0.87
Glutamate decarboxylase	0.01	0.68	-0.84	-	-	-	0	0.69	-0.53
Malic enzyme	0.05	0.74	-0.73	-	-	-	0.01	0.77	-0.38
Glutamate decarboxylase	0.01	0.74	-0.72	-	-	-	0	0.73	-0.45
Cytochrome P450 monooxygenase	0.04	0.75	-0.71	-	-	-	0.02	0.74	-0.44
Triosephosphate isomerase	0.01	0.76	-0.69	-	-	-	0.01	0.8	-0.33
Carbohydrate-binding module family 12	0.01	0.76	-0.69	-	-	-	0.01	0.79	-0.33
Malate synthase A	0.01	0.78	-0.65	-	-	-	0	0.79	-0.35
Family 18 glycoside hydrolase	0.02	0.79	-0.64	-	-	-	0.02	0.86	-0.22
Endoglucanase V	0.02	0.79	-0.63	-	-	-	0.01	0.75	-0.42
Mitochondrial ATP carrier	0.03	0.8	-0.61	-	-	-	0.03	0.86	-0.21
Glutamine-dependent NAD() synthetase	0.04	0.8	-0.61	-	-	-	0.01	0.84	-0.26
Fumarate mitochondrial	0.01	0.8	-0.61	-	-	-	0	0.83	-0.26
2,4-dienoyl- reductase (NADPH2)	0.01	0.81	-0.59	-	-	-	0	0.84	-0.25
Acyl- oxidase	0.01	0.82	-0.58	-	-	-	0.01	0.84	-0.25
UTP-glucose-1-phosphate uridylyltransferase	0.01	0.82	-0.58	-	-	-	0	0.8	-0.32
Aldehyde dehydrogenase 7 family, member A1	0.01	0.82	-0.58	-	-	-	0.03	0.86	-0.22
3-hydroxybutyryl- dehydrogenase	0.01	0.83	-0.57	-	-	-	0.01	0.89	-0.17
Telomerase reverse transcriptase	0.03	0.83	-0.56	-	-	-	0.01	0.83	-0.28
Saccharopine dehydrogenase-domain-containing	0.03	0.83	-0.56	-	-	-	0.01	0.86	-0.22
Citrate synthase	0.02	0.84	-0.54	-	-	-	0	0.85	-0.24
Diazepam-binding inhibitor (GABA receptor acyl- -binding)	0.02	0.84	-0.54	-	-	-	0.02	0.84	-0.24
Enolase	0.04	0.85	-0.52	-	-	-	0.01	0.86	-0.21
Enoyl- hydratase	0.02	0.86	-0.52	-	-	-	0.01	0.87	-0.2
Lactoylglutathione lyase	0.04	0.86	-0.51	-	-	-	0.01	0.86	-0.22
Malate dehydrogenase	0.01	0.86	-0.5				0.01	0.86	-0.22
Adenylosuccinate synthase	0.03	0.87	-0.49	-	-	-	0.02	0.89	-0.17
1,4-alpha-glucan-branching enzyme	0.04	0.87	-0.49	-	-	-	0.01	0.9	-0.15
Carbohydrate-binding module family 32	0.02	0.87	-0.49	-	-	-	0.01	0.89	-0.17
Amylo-1,6-glucosidase	0.03	0.87	-0.49	-	-	-	0.01	0.86	-0.21

Related to Ribonuclease P subunit p30	0.01	0.88	-0.48	-	-	-	0.04	0.94	-0.09
UPF0061 family protein	0.01	0.88	-0.48	-	-	-	0.01	0.9	-0.15
Electron transfer flavoprotein alpha subunit	0.01	0.88	-0.47	-	-	-	0	0.89	-0.17
Tryptophan synthase	0.01	0.88	-0.47	-	-	-	0.02	0.94	-0.09
Cyclopropane-fatty-acyl-phospholipid synthase	0.04	0.89	-0.46	-	-	-	0.04	0.91	-0.14
V-type H+transporting ATPase 21kDa proteolipid subunit	0.03	0.89	-0.46	-	-	-	0.01	0.88	-0.18
Secreted protein (Melampsora larici-populina (…)	0.02	0.89	-0.46	-	-	-	0.02	0.93	-0.11
Adenylosuccinate lyase	0.03	0.89	-0.46	-	-	-	0.03	0.93	-0.1
26S proteasome regulatory subunit N12	0.03	0.89	-0.46	-	-	-	0.05	0.92	-0.12
Acetyl- acyltransferase	0.04	0.89	-0.45	-	-	-	0.01	0.94	-0.09
Phosphoglycerate mutase	0.01	0.89	-0.45	-	-	-	0.03	0.94	-0.1
3-deoxy-7-phosphoheptulonate synthase	0.04	0.9	-0.44	-	-	-	0.02	0.9	-0.16
Isocitrate lyase	0.02	0.9	-0.44	-	-	-	0.04	0.92	-0.11
Omega-6 fatty acid desaturase (delta-12 desaturase)	0.01	0.91	-0.43	-	-	-	0.04	0.95	-0.07
Glutamate dehydrogenase	0.03	0.91	-0.43	-	-	-	0.03	0.93	-0.11
20S proteasome subunit beta 5	0.02	0.91	-0.43	-	-	-	0.04	0.93	-0.1
Ribose-phosphate pyrophosphokinase	0.03	0.91	-0.42	-	-	-	0.01	0.92	-0.12
Aconitate mitochondrial	0.03	0.91	-0.42	-	-	-	0.04	0.96	-0.06
Beta-hexosaminidase	0.05	0.91	-0.42	-	-	-	0.01	0.9	-0.15
Proteasome subunit alpha type-6	0.05	0.92	-0.4	-	-	-	0.02	0.93	-0.1
Nascent polypeptide-associated complex subunit	0.04	0.92	-0.4	-	-	-	0.03	0.93	-0.11
60S ribosomal protein L12	0.03	0.94	-0.39	-	-	-	0.01	0.93	-0.1
Ubiquitin 5	-	-	-	0.02	0.82	-0.29	0.04	0.88	-0.19
60S acidic ribosomal P1	-	-	-	0.05	0.82	-0.28	0.03	0.83	-0.26
Family 22 glycosyltransferase	-	-	-	0.03	0.86	-0.22	0.02	0.89	-0.17
Methylthioribose-1-phosphate isomerase	-	-	-	0.03	0.87	-0.2	0.04	0.93	-0.11
Cell wall integrity scw1	-	-	-	0.04	0.89	-0.18	0	0.9	-0.16
Methylsterol monooxygenase	-	-	-	0.03	0.89	-0.16	0.03	0.93	-0.1
D-3-phosphoglycerate dehydrogenase	0.04	0.8	-0.61	-	-	-	-	-	-
Beta-hexosaminidase	0.05	0.83	-0.56	-	-	-	-	-	-
Adenosinetriphosphatase	0.03	0.85	-0.52	-	-	-	-	-	-
Geranylgeranyl diphosphate type III	0.04	0.86	-0.51	-	-	-	-	-	-
Exosome complex component RRP4	0.02	0.86	-0.51	-	-	-	-	-	-
Succinyl- synthetase alpha subunit	0.05	0.87	-0.49	-	-	-	-	-	-
3-hydroxyisobutyrate dehydrogenase	0.01	0.88	-0.48	-	-	-	-	-	-
GDP-L-fucose synthase	0.02	0.89	-0.45	-	-	-	-	-	-
Glycoside hydrolase family 92	0.04	0.92	-0.41	-	-	-	-	-	-
MFS general substrate transporter	-	-	-	0.04	0.83	-0.26	-	-	-
Fatty acid synthase subunit beta	-	-	-	0.05	0.87	-0.2	-	-	-
Guanine nucleotide-binding subunit	-	-	-	0.05	0.89	-0.17	-	-	-

beta									
Aspartate aminotransferase, mitochondrial	-	-	-	0.03	0.89	-0.17	-	-	-
Heat shock HSS1	-	-	-	0.03	0.89	-0.17	-	-	-
40S ribosomal S4-A	-	-	-	0.03	0.9	-0.15	-	-	-
CDC7 (cell division control) protein kinase	-	-	-	0.04	0.9	-0.15	-	-	-
Reverse transcriptase domain protein	-	-	-	-	-	-	0.02	0.75	-0.41
Family 18 glycoside hydrolase	-	-	-	-	-	-	0.04	0.75	-0.41
Thiamine pyrophosphokinase	-	-	-	-	-	-	0.02	0.76	-0.4
Family 23 glycoside hydrolase	-	-	-	-	-	-	0.02	0.76	-0.4
Glutamate-cysteine ligase catalytic subunit	-	-	-	-	-	-	0.02	0.78	-0.36
60S acidic ribosomal protein P0	-	-	-	-	-	-	0.01	0.79	-0.34
Glycogen synthase	-	-	-	-	-	-	0.03	0.8	-0.33
Tryptophanyl-tRNA synthetase	-	-	-	-	-	-	0.04	0.85	-0.23
Mannosyltransferase	-	-	-	-	-	-	0.01	0.86	-0.22
26S proteasome regulatory subunit N6	-	-	-	-	-	-	0.01	0.86	-0.21
Phosphoglycerate kinase	-	-	-	-	-	-	0.02	0.88	-0.18
Peroxisomal-coenzyme A synthetase	-	-	-	-	-	-	0.01	0.88	-0.18
60S acidic ribosomal protein P0	-	-	-	-	-	-	0.02	0.89	-0.17
Fructose-1,6- cytosolic	-	-	-	-	-	-	0.03	0.89	-0.16
3-hydroxyanthranilate 3,4-dioxygenase 2	-	-	-	-	-	-	0.01	0.9	-0.15
Zinc finger 345-like	-	-	-	-	-	-	0.04	0.9	-0.15
Acyl-CoA desaturase	-	-	-	-	-	-	0.04	0.9	-0.15
Small subunit ribosomal S10e	-	-	-	-	-	-	0.01	0.9	-0.15
40S ribosomal S0	-	-	-	-	-	-	0.03	0.9	-0.15
Propionyl- carboxylase beta chain	-	-	-	-	-	-	0.02	0.91	-0.14
Protein phosphatase methylesterase 1	-	-	-	-	-	-	0.02	0.91	-0.14
Zinc metalloprotease	-	-	-	-	-	-	0.03	0.91	-0.13
Histone H2B	-	-	-	-	-	-	0.01	0.91	-0.13
Oligopeptide transporter	-	-	-	-	-	-	0.03	0.92	-0.13
Actin like 2 3 subunit 3	-	-	-	-	-	-	0.03	0.92	-0.13
Phosphoglycerate mutase	-	-	-	-	-	-	0.03	0.92	-0.12
Aspartic peptidase A1	-	-	-	-	-	-	0.05	0.92	-0.12
MFS SHS lactate transporter	-	-	-	-	-	-	0.03	0.92	-0.12
L-aminoadipate-semialdehyde dehydrogenase	-	-	-	-	-	-	0.03	0.92	-0.12
Family 16 glycoside hydrolase	-	-	-	-	-	-	0.03	0.92	-0.12
DNA-directed RNA polymerase II subunit A	-	-	-	-	-	-	0.03	0.92	-0.12
CMGC MAPK kinase	-	-	-	-	-	-	0.01	0.92	-0.12
Glycerol kinase	-	-	-	-	-	-	0.03	0.92	-0.11
Homeodomain-like containing	-	-	-	-	-	-	0.05	0.92	-0.11
CAMK CAMKL kinase	-	-	-	-	-	-	0.04	0.93	-0.11
CAMK CAMK1 CAMK1-RCK kinase	-	-	-	-	-	-	0.04	0.93	-0.11
Pyruvate kinase	-	-	-	-	-	-	0.01	0.93	-0.1

Galactan 1,3-beta-galactosidase	-	-	-	-	-	-	0.03	0.93	-0.1
Mitochondrial ABC transporter ATM	-	-	-	-	-	-	0.04	0.93	-0.1
Glucose-6-phosphate isomerase	-	-	-	-	-	-	0.02	0.93	-0.1
Peptidylprolyl isomerase	-	-	-	-	-	-	0.03	0.94	-0.09
Adenylate kinase	-	-	-	-	-	-	0.02	0.94	-0.09
Zinc finger, PHD-type protein	-	-	-	-	-	-	0.04	0.95	-0.08
Proteasome subunit alpha type	-	-	-	-	-	-	0.04	0.95	-0.08
Large subunit ribosomal L38e	-	-	-	-	-	-	0.02	0.95	-0.08
Serine threonine- kinase fhkC	-	-	-	-	-	-	0.05	0.95	-0.08
Ubiquitin-like-specific protease 2	-	-	-	-	-	-	0.05	0.95	-0.08
Kinase	-	-	-	-	-	-	0.05	0.95	-0.08
Carotenoid ester lipase precursor	-	-	-	-	-	-	0.03	0.95	-0.07

Legend: *q-value** $\leq$ 0.05 (*p-value* ajustado FDR). FC[1]: Fold-Change (FC): mean of TPM (transcripts per kilobase million) obtained by reason: TPM treatment/TPM control; Log2FC[2]: Base log (2) of FC.